2.2 Waste Management

WASTE MANAGEMENT

Annual Technical Project Report
for the Period July 1, 1989 through June 30, 1990

Including

the Quarterly Technical Progress Report
for the Period April through June 1990

by

Charles J. Moretti, David J. Hassett,
Debra Pflughoeft-Hassett, Gale G. Mayer
Daniel J. Stepan

University of North Dakota
Energy and Environmental Research Center
Box 8123, University Station
Grand Forks, North Dakota 58202

Contracting Officer's Technical Representative: Jerry Harness

for

United States Department of Energy
Office of Fossil Energy
Morgantown Energy Technology Center
Morgantown, West Virginia 26506

September 1990

Work Performed Under Cooperative Agreement No. DE-FC21-86MC10637

TABLE OF CONTENTS

LIST OF FIGURES

LIST OF TABLES

WASTE MANAGEMENT

1.0 INTRODUCTION

The objective of the Waste Management project is to characterize waste materials and by-products from advanced coal utilization processes, evaluate potential uses for these materials, and identify potential adverse environmental impacts associated with their use and/or disposal. Research is also being done to develop innovative waste management techniques for conventional and advanced coal utilization processes to comply with existing and/or future environmental regulations.

The activities of the Waste Management project include the following tasks:

Task 1. Activated Carbon Evaluation
Purpose - to evaluate the use of coal gasification char as activated carbon.

Task 2. Waste Characterization
Purpose - to characterize solid wastes from advanced coal utilization processes being developed at the Energy and Environmental Research Center (EERC).

Task 3. Coal Utilization Waste Conditioning Study
Purpose - to evaluate conditioning procedures for advanced coal utilization wastes.

Task 4. Bituminous Coal Fly Ash Data Collection and Evaluation
Purpose - to collect and evaluate data concerning the chemical and mineral compositions and physical properties of bituminous coal fly ash.

2.0 ACCOMPLISHMENTS

The following are the accomplishments of the Waste Management Project for the period July, 1989 to June, 1990.

2.1 Activated Carbon Evaluation

Based on a review of literature, several methods of characterizing activated carbons were selected for evaluation and methods development. These methods included determination of surface area, sieve analysis, iodine number, real density, apparent density, hardness number, abrasion number, and ash content. Selected methods were used to evaluate and verify the characteristics of four different commercially-available granular activated carbons. Results of these evaluations are described herein.

2.2 Waste Characterization

During the final quarter, the remaining chemical characterization leaching procedures were completed, as were the analyses of the resulting leachates. An as received unreacted limestone bed material was also chemically characterized. The results from this blank are provided for comparison to the spent bed materials under investigation in this task. The leaching procedures used for the chemical characterization of the limestone bed materials from the hydrogen production project and the limestone blank are as follows:

1. EPA-EP (1). The EPA-EP method is an U.S. EPA prescribed procedure which defines whether a solid waste is to be regulated as a hazardous waste under RCRA. The test is designed to simulate a municipal landfill where the presence of organic matter would presumably produce mildly acidic conditions due to the generation of acetic acid from the microbial degradation of cellulosic and other organic materials. The test uses dilute acetic acid as the leaching solution. A liquid-to-solid ratio of 20:1 is used in this test, with an equilibrium time of 24 hours and agitation on an orbital shaker. The test calls for the addition of 0.5 N acetic acid solution up to a limit of 4 ml/gm of ash to maintain a pH of 5.0.

2. Toxicity Characterization Leaching Procedure (TCLP) (2). This test is designed to provide information relevant to leaching in a sanitary landfill under codisposal conditions. This test will soon become the official EPA regulatory leaching test and will replace the EPA-EP toxicity procedure. The major changes are:

   A. End-over-end agitation.

   B. Addition of all of the acid at once as a dilute acetic acid solution, or as an acetate buffer, depending on the alkaline nature of the waste material being tested.

   C. An 18-hour equilibrium time instead of 24 hours.

3. The Synthetic Groundwater Leaching Procedure (SGLP) (3). The SGLP differs from the TCLP only in that the leaching solution is defined as whatever is appropriate to simulate the conditions the waste material is likely to encounter under natural disposal conditions. For this task distilled water was used as the leaching solution.

4. Long-Term Leaching (LTL). Long-term leaching tests are leaching tests over 48 hours in duration. The purpose of long-term leaching is primarily to allow time for secondary phase formation to, which has an effect on the concentrations of elements in the leachate, and to measure changes in concentration of analytes in leachates as slow, long-term reactions influence equilibrium conditions. Two LTL experiments were performed in a manner similar to the SGLP procedure, utilizing distilled water and an identical solid-to-liquid ratio. Duration of the first LTL experiment was one week. Duration of the second LTL experiment was 3 months.

The four limestone bed materials generated from the hydrogen production project have been fully characterized chemically and physically during the past year. Analytical results from chemical analyses were entered into a computer spreadsheet to facilitate evaluation of the chemical characterization portion of this task. Interpretation and evaluation of the analytical results were also completed during this quarter.

2.3 Ash Conditioning Study

A research study was conducted to determine the effects of conditioning moisture level on several disposal related properties of coal utilization wastes. The study was designed to determine the effect of various water addition levels on the compacted dry density, unconfined compressive strength, permeability coefficient, and trace element leaching potential of the wastes.

The wastes which were studied included a composite cyclone ash and baghouse fly ash from the Shawnee AFBC unit, an ESP fly ash from the Black Dog AFBC unit, a spent bed material from the KRW fluidized-bed gasifier, and a fly ash from a conventional cyclone-fired boiler burning a western subbituminous coal.

Activities conducted for the Ash Conditioning Study are as follows:

* The four coal utilization wastes were characterized to provide baseline elemental composition, mineral composition, and physical property data for the Ash Conditioning Study.

* Experiments were performed to determine the effects of varied moisture levels on the dry densities, unconfined compressive strengths, and permeability coefficients of the conditioned and compacted waste materials.

* Experiments were performed on the fly ashes to study the effects of varied moisture levels on the leaching behaviors of the conditioned and compacted wastes.

* The mineral transformations which occurred in the conditioned wastes were studied to determine the mechanisms which caused the observed increases in strength and reductions in permeability coefficient and leachate trace element concentrations.

* Optimal conditioning moisture levels were selected for the four coal utilization wastes based on the results of the experiments performed for the Ash Conditioning Study.

2.4 Bituminous Coal Fly Ash Data Collection and Evaluation

Identification of sources for bituminous coal fly ash information has been ongoing through the last quarter. The major effort has been to contact individuals or groups with access to the type of information desired, and request their participation in this task. Potential participants have been informed of the objectives of the task and have been sent packets detailing

the requested information. Additionally, these potential participants have been notified that information not available to them on specific bituminous fly ashes can be generated at our facility as part of this task.

The source lists for potential participants have been categorized to identify groups having bituminous coal fly ash information available and those agreeing or declining to participate.

Information and samples of bituminous coal fly ash have been received during the last quarter, and this information and corresponding samples have been cataloged for future input into the database.

The first year effort of this task has focused on the identification of sources of information on bituminous coal fly ash. A large number of contacts have been made by mail and telephone in an effort to identify potential participants, and this effort will continue through year two.

3.0 PROJECT TASK SUMMARIES

3.1 Activated Carbon Evaluation

3.1.1 Introduction

Activated carbons have many uses in industry. Most uses are associated with manufacturing and water purification, such as color removal in sugar manufacturing, drinking water treatment, and the removal of toxic or refractory compounds from waste streams. Additional uses are the removal of odorous compounds from industrial gas discharges and the adsorption of solvent vapor after air stripping of contaminated water.

Common materials utilized for the production of activated carbon include lignite and bituminous coals, wood, peat, heavy petroleum fractions, and waste materials from pulping. In the process of activation, the carbon materials acquire a high surface area that provides a high adsorption efficiency. Typical operations in the formation of activated carbons include devolatilization at approximately 1100°F, followed by activation with steam or carbon dioxide at around 1650°F to 1850°F. Activation results in weight loss in the range of 30 to 60%. The loss of weight follows the enlargement of pores during the oxidation that causes the increase in activation. Following activation, the carbon may be crushed, ground, grated, washed to reduce ash content, and dried.

The structure of activated carbon is believed to be that of a lattice crystal structure mixed with amorphous carbon, all of which are interspersed with micropores and macropores. Micropores are classified as pores having diameters from about 10 to 1000 angstroms. Macropores have diameters greater than 1000 angstroms. The function of macropores is to facilitate access to the smaller micropores where adsorption actually occurs.

Mild gasification is a developing coal conversion process that produces chars with a high potential for direct use as, or conversion to, activated

carbon. The main focus of this work is the characterization and evaluation of mild gasification chars, with and without activation, for use in wastewater treatment either as a competitive commercial product or as a cost-effective means of treating wastes generated during and from the mild gasification process.

3.1.2 Research Scope

The objective of this research task is to characterize and evaluate chars produced from the mild gasification of lignite for use in the commercial activated carbon market or for cost-effective treatment of wastes generated from the mild gasification process. This will be accomplished through characterization and evaluation of lignite char for direct use as activated carbon, and following varying degrees of activation.

3.1.3 Activated Carbon Evaluation Results

A review of the literature pertaining to methods of characterizing and evaluating activated carbons was conducted. Based on this review, the following methods were selected for laboratory evaluation:

(i) Surface Area
(ii) Sieve Analysis
(iii) Iodine Number
(iv) Real Density
(v) Apparent Density
(vi) Hardness Number
(vii) Abrasion Number
(viii) Ash Content

Surface Area - This is the amount of surface area per unit weight of carbon. It is determined from the nitrogen adsorption isotherm using the BET method.

Sieve Analysis - This is the distribution of particle sizes in a given sample and is obtained by mechanically shaking a weighed amount of material through a series of test sieves. Effective size, mean particle diameter, and uniformity coefficient can be determined by the interpolation of a cumulative particle-size distribution curve.

Iodine Number - This is the number of milligrams of iodine adsorbed by one gram of carbon at an equilibrium filtrate concentration of 0.02N iodine. It is measured by contacting a single sample of carbon with an iodine solution and extrapolating to 0.02N by an assumed isotherm slope. The iodine number can be correlated with the ability to adsorb low molecular weight substances.

Real Density - This is the density of the skeleton of a carbon particle. It is determined through helium displacement.

Apparent Density - This is the weight per unit volume of a homogeneous activated carbon. The density of a saturated activated carbon relative to the density of a regenerated carbon is used to indicate the degree of regeneration.

Hardness Number - This is a measure of the resistance of a granular carbon to the degradation action of steel balls in a pan on a Ro-Tap machine. It is calculated by using the weight of granular carbon retained on a particular sieve after the carbon has been in contact with steel balls.

Abrasion Number - This is a measure of the resistance of the particles to degrading upon being mechanically abraded. This value can be obtained by contacting the carbon sample with steel balls in a pan on a Ro-Tap machine. The abrasion number is the ratio of the final average particle diameter to the original particle diameter times 100.

Ash Content - This is the mineral content of the activated carbon. It is normally defined as a weight percent after a given amount of carbon has been reduced to ash.

Laboratory evaluations of selected methods were conducted on four commercially-available granular activated carbons which included: Calgon Filtrasorb 300 (F-300), Calgon Filtrasorb 400 (F-400), Hydrodarco 3000, and Hydrodarco 4000. Table 1 summarizes test results for commercially-available activated carbons, along with manufacturer's specifications.

Sieve analysis, giving the particle-size distribution of given samples, was obtained by shaking a weighed amount of activated carbon through a series of test sieves (1). Figures 1 through 4 illustrate particle-size distribution curves for the granular activated carbons, Calgon F-300, Calgon F-400, Hydrodarco 3000, and Hydrodarco 4000, respectively. As indicated in Table 1, with the exception of the Hydrodarco 4000 sample, all the activated carbon particle sizes fell within the specified range. The sample size larger than the No. 12 mesh for the Hydrodarco 4000 was 9.8 %, which is higher than the maximum 5%. Effective size and uniformity coefficients are determined using the particle-size distribution curves.

Effective size is the size of the particle that is coarser than 10% of the material, and was determined by interpolation of the particle-size distribution curve. Effective sizes were determined to be 0.85, 0.68, 0.90, and 0.65 for Calgon F-300, Calgon F-400, Hydrodarco 3000, and Hydrodarco 4000, respectively. These values are all within the ranges specified by the manufacturers.

Uniformity coefficient was obtained by determining the sieve opening (in millimeters) which pass 60% of the carbon sample, and dividing this by the sieve opening (in millimeters) which will pass 10% of the sample. Uniformity coefficients were calculated to be between 2.0 and 2.2 for all samples tested.

The mean particle diameter of an entire sample was computed by multiplying the weight of the fraction retained on each sieve by the corresponding mean sieve opening, summing those weighted values, and dividing by the total weight of material retained on the sieves and pan. Mean particle diameters were calculated to be 1.5, 1.1, 1.5, and 1.2 millimeters for Calgon F-300, Calgon F-400, Hydrodarco 3000, and Hydrodarco 4000, respectively.

TABLE 1

COMPARISON OF GRANULAR ACTIVATED CARBON CHARACTERISTICS

Parameter	Calgon Filtrasorb 8*30	Calgon Filtrasorb 12*40	Norit Hydrodarco 8*30	Norit Hydrodarco 12*40
Sieve Analysis (max %)				
Larger than No. 8	15.0 **7.7**	-- --	8.0 **1.5**	-- --
Larger than No. 12	-- --	5.0 **0.6**	-- --	5.0 **9.8**
Smaller than No. 30	4.0 **0.7**	-- --	4.0 **0.5**	-- --
Smaller than No. 40	-- --	4.0 **0.4**	-- --	5.0 **0.4**
Effective Size (mm)	0.8-1.0 **0.9**	0.55-0.75 **0.7**	0.8-1.0 **0.9**	0.6-0.7 **0.6**
Uniformity Coefficient	-- **2.1**	-- **2.1**	<1.9 **2.0**	<1.9 **2.2**
Mean Particle Diameter (mm)	-- **1.6**	-- **1.1**	-- **1.5**	-- **1.2**
Iodine Number (mg/gm)	900 **1010**	1000 **1150**	600 **625**	600 **610**
Real Density (gm/cm^3)	-- **1.94**	-- **1.85**	0.7-0.75 **1.72**	0.7-0.75 **1.87**
Apparent Density (kg/m^3)	-- **0.51**	0.48 **0.48**	0.4-0.42 **0.45**	0.4-0.42 **0.43**
Hardness Number (100 max)	-- **71**	-- **73**	-- **67**	-- **57**
Abrassion Number (%)	75 **71**	75 **73**	75 **60**	70 **52**
Ash Content (%)	0.5 **6.3**	0.5 **7.1**	-- **17.9**	-- **19.6**

Note: Bold values are results obtained at the EERC laboratories.

Figure 1. Particle size distribution curve-Calgon F-300.

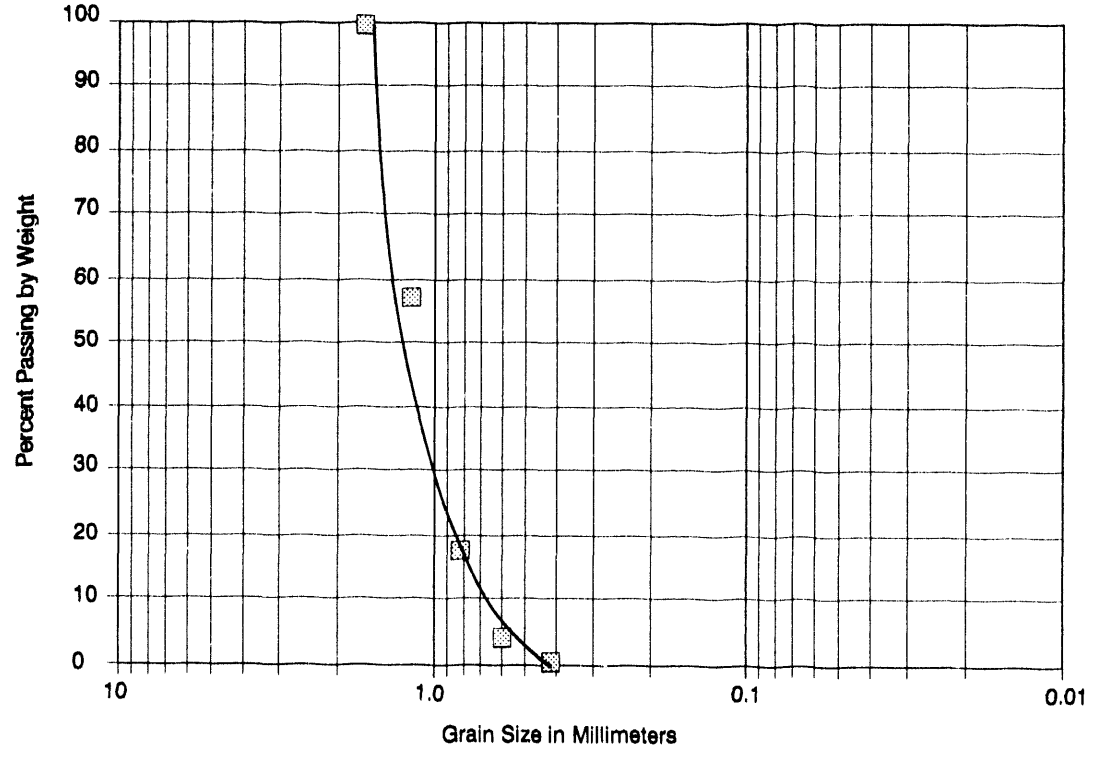

Figure 2. Particle size distribution curve-Calgon F-400.

Figure 3. Particle size distribution curve-Hydrodarco 3000.

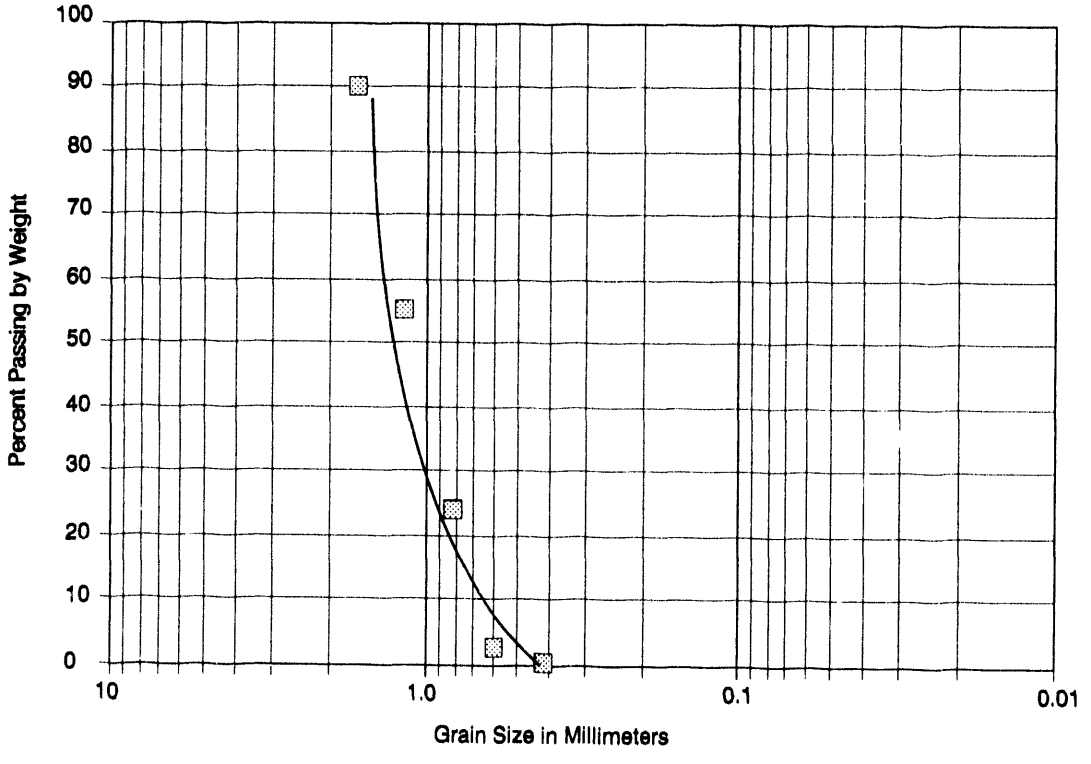

Figure 4. Particle size distribution curve-Hydrodarco 4000.

The iodine number is a relative indicator of the porosity of an activated carbon. It is measured by contacting the respective activated carbon samples with an iodine solution and extrapolating to 0.02N by an assumed isotherm slope (2). Figures 5 through 8 illustrate plots used in iodine number determinations for the various commercial activated carbons. Iodine number determinations for Calgon F-300, Calgon F-400, Hydrodarco 3000, and Hydrodarco 4000 yielded values of 1010, 1150, 625, and 610, respectively. The Calgon samples tested within 15% of the specified values, while the Hydrodarco samples were within 5%.

Real density describes the density of the skeleton of a carbon particle and was determined by helium displacement. It was measured as the mass of carbon per cubic centimeter of helium displaced, using a helium-air pycnometer (3). Real density determinations made at the EERC were approximately 2.5 times greater than the specified values for the activated carbons tested.

Apparent density is the weight per unit volume of a homogeneous activated carbon. A representative sample of granular activated carbon was added to a 100-ml graduated cylinder at a uniform rate, not exceeding 10 ml/sec, to obtain a maximum packing density. Test results for the commercially-available activated carbons tested were reproducible and were consistent with specified values (Table 1).

The hardness number is the resistance of activated carbon to degradation when subjected to the action of steel balls on a Ro-Tap machine (5). It is a measure of the resistance of a granular activated carbon to the effects of handling and carbon attrition. The GAC hardness number has no relation to the hardness scale used for plastics, metals, or minerals, and is used as a measurable characteristic for comparison to other activated carbons. Hardness number determinations for Calgon F-300, Calgon F-400, Hydrodarco 3000, and Hydrodarco 4000, yielded values of 73, 80, 66, and 56, respectively (Table 1). A hardness number of 100 indicates no degradation. The values obtained during hardness evaluations were all within 2% of calculated values used to check the accuracy of the results.

The abrasion number defines the resistance of carbon particles to degradation by the action of steel balls on a Ro-Tap machine. It is calculated as the percent change in mean particle diameter (6). The maximum abrasion number is 100. Abrasion numbers for Calgon F-300 and F-400 were determined to be 71 and 73%, respectively, within 5% of manufacturer's specifications. Abrasion number determinations for the Hydrodarco 3000 and 4000 samples resulted in values of 60 and 52, respectively, 20% lower than the manufacturers values.

3.2 Waste Characterization

3.2.1 Introduction

Wastes from advanced coal utilization processes being developed at UNDEERC are characterized for the selection of appropriate waste management techniques and to identify any significant or unusual problems associated with the advanced process wastes. The characterization protocol determines the

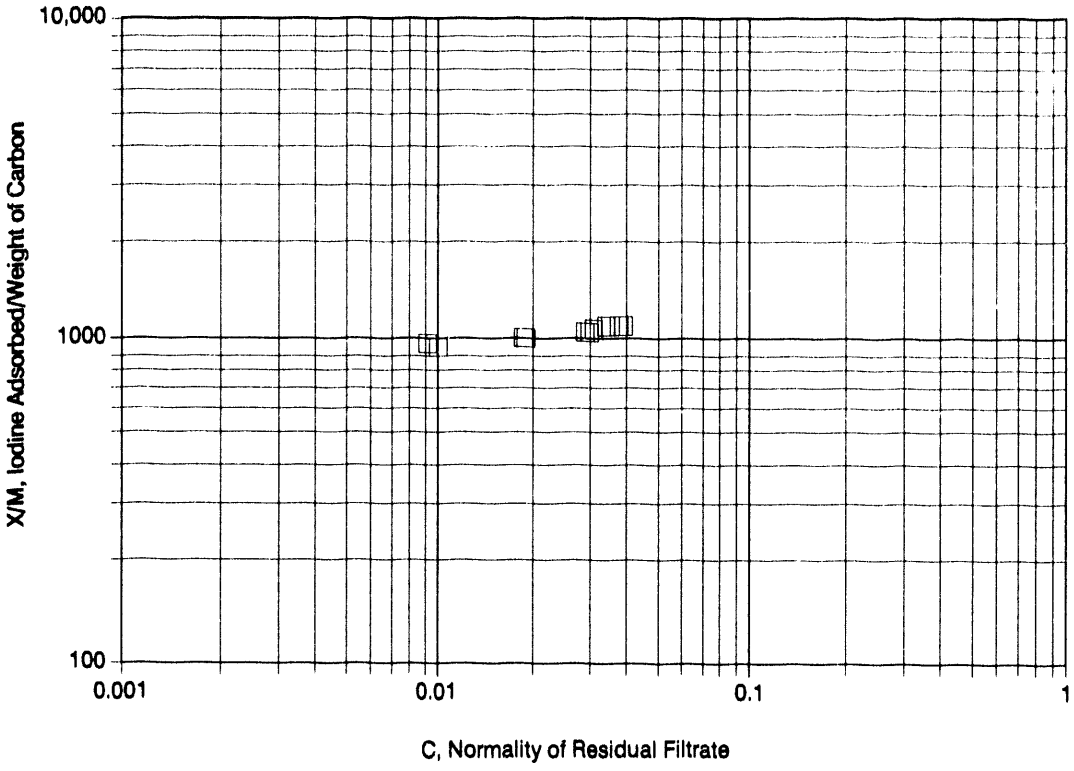

Figure 5. Iodine number determination-Calgon F-300.

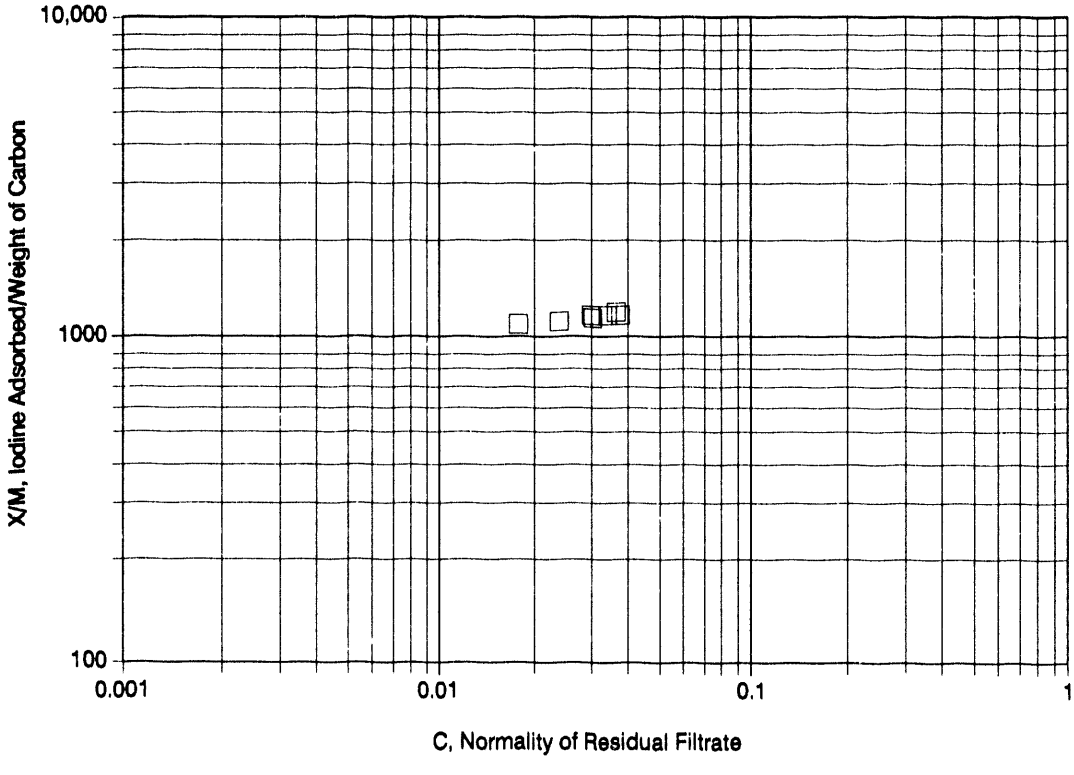

Figure 6. Iodine number determination-Calgon F-400.

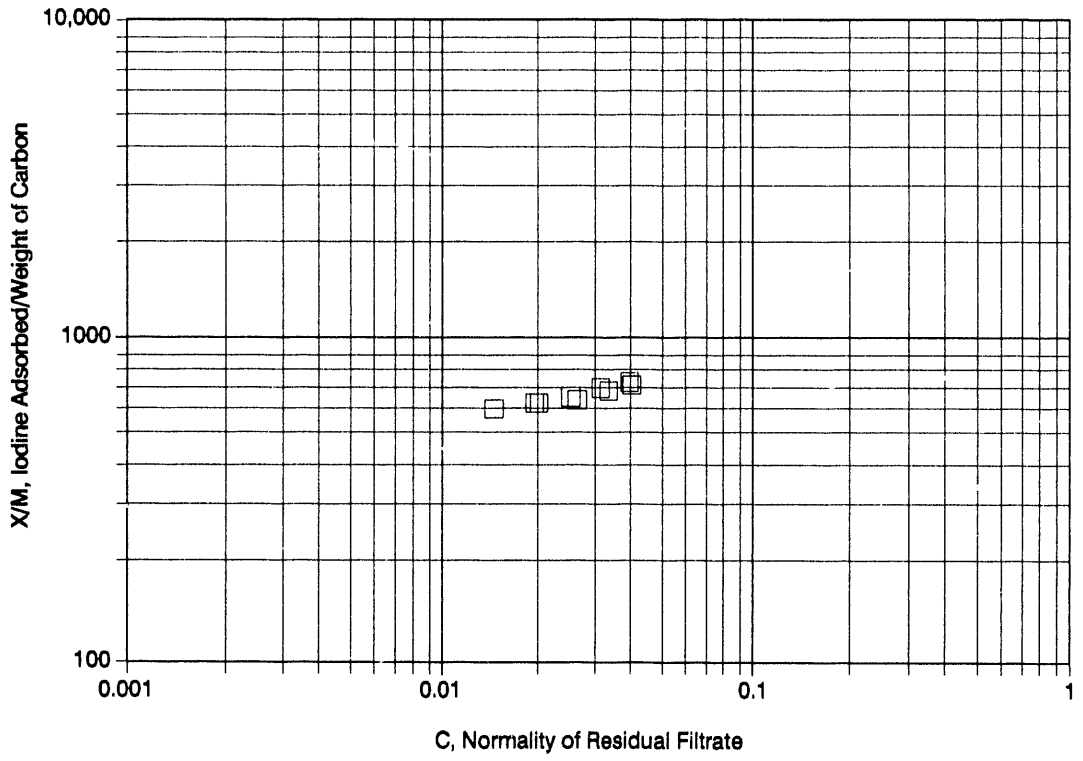

Figure 7. Iodine number determination-Hydrodarco 3000.

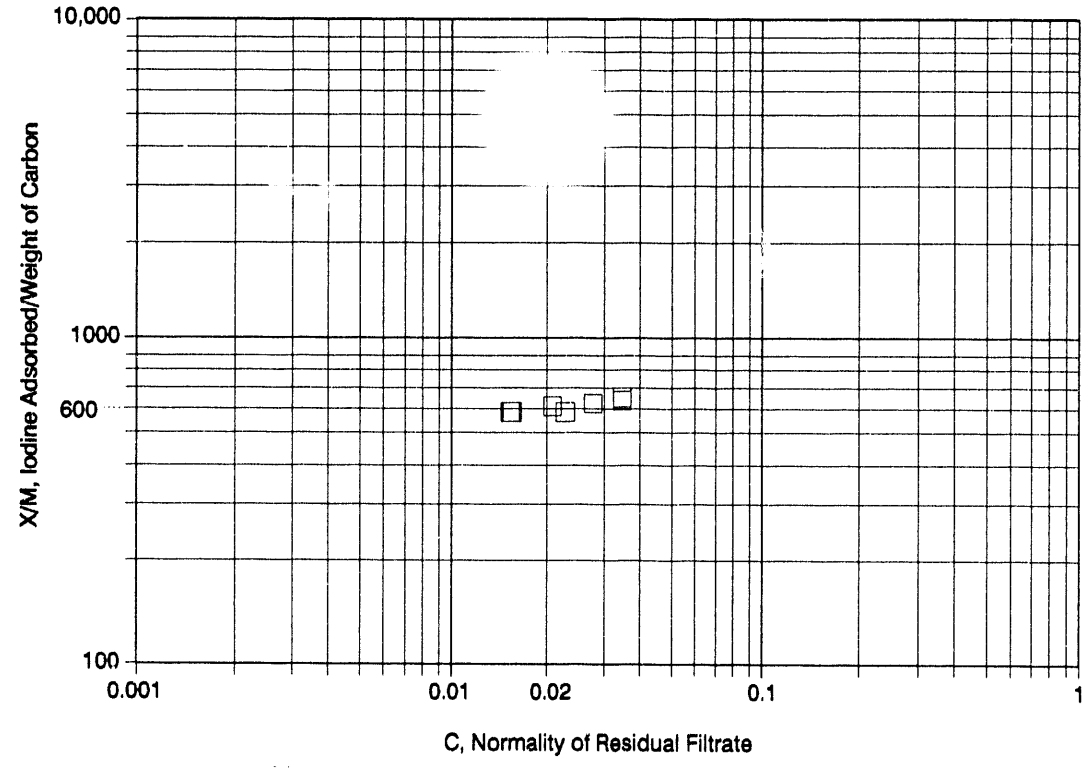

Figure 8. Iodine number determination-Hydrodarco 4000.

chemical and mineralogical composition, physical properties, and leaching behavior of the waste materials. The information obtained from the characterization studies can be used to assess the environmental impacts, handling properties, and utilization potential of the advanced process wastes.

3.2.2 Research Scope

The wastes to be characterized in this task will be obtained from ongoing coal utilization research at UNDEERC. Wastes considered for this task may include materials from the low-temperature coal gasifier and the circulating fluidized-bed combustor (CFBC). Emphasis for the waste characterization task for the current year is on limestone bed materials from the Hydrogen Production project.

3.2.3 Waste Characterization Results

The analytical results of the 3 month, long-term leaching experiments were completed for the identified characterization parameters listed in Table 2. Analytical results from these leaching experiments are included with the chemical characterization results in Appendix A.

The same chemical characterization procedures applied to the limestone bed materials generated by the hydrogen production project were applied to a limestone material that was not subjected to any treatment or combustion. This material was characterized chemically as a blank limestone material for comparison with the spent bed materials under investigation. The results of the characterization procedures for the blank limestone are also included in Appendix A.

The limestone bed materials generated by the hydrogen production project were fully characterized chemically and physically over the duration of this task. Complete physical characterization results are included in Table 3 and complete chemical characterization results are included in Appendix A.

TABLE 2

TRACE ELEMENTS SELECTED FOR CHARACTERIZATION STUDY OF BED MATERIALS

Designated RCRA Trace Elements	Trace Elements Identified by PIXE Screening
Arsenic	Copper
Barium	Maganese
Cadmium	Molybdenu
Chromium	Nickel
Mercury	Rubidium
Lead	Strontium
Selenium	Titanium
Silver	Zinc
	Zirconium

TABLE 3

PHYSICAL PROPERTIES OF HYDROGEN PRODUCTION BED MATERIALS

	6-W380L	10R-W180L	12R-W275L	14-W170L
Bulk Density (g/ml)	2.40	3.15	2.39	2/45
Exothermic?	Yes, very hot	Yes, but not immediate	Not noticeable	Not noticeable
Fineness (% retained #325 sieve)	105.24	132.92	118.45	119.13
Soundness (autoclave expansion %)	0.42	over	over	over
Specific Gravity	2.82	2.96	2.62	2.44
Water Requirement (% control)	133	125	113	114

6-W380L: Wyodak coal, reducing atmosphere, etc.

Chemical characterization results show the limestone bed materials to be non-hazardous according to the currently mandated regulatory leaching test, the EP Toxicity, and its soon to be replacement, the TCLP. Concentrations in the leachate for each bed material were determined to be below the hazardous limit as defined by RCRA and listed in Table 4.

Results from the SGLP and the long term leaching tests show these materials to be non-hazardous for the RCRA elements as well. The RCRA trace element concentrations in the SGLP leachate were well below the limits listed above. The concentrations of elements determined in the SGLP and the TCLP are quite different. This is important from the standpoint of interpretation of the regulatory leaching test. The use of results from the TCLP as predictive of leachate makeup for this type of material in a monofill would be misleading. The only valid use of the TCLP for any type of waste material in to simulate leaching under codisposal conditions in a sanitary landfill. Additional elements were determined in the various leachates generated. These results may be useful in the future as additional trace elements may be regulated or these materials may be investigated for potential utilization applications. These analyses indicated no additional elements at concentrations likely to present a future environmental problem.

3.3 ASH CONDITIONING STUDY

3.3.1 Introduction

Dry coal combustion wastes are usually non-cohesive materials which flow freely if not confined and are readily susceptible to dusting. Water is often mixed with these materials prior to ultimate disposal to increase cohesion, reduce dusting, and promote better compaction. This process is referred to as waste conditioning.

TABLE 4

RCRA ELEMENTS AND LEACHATE CONCENTRATION LIMITS

RCRA Element	Concentration Limit (mg/l)
Arsenic	5
Barium	100
Cadmium	1
Chromium	5
Lead	5
Mercury	0.2
Selenium	1
Silver	5

Conditioning of conventional fly ash usually involves the addition of between 10 and 15% water. For wastes from advanced processes, such as atmospheric fluidized-bed combustion (AFBC) using limestone addition for sulfur capture, conditioning accomplishes an additional function because the added water serves to hydrate the excess lime (CaO) created during combustion. Thus, for wastes that contain substantial amounts of unhydrated lime, a significantly higher conditioning water level may be required compared to conventional coal combustion wastes.

In addition to controlling dust and increasing compaction, the conditioning process can also affect the extent to which cementitious and pozzolanic reactions occur in the waste after it has been placed at the disposal site.

Cementitious reactions occur when compounds such as tricalcium aluminate, tricalcium silicate, and dicalcium silicate react with water and hydrate. As the hydrated compounds precipitate from solution, they tend to form a strong interlocking matrix that binds the ash particles together. Pozzolanic reactions occur when finely divided aluminate and silicate particles, such as fly ash, react with free lime and water to form adhesions between the particles. Both types of reactions can greatly increase the compressive strength of an ash after it has been placed at a disposal site.

Functionally, the principal difference between cementitious and pozzolanic reactions is the rate at which they occur. Cementitious reactions tend to occur faster than pozzolanic reactions. For example, cementitious reactions involving tricalcium aluminate may occur within a few minutes after the water has been added to the ash, while reactions involving dicalcium silicate and tricalcium silicate may take weeks or months to be completed. Pozzolanic reactions, however, tend to occur over a period of months or years after the ash has been placed at the disposal site.

In addition to increasing the compressive strength of the ash after placement at the disposal site, previous research has shown that cementitious and pozzolanic reactions tend to reduce the permeability coefficient and to immobilize toxic trace elements (10.) Thus the net result of the conditioning process, when it initiates cementitious and pozzolanic reactions, is to

decrease the environmental impact of the ash. If trace element leaching is reduced sufficiently, the need for including a liner and/or leachate collection system in the disposal site design could be eliminated, which would significantly reduce the ash disposal costs.

3.3.2 Objective and Scope

The objective of this research task is to develop effective conditioning methods for solid wastes from three different advanced coal utilization processes. To accomplish this, a laboratory testing program is being conducted to determine appropriate water addition levels for each waste to minimize their potential environmental impacts. The testing program is designed to determine the effect of various water addition levels on the compacted dry density, unconfined compressive strength, permeability coefficient, and trace element leaching potential of the wastes. The optimal water addition level for conditioning each waste will be selected to yield the highest dry density and compressive strength and the lowest permeability and leachate trace metal content.

The advanced process wastes being studied include a composite cyclone ash and baghouse fly ash from the Shawnee AFBC unit, an ESP fly ash from the Black Dog AFBC unit, and a spent bed material from the KRW fluidized-bed gasifier. All three wastes were produced from processes that used some type of limestone addition to the bed for sulfur capture.

The two AFBC units are both commercial plants. The Black Dog Plant is owned by the Northern States Power Company; it has a 125-MW generating capacity and burns western subbituminous coal. The Shawnee Plant is owned by the Tennessee Valley Authority; it has a 160-MW generating capacity and burns bituminous coal.

The KRW gasifier is a pilot-scale unit. It is being developed for integrated gasification combined cycle (IGCC) applications. The spent bed material being used for this study was obtained from a gasification run that used a Pittsburgh #2 bituminous coal.

In addition to the three advanced process wastes, a fly ash from a conventional cyclone-fired boiler burning a western subbituminous coal was included in the conditioning study. The fly ash was produced at the Riverside Plant which is owned by the Northern States Power Company. This ash was included in the study because it exhibits some of the same types of problematic behaviors as the advanced process wastes. Fly ashes from western subbituminous coals, for example, often display self-hardening and self-heating behavior. It was thought that if the behaviors of the Riverside fly ash and the advanced process wastes are fundamentally related, this would indicate that the conditioning procedures which have been developed for western bituminous coal fly ash may be successfully applied to advanced process wastes.

The laboratory testing plan for this study consisted of an initial characterization program to establish baseline elemental composition, mineral composition, and physical property data for the advanced process wastes and

the Riverside fly ash. Moisture-density tests were conducted to determine optimum moistures and maximum compacted dry densities. Based on the results of the moisture-density tests, sets of specimens were prepared for each waste to determine the maximum strength, minimum permeability, and minimum leachate trace metal contents as a function of conditioning moisture. The results of these tests were used to select an optimal moisture addition level for conditioning each waste.

3.3.3 Ash Conditioning Results

3.3.3.1 Ash Characterization

The bulk chemical compositions of the four wastes included in the ash conditioning study are listed in Table 5. The three advanced process wastes all had relatively high calcium and sulfur contents due to the fact that limestone was added to the Shawnee and Black Dog AFBC beds and the KRW gasifier bed for sulfur capture. The Riverside fly ash also had a high calcium content but this was due to the presence of calcium-bearing minerals in the coal rather than to an added sorbent.

The various mineral phases identified in the wastes are listed in Table 6. Lime (CaO) and Anhydrite ($CaSO_4$) were both major constituents in the Shawnee and Black Dog AFBC ashes. The lime was produced by calcination of limestone in the combustor bed, and the anhydrite was formed when lime reacted with SO_2 in the flue gas.

Some selected physical properties of the wastes are listed in Table 7. All four ashes contained little or no moisture as received from the different plants. The loss-on-ignition (LOI) measurements for the Black Dog and Shawnee AFBC ashes were relatively high compared to most conventional coal combustion ashes. However, high LOI in AFBC ashes is typical and it is usually caused by the loss of carbonate from unreacted limestone rather than the presence of unburned carbon. The negative LOI obtained for the KRW gasifier bed material was probably caused by the oxidation of sulfide during the LOI test. A significant amount of sulfide was definitely present in this waste, evidenced

TABLE 5

BULK CHEMICAL COMPOSITION

	Waste Type			
	Black Dog Fly Ash	Shawnee Fly Ash	KRW Bed Material	Riverside Fly Ash
Silicon Dioxide (SiO_2)	12.5	11.4	22.8	23.5
Aluminum Dioxide (Al_2O_3)	4.8	4.7	11.0	13.1
Iron Oxide (Fe_2O_3)	2.3	7.2	8.5	6.2
Calcium Oxide (CaO)	28.3	47.9	36.5	29.2
Sulfur Trioxide	16.8	13.8	19.2	8.4

TABLE 6

WASTE MINERAL COMPOSITION

	Waste Type			
	Black Dog Fly Ash	Shawnee Fly Ash	KRW Bed Material	Riverside Fly Ash
Major Mineral Phases	$CaSO_4$-Anhydrite CaO SiO_2	$CaSO_4$-Anhydrite CaO	CaS Mgo	$CaSO_4$-Anhydrite Ca Fe_3 O_5 $Ca_2MgSi_2O_7$-Akermanite
Minor Mineral PHases	$Ca(OH)_2$	SiO_2-Quartz $Ca_3Fe_2(SiO_4)_3$	SiO_2-Quartz	CaO MgO SiO_2-Quartz

TABLE 7

SELECTED WASTE PHYSICAL AND CHEMICAL PROPERTY DATA

	Waste Type			
	Black Dog Fly Ash	Shawnee Fly Ash	KRW Bed Material	Riverside Fly Ash
Moisture Content (wt%)	<0.01	0.15	0.04	0.26
Loss on Ignition (Wt%)	27.6	11.4	<0.01	4.7
pH of Ash Slurry[a]	11.9	12.4	11.9	11.5
Specific Gravity	2.20	2.78	2.69	2.68
Maximum Compacted Dry Density[b] (lbs/ft^3)	74	77	78	93.5
Optimum Moisture Content[c] (% Dry Wt)	35	30	25	4
Median Particle Diameter (Wt Basis)	15.1	26.8	1000	7.9
Specific Surface Area (m^2/cm^3)	0.68	0.45	ND	1.3

[a] 10 grams of ash were mixed with 500 ml of distilled-deionized water to determine the pH values.

[b] Ash specimens were compacted approximately 35 minutes after they were mixed with water.

[c] Optimum moisture content was measured by drying ash at 110°F.

ND A reproducible value could not be determined.

by a strong characteristic sulfide odor when the material was titrated with sulfuric acid. The oxidation of sulfide to sulfate can produce a negative LOI value because sulfate has a higher molecular weight than sulfide.

In order to obtain additional information about the chemical properties of the advanced process wastes, the ashes were mixed with water and titrated with sulfuric acid. These titrations provided valuable data about the buffering capacities and chemical compositions of the wastes.

The titrations were performed by mixing 10 grams of ash with 500 ml of distilled-deionized water and then stirring the mixture for 30 minutes to dissolve any readily soluble components. The mixtures were then titrated with 10% (by volume) H_2SO_4 to an endpoint pH of 2.0. As the acid was incrementally added to the mixture, the pH was allowed to equilibrate before more acid was added.

The titration curves for the four wastes are shown in Figures 9 through 12. The curves for the Shawnee and Black Dog AFBC ashes indicate that these materials contain large amounts of free lime as indicated by their high initial pH values and large buffering capacities in the 11-12 pH range. In contrast to the AFBC ashes, the Riverside fly ash contained little free lime. The Riverside fly ash, however, displayed a large buffering capacity in the pH range of 5.5 to 2.0. The titration curves generally indicate that the AFBC ashes have different gross chemical compositions, at least in terms of acid neutralizing components, compared to the Riverside fly ash. The titration of the KRW gasifier bed material liberated a strong odor of hydrogen sulfide, indicating the presence of calcium sulfide in the waste. This was expected, since sulfur capture in the gasifier bed occurs under reducing conditions. The results of the KRW waste titration indicated that the calcium sulfide content was 5 to 10 wt%.

The free lime contents of the three advanced process wastes were estimated from their titration curves. The Shawnee AFBC ash was found to contain about 28% free lime, the Black Dog AFBC ash was found to contain about 11% free lime, and the KRW gasifier bed material was found to contain about 2% free lime.

3.3.3.2 Self-Heating and Self-Hardening Behavior

The three fly ashes and the gasifier bed material studied for this task all released various amounts of heat when they were mixed with water. For the fly ashes, the temperature was measured periodically for 35 minute after the water was added. Both the Shawnee and Black Dog AFBC fly ashes reached a maximum temperature of 100°C shortly after the water was added. When the temperature reached 100°C noticeable amounts of steam were released from both AFBC fly ashes. The Riverside fly ash did not get as hot as the AFBC ashes; the maximum temperature measured for the Riverside fly ash was 62°C. The KRW gasifier bed material released a small amount of heat when it was mixed with water, but it was much less than that released by the fly ashes.

The self-heating tendencies of the Black Dog and Riverside fly ashes are illustrated in Figures 13 and 14. The figures show the maximum ash

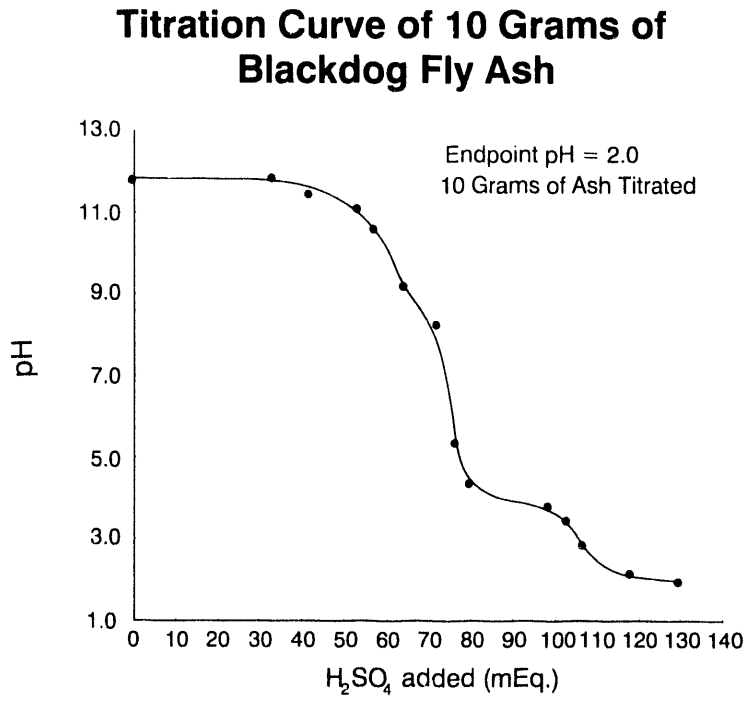

Figure 9. Titration curve of 10 grams of Black Dog AFBC.

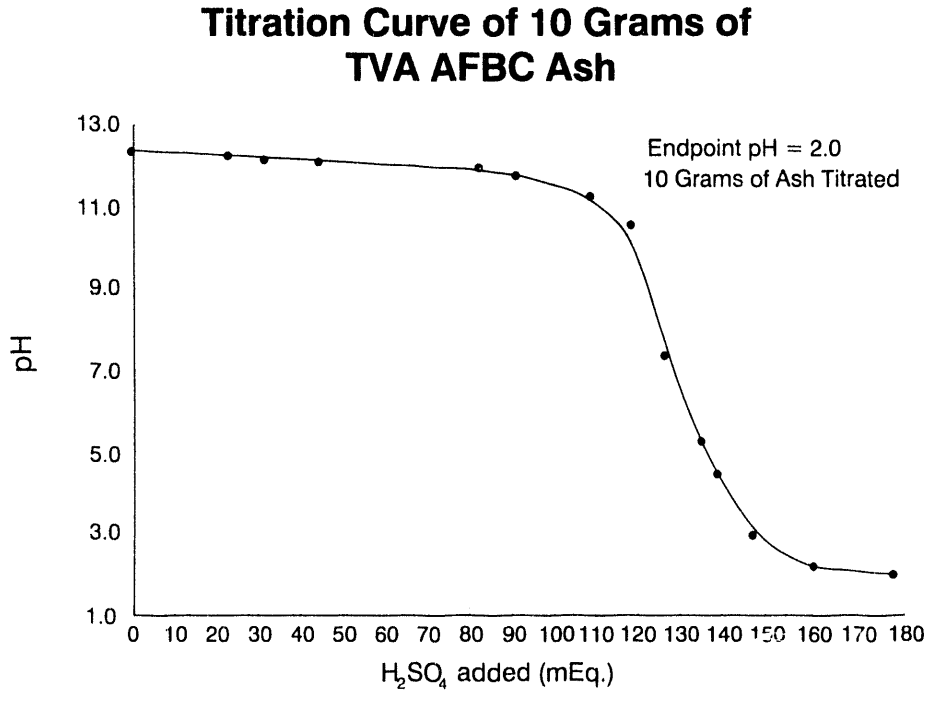

Figure 10. Titration curve of 10 grams of Shawnee AFBC Ash.

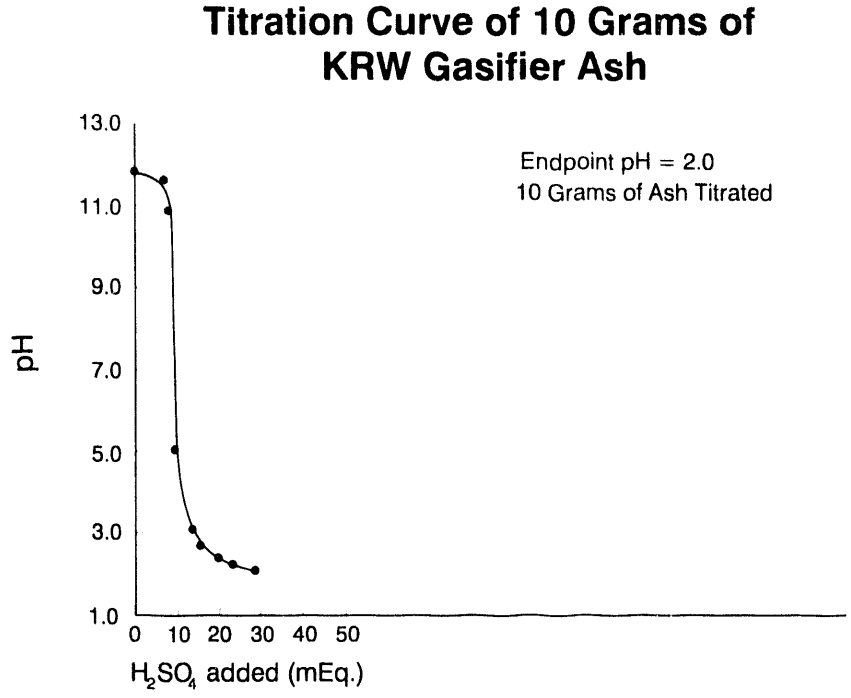

Figure 11. Titration curve of 10 grams of KRW spent gasifier bed materials.

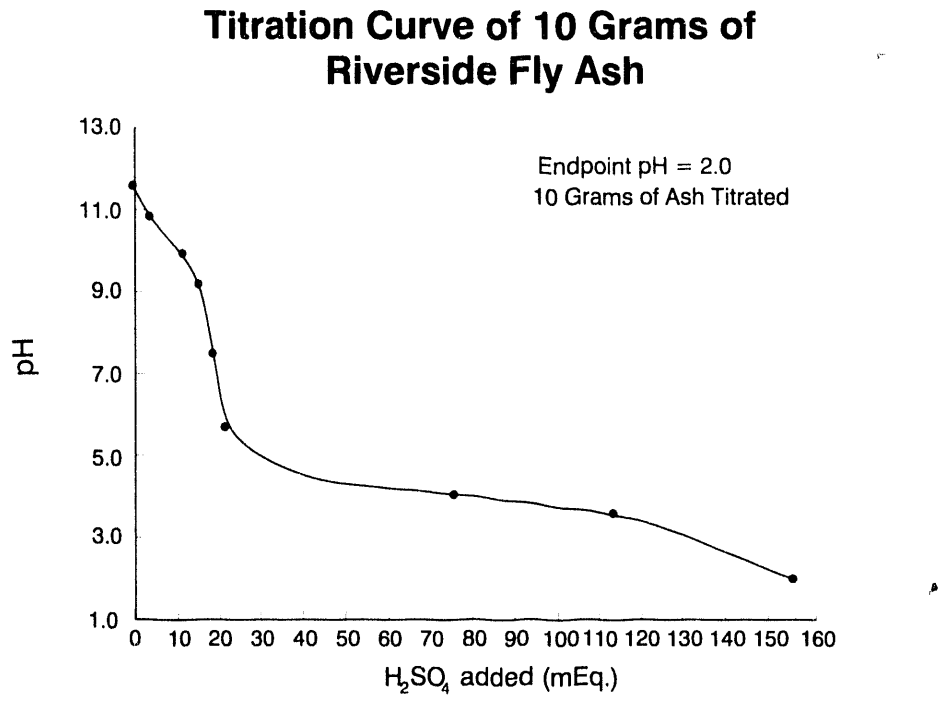

Figure 12. Titration curve of 10 grams of Riverside fly ash.

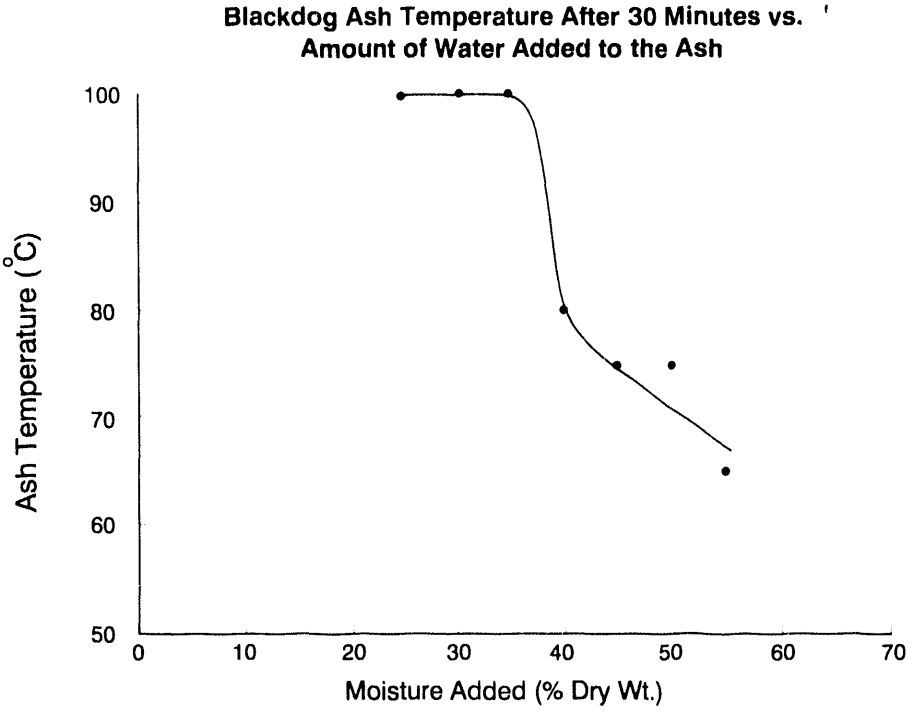

Figure 13. Maximum temperature of the conditioned Black Dog AFBC fly ash versus the amount of moisture added.

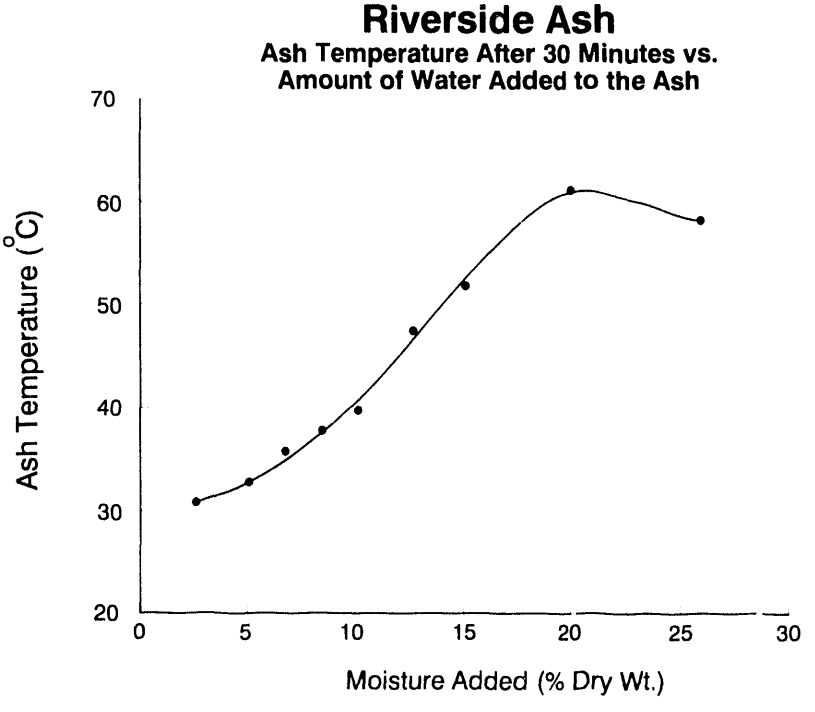

Figure 14. Maximum temperature of the conditioned Riverside fly ash versus the amount of moisture added.

temperature reached after conditioning as a function of the amount of moisture added. Figure 13 shows that when the amount of moisture added was less than 35% of dry weight, the Black Dog fly ash heated to 100°C (with an accompanying generation of steam). When the moisture added was greater than 35%, however, the maximum temperature decreased. Apparently the additional water absorbed enough of the liberated heat from lime hydration to keep the temperature below 100°C. The Shawnee fly ash acted much like the Black Dog fly ash except that its temperature reached 100°C even when the amount of moisture added ranged up to about 50% of dry weight.

The temperature curve for the Riverside fly ash (Figure 14) was quite different from the one obtained for the Black Dog fly ash (Figure 13). The Riverside fly ash showed a gradual increase in maximum temperature as the amount of conditioning moisture increased to about 20% of dry weight; above that level, the temperature decreased. The difference between the self-heating behaviors of the Black Dog and Shawnee AFBC fly ashes and the Riverside fly ash was probably due to the fact that the heat released from the AFBC fly ashes was caused by lime hydration, while the heat released from the Riverside fly ash must have resulted from hydration of other compounds, since no lime was detected in the Riverside fly ash.

All three of the fly ashes studied exhibited some degree of self-hardening behavior. The Riverside fly ash showed the greatest tendency to harden. It became quite stiff in a matter of minutes when it was mixed with about 15% water. The two AFBC fly ashes both stiffened when they were mixed with water and allowed to sit for 30 minutes, but it was fairly easy to remix these materials by hand after they had set up. The KRW gasifier bed material did not display any self-hardening behavior when it was mixed with water.

Some of the water added to the three fly ashes and the gasifier bed material appeared to have become chemically bound as a result of the conditioning process. This behavior is illustrated in Figures 15 and 16, which show the amounts of moisture initially added to the ashes and the amounts of moisture contained in the ashes after mixing and compaction. The difference between the moisture added and the moisture contained in the ash represents the water lost to either hydration reactions, evaporation, or steam release. For the Black Dog fly ash, the moisture loss (about 10%) was independent of the amount of moisture added, while for the Riverside fly ash, the moisture loss increased gradually to a maximum of about 10% as the amount of moisture added was increased. The Shawnee Fly Ash behaved similar to the Black Dog in terms of moisture loss.

Although the self-heating and moisture-loss relationships indicated by the conditioning tests appear well defined, caution must be used when applying this type of information to field disposal situations. The chief difference between laboratory tests and field conditions is the bulk quantities of ash handled. The small amounts of ash used for the laboratory tests may release heat more readily due to evaporation and steam generation than the large quantities of ash handled in the field. This means that ash handled in the field may stay hot longer and lose more moisture than the laboratory data indicates.

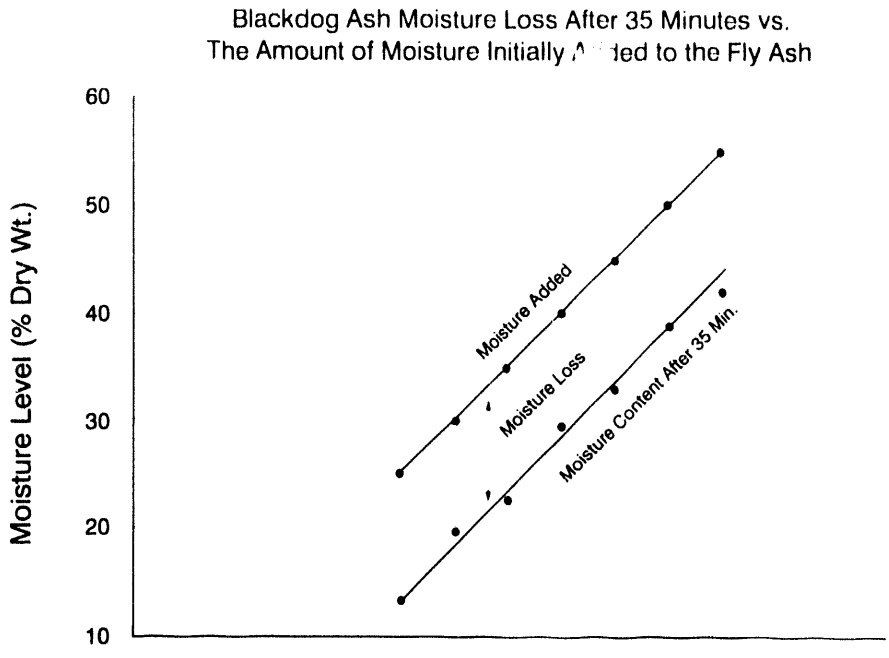

Figure 15. Comparison between the moisture content of the Black Dog AFBC fly ash and the amount of moisture added.

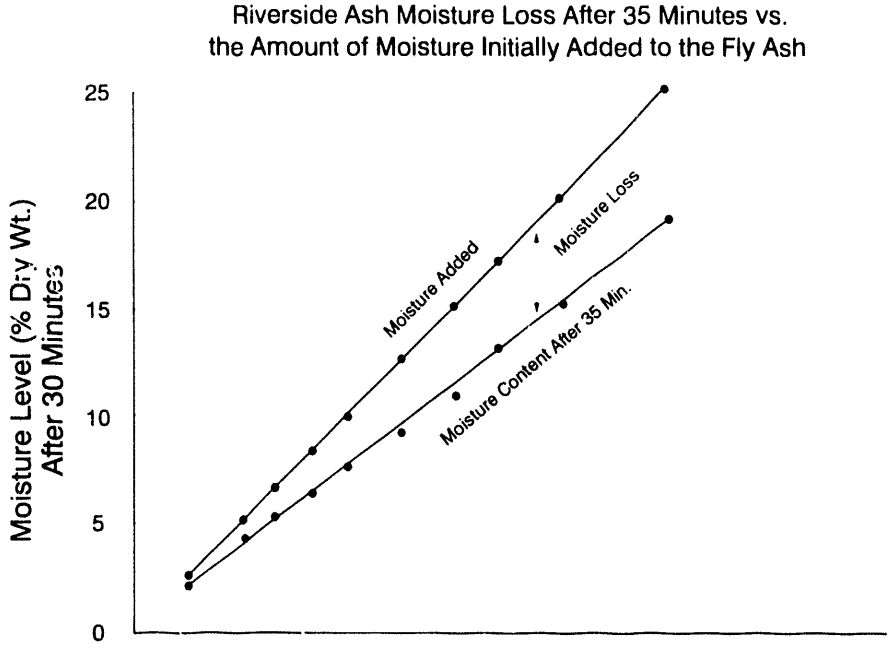

Figure 16. Comparison between the moisture content of the Riverside fly ash and the amount of moisture added.

3.3.3.3 Moisture-Density, Strength, and Permeability Tests

Moisture-density tests were performed on the Shawnee, Black Dog, and Riverside fly ashes and the KRW gasifier bed material. The tests were conducted in the laboratory by mixing the ash with different amounts of water using a paddle-type mixer, allowing the mixtures to stand for 35 minutes and then remixing by hand, preparing duplicate 1/30th ft^3 cylinders from each mix using standard Proctor compaction, then measuring the dry density and water content of the cylinders. The ash-water mixtures were set aside for 35 minutes to allow the materials to hydrate and cool somewhat before compacting. Since it would probably take at least 35 minutes to haul the conditioned ash to the disposal site and place it, this testing procedure was thought to be representative of in-field disposal conditions.

The ash cylinders prepared for the moisture-density tests were cured for 28 days at 70°F and then tested for unconfined compressive strength and coefficient of permeability. The purpose of these tests was to generate sufficient data to evaluate the relationship between the amount of conditioning moisture added to the ash and its compacted density, strength, and permeability.

The test results obtained from the Black Dog AFBC fly ash, mixed and compacted over a range of moisture contents, are presented graphically in Figure 17. For this fly ash, a maximum compacted dry density of 74 lbs/ft^3 occurred at an optimum moisture content of 35% of dry weight, a maximum unconfined compressive strength of 366 psi occurred at a moisture content of 42% of dry weight, and a minimum permeability coefficient of 1.2×10^{-6} cm/sec occurred at a moisture content of 44% dry weight.

A surprising feature of the Black Dog fly ash was that the permeability coefficient continued to decrease as the moisture content was raised to 8% age points above the optimum moisture (for maximum compacted density). An attempt was made to compact the ash with a moisture content above 44% of dry weight to see if the permeability would continue to decrease, but the compacted ash was so wet that it would not hold its shape after it was extruded from the mold.

The test results obtained from the Shawnee AFBC fly ash, mixed and compacted over a range of moisture contents, are presented graphically in Figure 18. For this fly ash, a maximum compacted dry density of 77 lbs/ft^3 occurred at an optimum moisture content of 30% of dry weight, a maximum unconfined compressive strength of 366 psi occurred at a moisture content of 30% of dry weight, and a minimum permeability coefficient of 3.9×10^{-6} cm/sec occurred at a moisture content of 35% of dry weight.

The results show that the Shawnee fly ash developed maximum strength and maximum compacted dry density at the same moisture content, while the minimum permeability was obtained when the moisture content was 5% age points higher. Comparing the results obtained for the two AFBC fly ashes, it is interesting to note that both fly ashes exhibited identical maximum compressive strengths and similar minimum permeability coefficients and maximum compacted densities. The optimum moisture content of the Black Dog fly ash was about 6% age points higher than the optimum moisture measured for the Shawnee fly ash, and this

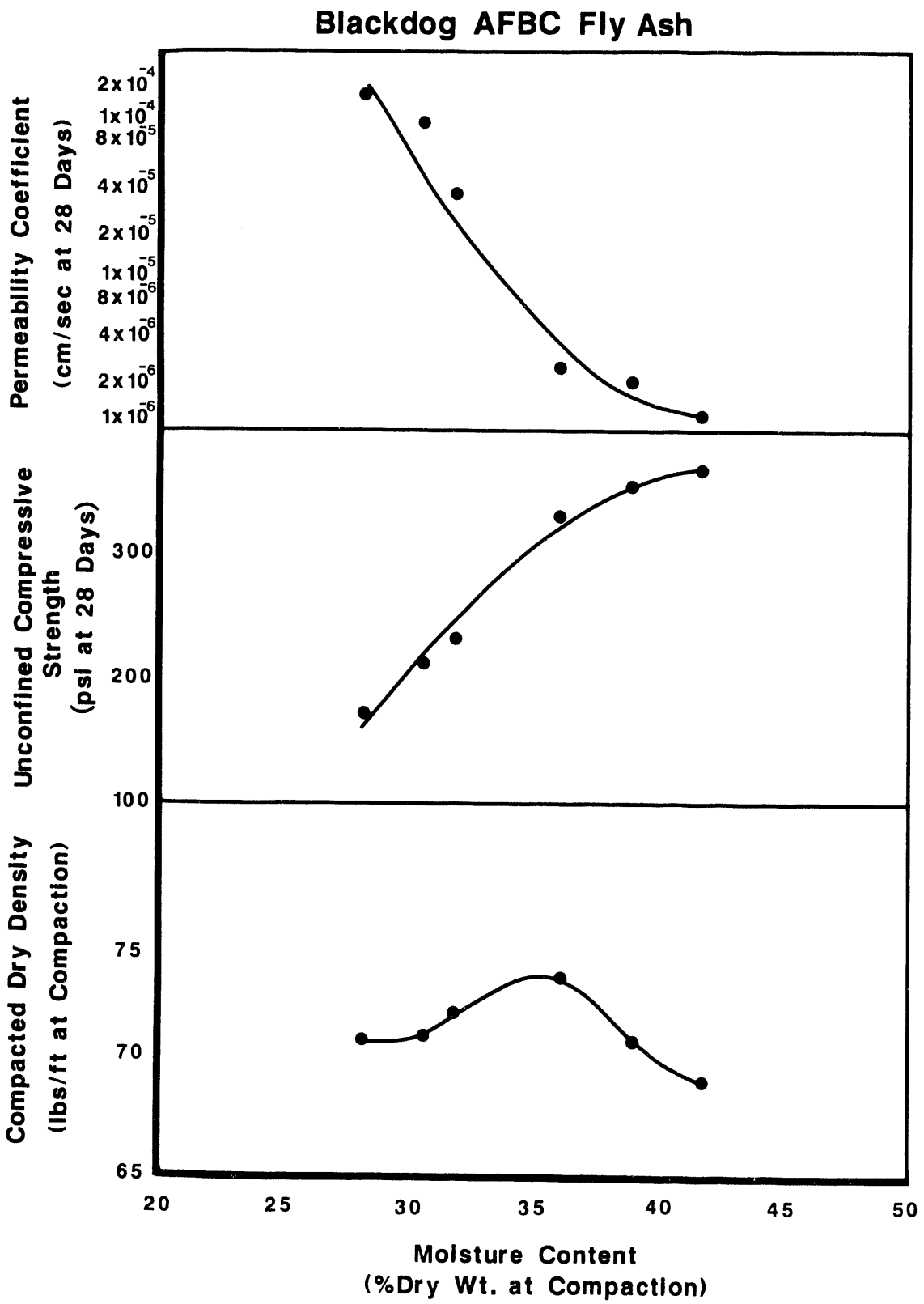

Figure 17. Density, strength, and permeability of the Black Dog AFBC ash as a function of moisture content at compaction.

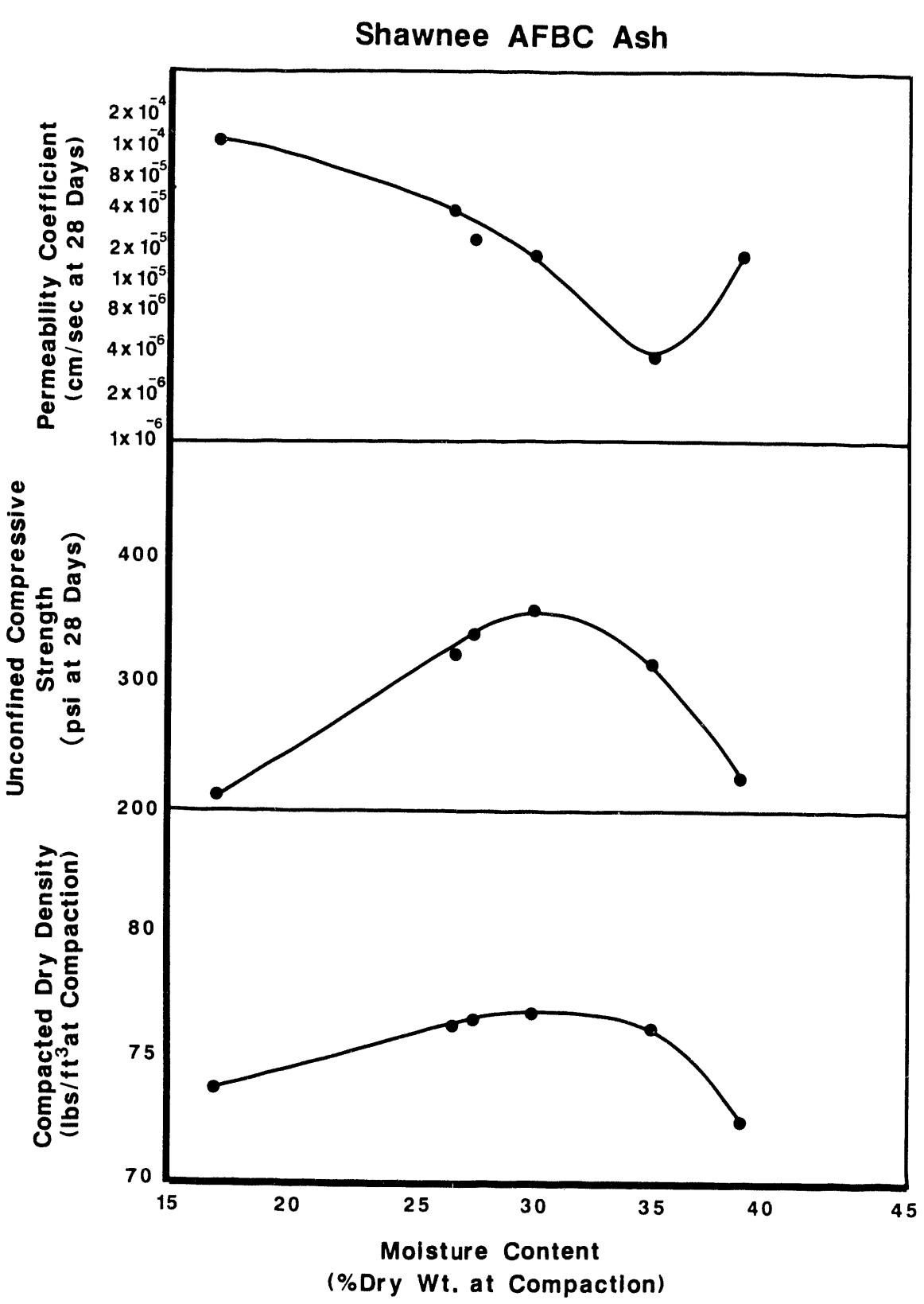

Figure 18. Density, strength, and permeability of the Shawnee AFBC ash as a function of moisture content at compaction.

difference was probably due to the fact that the Black Dog fly ash had a smaller mean particle diameter. Generally, the smaller the particles, the more moisture will be needed to achieve maximum compacted dry density.

The test results obtained from the Riverside fly ash, mixed and compacted over a range of moisture contents, are presented graphically in Figure 19. For this fly ash, a maximum compacted dry density of 93.5 lbs/ft^3 occurred at an optimum moisture content of 4% of dry weight, a maximum unconfined compressive strength of 430 psi occurred at a moisture content of 6.5% of dry weight, and a minimum permeability coefficient of 1.7×10^{-5} cm/sec occurred at a moisture content of 9% of dry weight.

The Riverside fly ash reacted differently to moisture addition than either of the AFBC fly ashes. This was because the Riverside fly ash showed a greater tendency to self-harden during the 35 minute period between mixing and compaction. As the Riverside fly ash hardened, it tended to change from an initially fine grained material into a coarser and less cohesive material. Further, as the moisture content was increased, the self-hardening behavior also increased and the material became more granular. This is why the dry density of the Riverside fly ash only decreased as the moisture content increased.

The test results obtained from the KRW gasifier bed material, mixed and compacted over a range of moisture contents, are presented graphically in Figure 20. For this material, a maximum compacted dry density of 78 lbs/ft^3 occurred at an optimum moisture content of 25% of dry weight. Since the gasifier bed material was composed of much larger particles than the three fly ashes studied, it did not "set up" to any significant extent during the 28 day curing period. For this reason, the cured bed material displayed much lower strengths and higher permeabilities than the fly ashes. Further, there was no trend observed toward development of a maximum strength or minimum permeability as a function of the change in moisture content as was observed with the fly ashes.

3.3.3.4 Leaching Tests

Leaching tests were performed on the compacted and cured fly ashes to evaluate the effect of conditioning moisture on the immobilization of trace elements. Leaching tests were not performed on the KRW gasifier bed material because the preceding tests had shown that this material was not chemically reactive to any significant degree, and therefore the conditioning process would not be expected to affect its leaching behavior.

The results of the leaching tests performed on the Black Dog and Shawnee AFBC fly ashes and the Riverside fly ash are contained in Tables 8, 9, and 10 respectively. Some of the leaching test results for selenium, barium, chromium, and molybdenum are plotted as a function of conditioning moisture content in Figures 21, 22, 23, and 24.

For the leaching tests, fragments from the cylinders used for the compressive strength tests were crushed and passed through a no. 16 sieve. Trace elements were then extracted from the sieved material using a generic

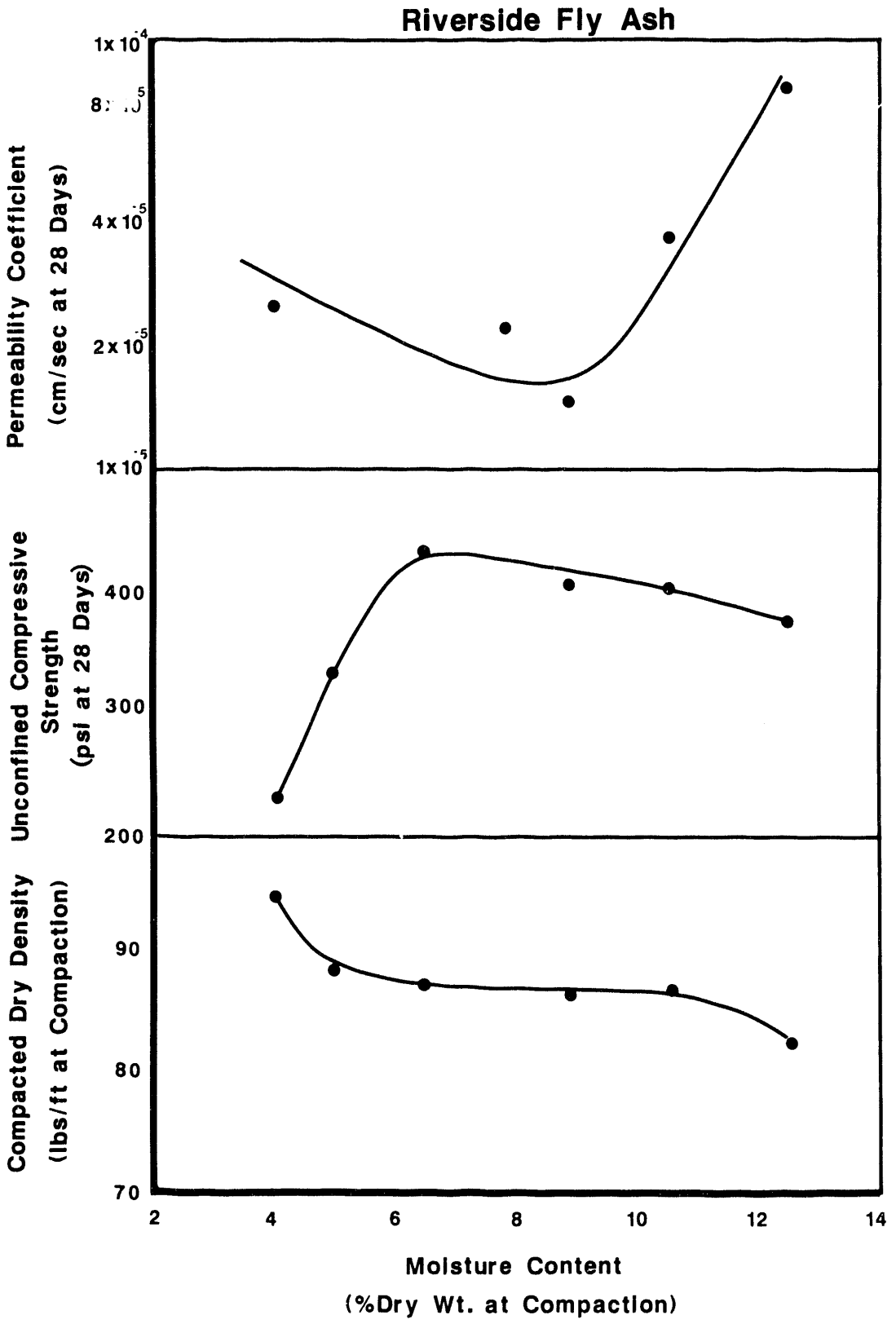

Figure 19. Density, strength, and permeability of the Riverside fly ash as a function of moisture content at compaction.

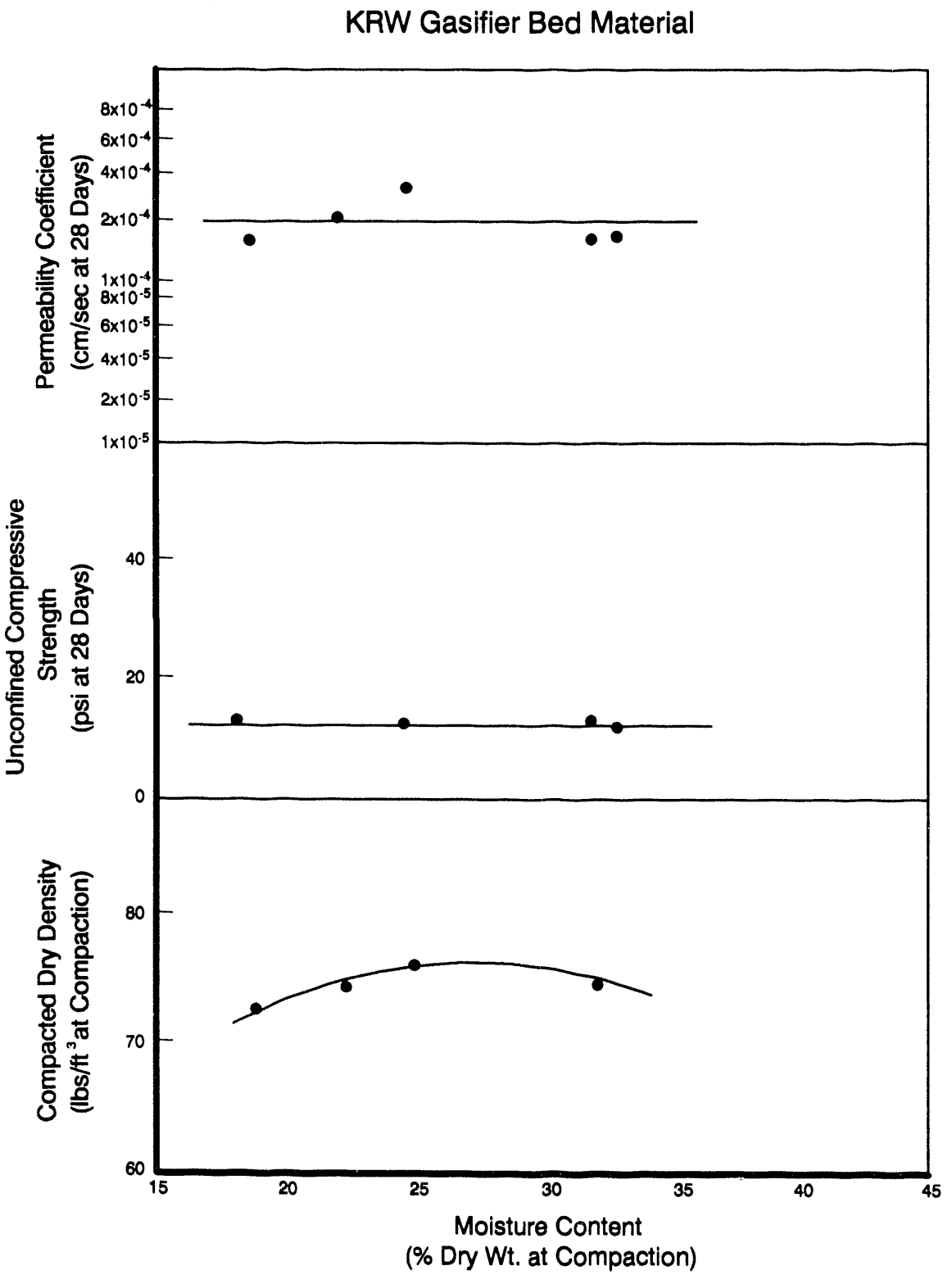

Figure 20. Density, strength, and permeability of the KRW gasifier bed material as a function of moisture content at compaction.

TABLE 8

LEACHING TEST RESULTS FOR THE CONDITIONED BLACK DOG AFBC ASH

	Specimen No.					
	1	2	3	4	5	6
Conditioning Moisture Assition Level (% Dry Wt.)	0.00	28.10	31.90	36.00	41.90	44.10
Leachage Arsenic Conc. (μg/l)	<2.00	<2.00	<2.00	<2.00	<2.00	<2.00
Leachage Barium Conc. (mg/l)	<0.02	0.28	0.26	0.23	0.23	0.25
Leachage Cadmium Conc. (mg/l)	<0.02	0.03	<0.02	<0.02	<0.02	<0.02
Leachate Chromium Conc. (mg/l)	<0.02	0.17	<0.02	0.08	0.08	0.13
Leachage Lead Conc. (μg/l)	<10.00	<10.00	<10.00	<10.00	<10.00	<10.00
Leachage Mercury Conc. (μg/l)	<0.60	<0.60	<0.60	<0.60	<0.60	<0.60
Leachage Selenium Conc. (μg/l)	6.80	<2.00	2.00	<2.00	<2.00	<2.00
Leachage Silver Conc. (μg/l)	<1.00	<1.00	<1.00	<1.00	<1.00	<1.00
Leachage Boron Conc (mg/l)	<0.50	<0.50	<0.50	<0.50	<0.50	<0.50
Leachage Molybdenum Conc. (mg/l)	0.39	0.37	0.42	0.49	0.40	0.39

TABLE 9

LEACHING TEST RESULTS FOR THE CONDITIONED SHAWNEE AFBC ASH

	Specimen No.					
	1	2	3	4	5	6
Conditioning Moisture Assition Level (% Dry Wt.)	0.00	17.00	26.40	29.80	34.60	39.20
Leachage Arsenic Conc. (μg/l)	<2.00	<2.00	<2.00	<2.00	<2.00	<2.00
Leachage Barium Conc. (mg/l)	0.20	0.22	0.22	0.20	0.20	0.20
Leachage Cadmium Conc. (mg/l)	<0.02	0.03	0.03	<0.02	<0.02	<0.02
Leachate Chromium Conc. (mg/l)	0.14	<0.02	0.12	0.08	0.08	0.12
Leachage Lead Conc. (μg/l)	<10.00	<10.00	<10.00	<10.00	<10.00	<10.00
Leachage Mercury Conc. (μg/l)	<0.60	<0.60	<0.60	<0.60	<0.60	<0.60
Leachage Selenium Conc. (μg/l)	8.50	3.80	4.50	2.90	2.90	2.50
Leachage Silver Conc. (μg/l)	<1.00	<1.00	<1.00	<1.00	<1.00	<1.00
Leachage Boron Conc (mg/l)	<0.50	<0.50	<0.50	<0.50	<0.50	<0.50
Leachage Molybdenum Conc. (mg/l)	0.17	0.14	0.24	0.11	0.11	0.20

TABLE 10

LEACHING TEST RESULTS FOR THE CONDITIONED RIVERSIDE FLY ASH

	Specimen No.					
	1	2	3	4	5	6
Conditioning Moisture Assition Level (% Dry Wt.)	0.00	4.10	5.10	8.90	10.60	12.60
Leachage Arsenic Conc. (μg/l)	<2.00	<2.00	<2.00	<2.00	<2.00	<2.00
Leachage Barium Conc. (mg/l)	0.91	0.73	0.37	0.46	0.28	0.08
Leachage Cadmium Conc. (mg/l)	<0.02	<0.02	<0.02	<0.02	<0.02	<0.02
Leachate Chromium Conc. (mg/l)	0.31	0.20	0.28	0.27	0.30	0.33
Leachage Lead Conc. (μg/l)	<10.00	<10.00	<10.00	<10.00	<10.00	<10.00
Leachage Mercury Conc. (μg/l)	<0.60	<0.60	<0.60	<0.60	<0.60	<0.60
Leachage Selenium Conc. (μg/l)	55.00	55.00	49.00	50.00	48.00	64.00
Leachage Silver Conc. (μg/l)	<1.00	<1.00	<1.00	<1.00	<1.00	<1.00
Leachage Boron Conc (mg/l)	<0.50	<0.50	<0.50	<0.50	<0.50	<0.50
Leachage Molybdenum Conc. (mg/l)	0.79	0.49	0.60	0.52	0.49	0.46

leaching test developed at EERC (the synthetic groundwater leaching procedure). Each leachate was analyzed for arsenic, barium, cadmium, chromium, lead, mercury, selenium, silver, boron, and molybdenum concentrations. The data thus generated were evaluated to determine whether a functional relationship existed between the moisture level used to condition the ash and the amounts of trace elements leached.

Based on the plots of the leaching data, several different types of functional relationships appear to exist between the leachate trace element concentrations and the conditioning moisture levels. In some cases, the addition of moisture and the curing of the compacted fly ash cylinders clearly did produce lower leachate trace element concentrations, while in a few cases, conditioning and curing actually produced higher trace element contractions. In those cases where trace element concentrations decreased, the data indicated that either the concentrations decreased continually as the moisture level increased or that the levels reached a minimum value at some intermediate moisture addition level.

The results of the leaching studies generally suggest that conditioning with moisture, compacting, and curing the fly ashes did affect their leaching behavior.

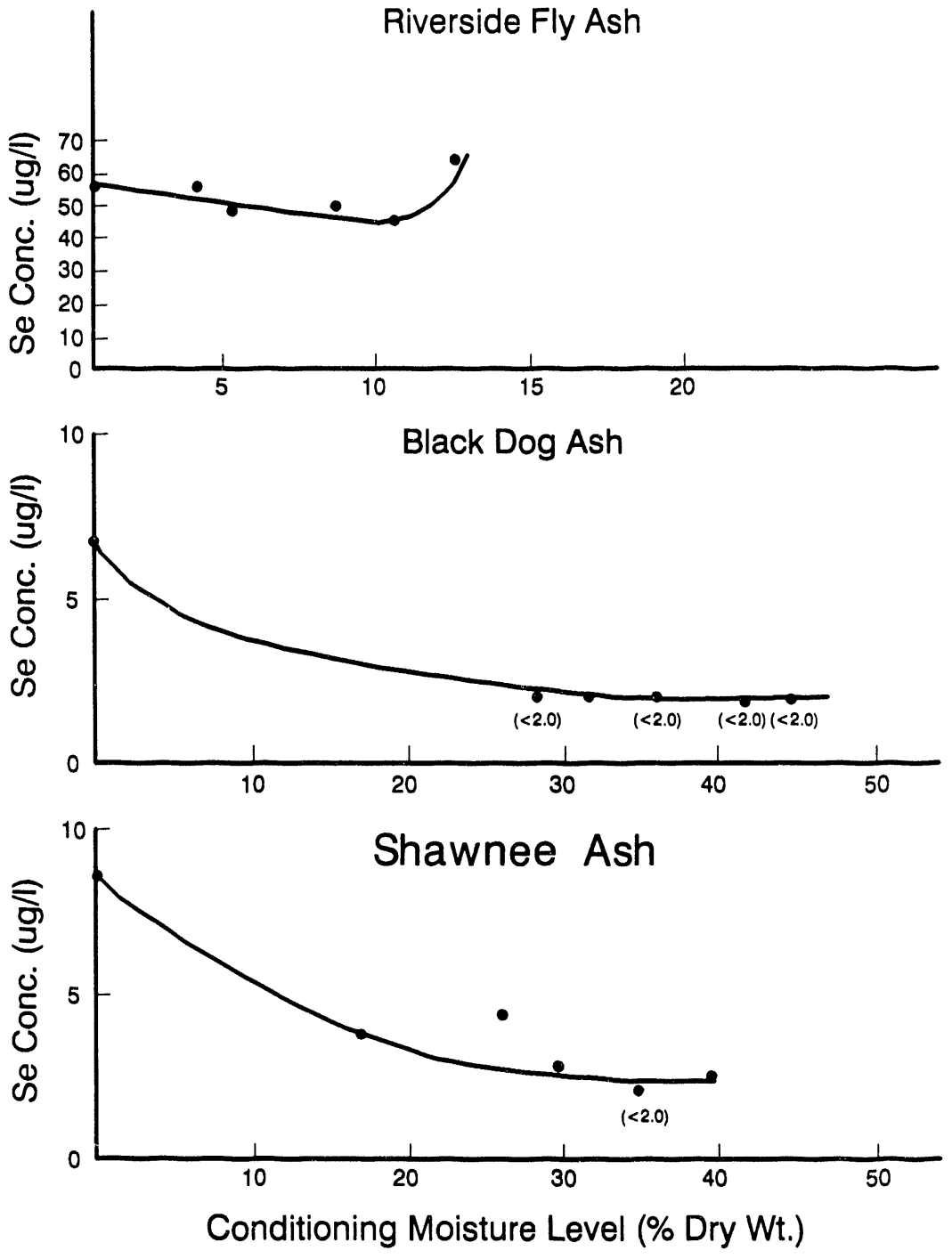

Figure 21. Leachate selenium concentration vs. conditioning moisture level for the Riverside, Black Dog, and Shawnee ashes.

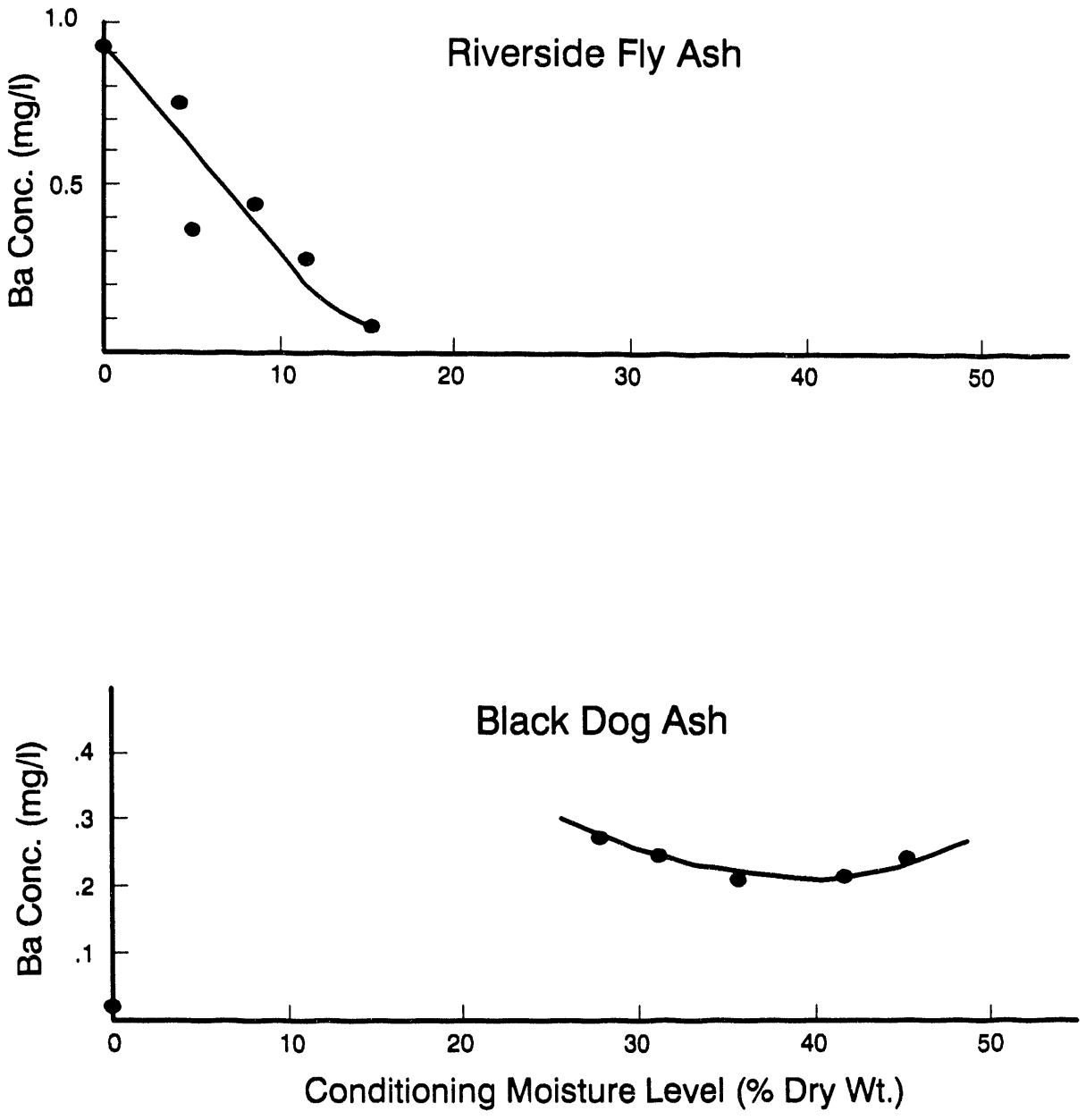

Figure 22. Leachate barium concentration vs. conditioning moisture level for the Riverside and Black Dog ashes. The Shawnee graph showed negligible data.

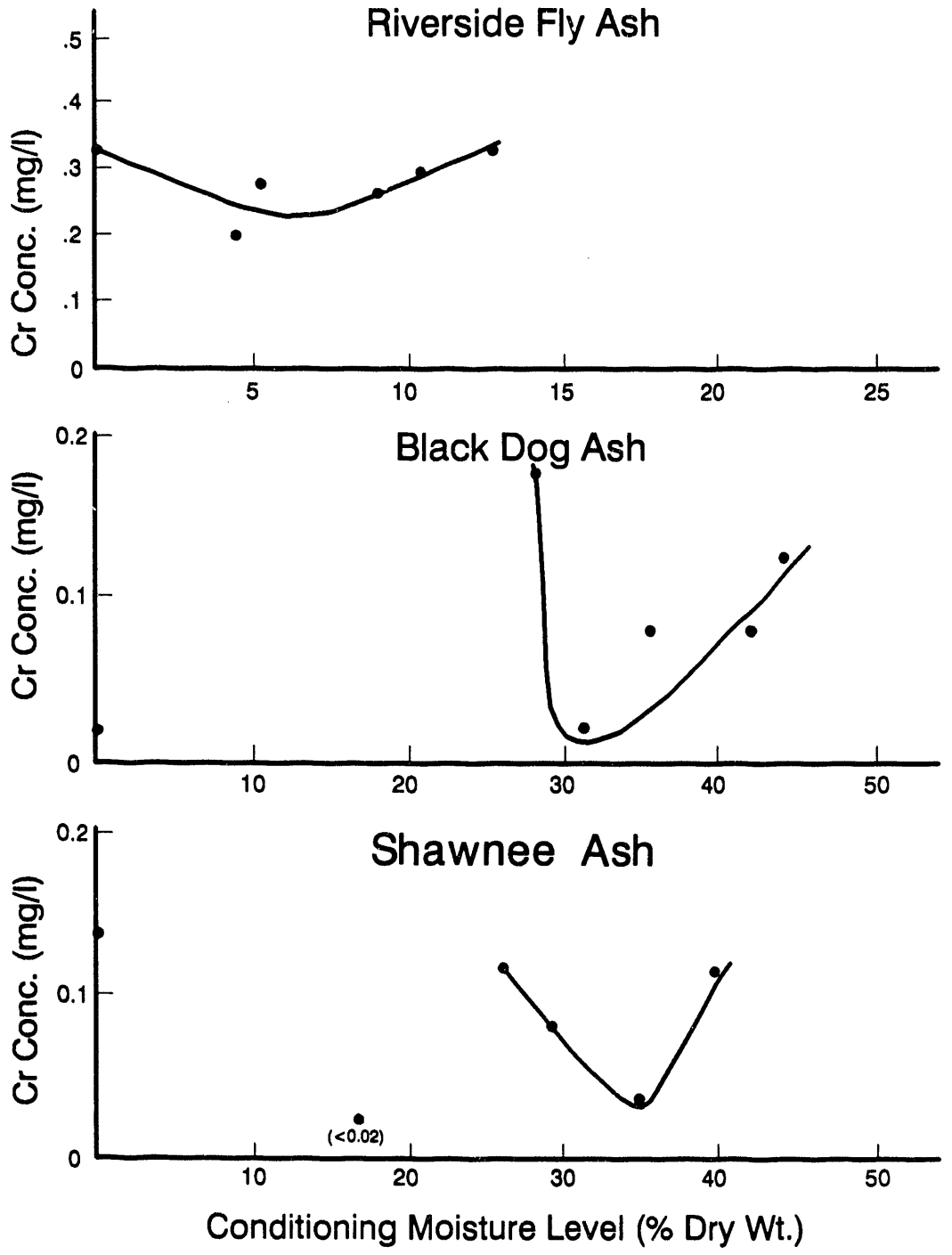

Figure 23. Leachate chromium concentration vs. conditioning moisture level for the Riverside, Black Dog, and Shawnee ashes.

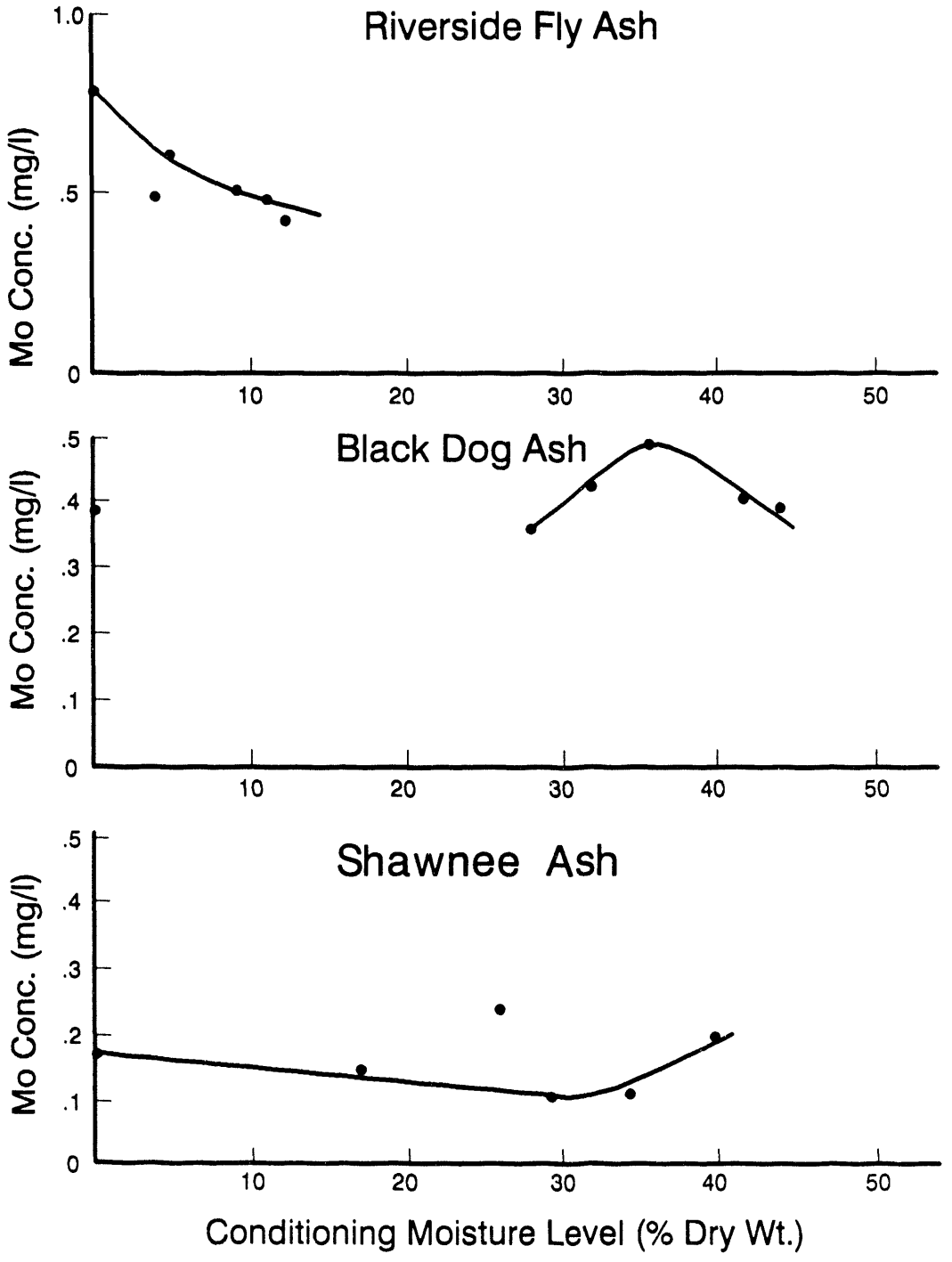

Figure 24. Leachate molybdenum concentration vs. conditioning moisture level for the Riverside, Black Dog, and Shawnee ashes.

3.3.3.5 Mineralogical Analysis

The mineral compositions of the four coal combustion wastes were analyzed before and after conditioning to determine the mineral transformations which may have caused the increased strengths, reduced permeabilities, and lowered leachate trace element concentrations observed for the Shawnee, Black Dog, and Riverside fly ashes. The mineral compositions were determined using X-ray diffraction analysis. The results of the analyses are listed in Table 11.

From the table it can be seen that significant transformations occurred in the mineral compositions of the Shawnee, Black Dog, and Riverside fly ashes after the materials were conditioned, compacted, and cured for 28 days. The general trend with these fly ashes was a change from relatively simple compounds such as lime and anhydrite to more complex mineral forms such as ettringite. Significant amounts of ettringite formed in all three fly ashes. In contrast to the mineral transformations observed with the fly ashes, the composition of the KRW gasifier bed material changed very little after conditioning.

In addition to the mineral phases listed in Table 11, it must be remembered that the Shawnee, Black Dog, and Riverside fly ashes also contained large amounts of amorphous glassy components which cannot be detected as distinct mineral phases because they do not have crystalline structures. Although not detected, the glassy components probably played a role in the mineral transformations brought about by the conditioning process. For example, it is probable that the aluminum in the ettringite phases, which formed in all three fly ashes after conditioning, was contributed from glassy components because there was no aluminum detected in any of the crystalline mineral phases prior to conditioning.

Since ettringite was the only major hydrated mineral phase formed in each of the three fly ashes after conditioning, it appears to be largely responsible for the observed self-hardening behavior. Ettringite is commonly produced during the hydration of Portland cement through a reaction between tricalcium aluminate and gypsum, and it is believed to contribute to the development of early strength in the cement paste. Other studies conducted with cementitious fly ashes have shown that when these materials are mixed with water, a mass of rod-like ettringite structures form, which bond the fly ash particles into a continuous matrix (11).

The ettringite formation caused by the conditioning process probably accounts for the increased strengths and reduced permeabilities observed with the Shawnee, Black Dog, and Riverside fly ashes due to the formation of interparticle bridges. Ettringite formation may also account for the observed reductions in the amounts of some trace elements which leached from these fly ashes. The immobilization mechanism is probably substitution of the trace elements into the ettringite molecular structure during compound formation. The leachate trace elements affected to the greatest extent by the conditioning process were selenium, chromium, and barium. If these elements were present in solution as negatively charged oxides, they may have simply been substituted for sulfate ions in the ettringite molecular structure, thereby reducing their concentration in the leachate.

TABLE 11

TRANSFORMATIONS IN MINERAL COMPOSITION RESULTING FROM ASH CONDITIONING

	Initial Mineral Composition	Mineral Composition after Conditioning
Shawnee AFBC Fly Ash		
Major Phases:	$CaSO_4$ - Anhydrite CaO - Lime	$Ca(OH)_2$ - Portlandite $Ca_6Al_2(SO_4)_3(OH)_{12}$ $26H_2O$-Ettringite
Minor Phases:	SiO_2 - Quar $Ca_3Fe_2(SiO_4)_3$	$CaSO_4$ $2H_2O$ - Gypsum $CaCO_3$ - Calcite SiO_2 - Quartz
Black Dog AFBC Fly Ash		
Major Phases:	$CaSO_4$ - Anhydrite CaO - Lime SiO_2 - Quartz	$Ca(OH)_2$ - Portlandite $Ca_6Al_2(SO_4)_3(OH)_{12}26H_2O$ - Ettringite
Minor Phases:	$Ca(OH)_2$ - Portlandite	$CaSO_4$ $2H_2O$ - Gypsum SiO_2 - Quartz $CaSO_4$ - Anhydrite
Riverside Fly Ash		
Major Phases:	$CaSO_4$ - Anhydrite $CaFe_3O_5$ Akermanite MgO - Periclase	$Ca_3Mg(SiO_4)_2$ - Merwinite $Ca_6Al_2(SO_4)_3(OH)_{12}$ $26H_2O$-Ettringite
Minor Phases:	SiO_2 - Quartz Ca_o -Lime MgO - Periclase	$Ca_2A_{12}SiO_7$ - Gehlenite SiO_2 - Quartz
KRW Gasifier Bed Material		
Major Phases:	CaS - Oldhamite MgO - Periclase	CaS - Oldhamite MgO - Periclase $Ca(OH)_2$ - Portlandite
Minor Phases:	SiO_2 - Quartz	

3.3.4 Summary and Conclusions

This research has demonstrated that the strength, permeability, and leaching behavior of the Shawnee, Black Dog, and Riverside fly ashes was profoundly affected by the ash conditioning process. Test results showed that conditioning with water followed by compaction and curing increased the strength, decreased the permeability, and reduced the amounts of certain leachate trace elements for all three of these fly ashes. Mineralogical

analyses of the conditioned fly ashes indicated that the formation of ettringite may have been the chief cause of the altered properties of the materials.

The KRW gasifier bed material was affected to a much lesser extent by the conditioning process than the fly ashes. This was probably due to the fact that the KRW bed material was much less chemically reactive when mixed with water compared to the fly ashes and that no ettringite formed in the conditioned KRW gasifier bed material.

All of the data generated for the ash conditioning study was examined in order to select the best moisture levels for conditioning the Shawnee, Black Dog, and Riverside fly ashes, and the KRW gasifier bed material. The factors which were used to select a specific moisture level for conditioning each ash included the effects of moisture content on the compacted dry density, unconfined compressive strength, minimum permeability coefficient, and leachate trace element concentrations for each material. Since all of these factors were usually not optimized at one particular moisture level, it was necessary to trade off between the different factors to arrive at a single moisture level which produced the best combination of effects in the conditioned ashes.

The optimized conditioning moisture levels selected for the three fly ashes and the gasifier bed material are listed in Table 12. The suggested moisture content for each material is the level present after the ash or bed material has been conditioned and compacted. The second column in the table is the amount of moisture which must be initially added to each material to achieve the suggested moisture content allowing for moisture loss due to hydration, evaporation, and steam generation. It must be noted that the levels of added moisture were determined in the laboratory on relatively small amounts of material. In the field, the amount of moisture which must be added to the waste to achieve the suggested moisture content may be significantly higher due to the fact that more evaporation may occur.

TABLE 12

OPTIMIZED CONDITIONING MOISTURE LEVELS

Waste Type	Suggested Conditioning Moisture Content (% Dry Wt.)	Moisture Added to Achieve Suggested Content (% Dry Wt.)
Shawnee AFBC Fly Ash	30	53
Black Dog AFBC Fly Ash	35	49
Riverside Fly Ash	6	8
KRW Gasifier Bed Material	25	30

For the Shawnee AFBC fly ash, the suggested conditioning moisture content of 30% of dry weight was selected because it produced the maximum compacted dry density and maximum unconfined compressive strength. It also produced significant reductions in the amounts of selenium and chromium which leached from the ash.

For the Black Dog AFBC fly ash, the suggested conditioning moisture content of 35% of dry weight was selected because it produced the maximum compacted dry density, a significant increase in the unconfined compressive strength, and a significant reduction in the permeability coefficient. The moisture also reduced the amount of selenium that leached from the ash.

For the Riverside fly ash, the suggested conditioning moisture content of 6% of dry weight was selected because it produced the maximum unconfined compressive strength, a relatively high compacted dry density, and some reduction in the permeability coefficient. This moisture level also produced reductions in the amount of barium which leached from the ash. If a 6% moisture content is not sufficient to control dusting of the fly ash at the plant, it may be necessary to increase the moisture content to the more typical range of 10% to 15%.

For the KRW gasifier bed material, the suggested conditioning moisture content of 25% of dry weight was selected because it produced the maximum compacted dry density. Since this material was not reactive, there were no increases in strength or reductions in permeability observed at any of the moisture levels tested.

3.4 Bituminous Coal Fly Ash Data Collection and Evaluation

3.4.1 Introduction

The objectives of the coal fly ash research during the first year were to identify and evaluate bituminous coal fly ash data. The effort for the second and third years of the project will be to collect and characterize samples of bituminous coal fly ash according to characterization protocols developed under the Western Fly Ash Research, Development, and Data Center and to expand the existing data base on western coal fly ashes to include information on bituminous coal fly ashes gained through this task.

3.4.2 Research Scope

Chemical, mineralogical, and physical characterization information on bituminous coal fly ashes from varying sources will be obtained and added to an existing coal fly ash data base currently containing information on over 500 western coal fly ashes. The information will be collected from voluntary participants who generate or market bituminous coal fly ash, or other research groups having access to this type of information. If sources of information being sought are inadequate, the information will be supplemented by characterization of submitted samples at the EERC Coal By-Products Laboratory and the NDSU Chemistry Department.

The addition of this information to the current Western Fly Ash Data Base will facilitate basic understanding of the character of bituminous coal fly

ash and the variability of the material. This information will be valuable in current and future coal ash research.

3.4.3 Bituminous Coal Fly Ash Data Collection and Evaluation Results

During the last quarter, several new participants for the bituminous coal fly ash data base have been identified and sent the appropriate information to facilitate their participation. Information on bituminous coal fly ash and corresponding bituminous fly ash samples have been received and cataloged for future reference.

The first years effort for this task has focused on determining the availability of information of interest on bituminous coal fly ash. As a result of this effort, it has been determined that physical and chemical ASTM testing has been generated by ash producers and marketers on bituminous coal fly ashes either being disposed or utilized, but that this information may not be generally available. Mineralogical characterization information and trace element characterization is generally not available. Additionally, information on the generation and collection of the bituminous coal fly ash samples, although generally available, must be specifically requested as it is not generally considered of importance for disposal or utilization purposes. This is extremely unfortunate since a complete history of ash formation, collection, and disposal is essential to a thorough scientific understanding of related phenomena such as leachate generation and the formation of secondary hydrated phases. Especially important is this phenomenon of secondary hydrated phase formation. It is now generally recognized that there exists a potential for ash to react with water in the environment and form mineralogical phases not present in the original ash. The implication of this is that over an extended period of time (months - years) ash may form phases that change the chemical makeup of leachate thus, producing leachate of a chemical composition quite dissimilar to laboratory produced leachate generated in short term leaching tests. It has been very important in contact with potential participants for this task to emphasize that information included in this data base will not be traceable to a specific power generation facility, company, or marketer, thus guaranteeing the anonymity of participants.

The effort to identify additional participants will continue throughout the upcoming year. Samples and information that are received will be cataloged and stored for future use.

4.0 REFERENCES

1. "Standard Test Method for Particle-size Distribution of Granular Activated Carbon," ASTM D2862-82, pp. 324-325 (1987).

2. "Standard Test Method for the Determination of Iodine Number of Activated Carbon," ASTM D4607-86, pp. 378-382.

3. Instruction Manual, Model 1302/1303 Helium-Air Pycnometer, October, 1976.

4. "Standard Test Method for Apparent Density of Activated Carbon," ASTM D2854-83, p. 321.

5. "Standard Test Method for Ball-Pan Hardness of Activated Carbon," ASTM D3802-79, pp. 350-352. (1986).

6. "Process Design Manual for Carbon Adsorption," USEPA Technology Transfer, P.B7, October, 1973.

7. U.S. Environmental Protection Agency, Federal Register, 45 (98) 33121-33133 (May 19, 1980), ISSN 0097-6326.

8. U.S. Environmental Protection Agency, Federal Register, 51 (9) 1750-1758 (January 14, 1986), ISSN 0097-6326.

9. American Society for Testing and Materials, 1983 Annual Book of ASTM Standards - Water and Environmental Technology, Part 31, p. 1258 (1979).

10. Moretti, C.J., "Development of Fly Ash-Based Liner Materials for Waste Disposal Sites", Topical Report Submitted to the U.S. Department of Energy by the University of North Dakota Energy and Environmental Research Center, November 1989.

11. Diamond, Sidney, "Hydration Reactions of C_3A Contained in an Unusual Flyash," U.S. Department of Energy, DOE/CS/40222--2, 1979.

APPENDIX A

Limestone Bed Materials from Hydrogen Production
Chemical Characterization

Sample Number	6-W380L	6-W380L	6-W380L	6-W380L	6-W380L	6-W380L	6-W380L
Temp (Ave.)	801.70	801.70	801.70	801.70	801.70	801.70	801.70
Steam/C (Ave.)	3.41	3.41	3.41	3.41	3.41	3.41	3.41
Atmosphere	Reducing	Reducing	Reducing	Reducing	Reducing	Reducing	Reducing
Coal Used	Wyodak	Wyodak	Wyodak	Wyodak	Wyodak	Wyodak	Wyodak
WAL #	38192	38192	38192	38192	38192	38192	38192
Sample Prep	Fusion	Digest	TCLP	EP Tox	SGLP-18	LTL 1WK	LTL 3MO
	% as oxide	ug/g	mg/L	mg/L	mg/L	mg/L	mg/L
Aluminum	0.48		0.48	0.53	0.26	0.38	0.3
Arsenic			<0.005	<0.005	<0.005	<0.005	<0.005
Barium		32	<5	<5	<5	<5	<5
Boron		360	0.56	0.5	0.46	0.5	0.9
Cadmium			<0.02	<0.02	<0.02	<0.02	<0.02
Calcium	60.42		2690	2690	950	950	864
Chromium		7.2	<0.1	<0.1	<0.1	<0.1	<0.1
Copper			<0.2	<0.2	<0.2	<0.2	<0.2
Iron	0.62		1	1	0.44	0.46	<0.2
Lead		0.7	<0.5	<0.5	<0.5	<0.5	<0.5
Magnesium	0.5		0.1	0.1	0.1	0.1	0.5
Manganese		280	<0.02	<0.02	<0.02	<0.02	<0.02
Mercury			<0.003	<0.003	<0.003	<0.003	
Molybdenum			<0.1	<0.1	<0.1	<0.1	<0.1
Nickel			<0.1	<0.1	<0.1	<0.1	<0.1
Phosphorous			<0.5	<0.5	<0.5	<0.5	<0.5
Potassium	0.02		0.9	1	1	1.6	5.9
Selenium			<0.005	<0.005	<0.005	<0.005	<0.005
Silicon	2.63		1.7	1.7	0.99	0.99	0.2
Silver			<0.2	<0.2	<0.2	<0.2	<0.2
Sodium	0.02		3	2.6	2.4	3	7.2
Strontium			14	14	14	17	18.8
Titanium		62	<0.2	<0.2	<0.2	<0.2	<0.2
Zinc			<0.1	<0.1	<0.1	<0.1	<0.1
Zirconium			<0.1	<0.1	<0.1	<0.1	<0.1

Limestone Bed Materials from Hydrogen Production
Chemical Characterization

Sample Number	10R-W180L	10R-W180L	10R-W180L	10R-W180L	10R-W180L	10R-W180L	10R-W180L
Temp (Ave.)	806.36	806.36	806.36	806.36	806.36	806.36	806.36
Steam/C (Ave.)	1.28	1.28	1.28	1.28	1.28	1.28	1.28
Atmosphere	Reducing	Reducing	Reducing	Reducing	Reducing	Reducing	Reducing
Coal Used	Wyodak	Wyodak	Wyodak	Wyodak	Wyodak	Wyodak	Wyodak
WAL #	38193	38193	38193	38193	38193	38193	38193
Sample Prep	Fusion	Digest	TCLP	EP Tox	SGLP-18	LTL 1WK	LTL 3MO
	% as oxide	ug/g	mg/L	mg/L	mg/L	mg/L	mg/L
Aluminum	1.01		0.59	0.68	0.35	0.43	0.32
Arsenic			<0.005	<0.005	<0.005	<0.005	<0.005
Barium		86	<5	<5	<5	<5	<5
Boron		360	1.12	0.92	0.98	0.5	0.2
Cadmium			<0.02	<0.02	<0.02	<0.02	<0.02
Calcium	61.46		2630	2650	955	915	888
Chromium		26	<0.1	<0.1	<0.1	<0.1	<0.1
Copper			<0.2	<0.2	<0.2	<0.2	<0.2
Iron	0.66		1	1	0.44	0.43	<0.2
Lead		1.7	<0.5	<0.5	<0.5	<0.5	<0.5
Magnesium	0.63		0.1	0.1	0.1	0.1	1
Manganese		312	<0.02	<0.02	<0.02	<0.02	<0.02
Mercury			<0.003	<0.003	<0.003	<0.003	
Molybdenum			<0.1	<0.1	<0.1	<0.1	<0.1
Nickel			<0.1	<0.1	<0.1	<0.1	<0.1
Phosphorous			<0.5	<0.5	<0.5	<0.5	<0.5
Potassium	0.06		0.7	0.7	0.7	1.6	7.2
Selenium			<0.005	<0.005	<0.005	<0.005	<0.005
Silicon	3.33		1.8	1.7	0.98	0.94	0.2
Silver			<0.2	<0.2	<0.2	<0.2	<0.2
Sodium	0.06		6.3	5.4	5.7	7.6	12.2
Strontium			15	15	15	19	20
Titanium		384	<0.2	<0.2	<0.2	<0.2	<0.2
Zinc			<0.1	<0.1	<0.1	<0.1	<0.1
Zirconium			<0.1	<0.1	<0.1	<0.1	<0.1

Limestone Bed Materials from Hydrogen Production
Chemical Characterization

Sample Number	12R-W275L	12R-W275L	12R-W275L	12R-W275L	12R-W275L	12R-W275L	12R-W275L
Temp (Ave.)	749.95	749.95	749.95	749.95	749.95	749.95	749.95
Steam/C (Ave.)	2.35	2.35	2.35	2.35	2.35	2.35	2.35
Atmosphere	Reducing	Reducing	Reducing	Reducing	Reducing	Reducing	Reducing
Coal Used	Wyodak	Wyodak	Wyodak	Wyodak	Wyodak	Wyodak	Wyodak
WAL #	38194	38194	38194	38194	38194	38194	38194
Sample Prep	Fusion	Digest	TCLP	EP Tox	SGLP-18	LTL 1WK	LTL 3MO
	% as oxide	ug/g	mg/L	mg/L	mg/L	mg/L	mg/L
Aluminum	0.44		0.7	0.63	0.3	0.39	0.29
Arsenic			<0.005	<0.005	<0.005	<0.005	<0.005
Barium		58	<5	<5	<5	<5	<5
Boron		559	0.13	0.24	0.17	0.5	0.32
Cadmium			<0.02	<0.02	<0.02	<0.02	<0.02
Calcium	41.59		2470	2600	945	940	850
Chromium		8.6	<0.1	<0.1	<0.1	<0.1	<0.1
Copper			<0.2	<0.2	<0.2	<0.2	<0.2
Iron	0.51		0.98	1	0.45	0.42	<0.2
Lead		2.3	<0.5	<0.5	<0.5	<0.5	<0.5
Magnesium	0.39		0.1	0.1	0.1	0.1	1
Manganese		91	<0.02	<0.02	<0.02	<0.02	<0.02
Mercury			<0.003	<0.003	<0.003	<0.003	
Molybdenum			<0.1	<0.1	<0.1	<0.1	<0.1
Nickel			<0.1	<0.1	<0.1	<0.1	<0.1
Phosphorous			<0.5	<0.5	<0.5	<0.5	<0.5
Potassium	0.03		1.1	0.9	1.7	2.3	5.5
Selenium			<0.005	<0.005	<0.005	<0.005	<0.005
Silicon	1.97		1.9	2.1	1	0.97	0.2
Silver			<0.2	<0.2	<0.2	<0.2	<0.2
Sodium	0.01		2.4	2.1	1.7	2.4	5.3
Strontium			3.2	3.2	1.3	2.4	2.8
Titanium		91	<0.2	<0.2	<0.2	<0.2	<0.2
Zinc			<0.1	<0.1	<0.1	<0.1	<0.1
Zirconium			<0.1	<0.1	<0.1	<0.1	<0.1

Limestone Bed Materials from Hydrogen Production
Chemical Characterization

Sample Number	14R-W170L	14R-W170L	14R-W170L	14R-W170L	14R-W170L	14R-W170L	14R-W170L
Temp (Ave.)	698.59	698.59	698.59	698.59	698.59	698.59	698.59
Steam/C (Ave.)	1.57	1.57	1.57	1.57	1.57	1.57	1.57
Atmosphere	Reducing	Reducing	Reducing	Reducing	Reducing	Reducing	Reducing
Coal Used	Wyodak	Wyodak	Wyodak	Wyodak	Wyodak	Wyodak	Wyodak
WAL #	38195	38195	38195	38195	38195	38195	38195
Sample Prep	Fusion	Digest	TCLP	EP Tox	SGLP-18	LTL 1WK	LTL 3MO
	% as oxide	ug/g	mg/L	mg/L	mg/L	mg/L	mg/L
Aluminum	0.46		0.72	1.7	0.32	0.4	0.29
Arsenic			<0.005	<0.005	<0.005	<0.005	<0.005
Barium		55	<5	<5	<5	<5	<5
Boron		219	0.1	0.07	0.45	0.5	0.07
Cadmium			<0.02	<0.02	<0.02	<0.02	<0.02
Calcium	39.98		2290	2360	960	940	880
Chromium		11	<0.1	<0.1	<0.1	<0.1	<0.1
Copper			<0.2	<0.2	<0.2	<0.2	<0.2
Iron	0.47		0.98	0.93	0.45	0.45	<0.2
Lead		1.2	<0.5	<0.5	<0.5	<0.5	<0.5
Magnesium	0.39		0.1	0.1	0.1	0.1	0.8
Manganese		137	<0.02	<0.02	<0.02	<0.02	<0.02
Mercury			<0.003	<0.003	<0.003	<0.003	
Molybdenum			<0.1	<0.1	<0.1	<0.1	<0.1
Nickel			<0.1	<0.1	<0.1	<0.1	<0.1
Phosphorous			<0.5	<0.5	<0.5	<0.5	<0.5
Potassium	0.03		1.4	1.6	5.6	4.5	8.6
Selenium			<0.005	<0.005	<0.005	<0.005	<0.005
Silicon	1.91		1.9	2.3	1	1	0.2
Silver			<0.2	<0.2	<0.2	<0.2	<0.2
Sodium	0.03		7	6.6	5.6	8.6	12.8
Strontium			3.3	3.3	1.5	2.3	3.3
Titanium		137	<0.2	<0.2	<0.2	<0.2	<0.2
Zinc			<0.1	<0.1	<0.1	<0.1	<0.1
Zirconium			<0.1	<0.1	<0.1	<0.1	<0.1

Limestone Bed Materials from Hydrogen Production
Chemical Characterization

Sample Number	BLANK	BLANK	BLANK	BLANK	BLANK	BLANK	BLANK
Temp (Ave.)							
Steam/C (Ave.)							
Atmosphere							
Coal Used							
WAL #							
Sample Prep	Fusion	Digest	TCLP	EP Tox	SGLP-18	LTL 1WK	LTL 3MO
	% as oxide	ug/g	mg/L	mg/L	mg/L	mg/L	mg/L
Aluminum	0.35		0.44	0.51	0.12	0.29	0.06
Arsenic			<0.005	<0.005	<0.005	<0.005	<0.005
Barium		8.4	<5	<5	<5	<5	<5
Boron		1146	0.16	0.1	<0.02	0.03	<0.02
Cadmium			0.08	0.04	<0.02	<0.02	<0.02
Calcium	53.18		2010	2090	29	28	39
Chromium		3.88	<0.1	<0.1	<0.1	<0.1	<0.1
Copper			<0.2	<0.2	<0.2	<0.2	<0.2
Iron	0.43		1.3	1	<0.2	<0.2	<0.2
Lead		6.4	<0.5	<0.5	<0.5	<0.5	<0.5
Magnesium	0.52		17	17	1.1	2.4	3.6
Manganese		528	3.26	3.12	<0.02	<0.02	<0.02
Mercury			<0.003	<0.003	<0.003	<0.003	
Molybdenum			<0.1	<0.1	<0.1	<0.1	<0.1
Nickel			<0.1	<0.1	<0.1	<0.1	<0.1
Phosphorous			<0.5	<0.5	<0.5	<0.5	<0.5
Potassium	0.04		0.8	0.8	0.4	1.1	0.7
Selenium			<0.005	<0.005	<0.005	0.007	<0.005
Silicon	2.74		1.8	1.9	0.46	1.1	1.2
Silver		0.6	<0.2	<0.2	<0.2	<0.2	<0.2
Sodium	0.06		3.5	2.8	2.8	3	2
Strontium			1.94	2.07	0.21	0.28	0.39
Titanium		52	<0.2	<0.2	<0.2	<0.2	<0.2
Zinc		21	<0.1	<0.1	<0.1	<0.1	<0.1
Zirconium			<0.1	<0.1	<0.1	<0.1	<0.1

2.3 Regional Energy Policy Program for the Northern Great Plains

REGIONAL ENERGY POLICY PROGRAM
FOR THE NORTHERN GREAT PLAINS

Annual Technical Progress Report
for the Period July 1, 1989 - June 30, 1990

Including

the Quarterly Technical Progress Report
for the Period April - June 1990

by

Daniel J. Daly, Geologist

University of North Dakota
Energy and Environmental Research Center
Box 8213, University Station
Grand Forks, ND 58202

Contracting Officer's Representative: John W. Byam, Jr.

for

U.S. Department of Energy
Morgantown Energy Technology Center
P.O. Box 880
Morgantown, West Virginia 26507-0880

August 1990

Work Performed Under Cooperative Agreement No. DE-FC21-86MC10637

TABLE OF CONTENTS

REGIONAL ENERGY POLICY PROGRAM FOR THE NOPTHERN GREAT PLAINS

1.0 INTRODUCTION

The United States is the world's leading consumer of energy. The production and consumption of energy varies across the country as a function of climate, the availability of natural resources, economics, and culture. The northern Great Plains region (Montana, Wyoming, North Dakota, and South Dakota), an area characterized by many similarities in climate, culture, and physiography:

- Accounts for over 10 percent of domestic hydrocarbon production, a major share of low-rank, low-sulfur coal production, a significant steam-generated electrical capability, and a significant portion of domestic uranium production.
- Contains significant oil shale, geothermal, nuclear, and conventional fossil fuel resources.
- Contains significant research capability, particularly with regard to coal conversion, and oil shale technologies and the environmental effects of fossil fuel production, conversion, and utilization.
- Is a net exporter of energy and fossil fuel materials.
- Is a significant consumer of fuel and fossil fuel by-products in the agricultural sector.
- Receives significant revenues and economic support from fossil fuel exploration, production, conversion, and transportation industries, as well as from ancillary industries.

2.0 PROGRAM OBJECTIVES

Energy-related activities are significant in the economy at the regional, state, and local levels. Fluctuations in energy markets can have marked effects on government revenues and programs as well as on the economy. Since the end of the Second World War, the northern Great Plains has experienced economic "booms" related to oil and gas, coal, oil shale, hydroelectric power, and uranium. Since the early 1970s, the energy market has had to deal with the increase in environmental awareness and the growth and diversification of energy sources and suppliers on a global scale. For example, prospects for the continued growth of the region's coal sector depend to a significant degree on the nature of federal actions with respect to air quality and waste management. Currently, an attempt is being made during the development of a National Energy Strategy (NES) to take into account the mix of environmental, fiscal, social, research, economic, national security, and resource issues that form the energy picture of the nation. Ensuring the optimal production

and utilization of the region's energy resources, within the framework of the developing NES, could be enhanced by responses and initiatives both at the state and regional levels. Once the basic framework of the strategy is in place, periodic review of the policy with respect to the region would be augmented by ready access to pertinent data for the region. To this end, the objectives of the Regional Energy Policy Program for the northern Great Plains as originally proposed were to:

- Gather, develop, and disseminate information necessary for well-founded energy initiatives in the region.
- Promote and assist in the integration and coordination of the energy-planning efforts of individual states in the region.
- Foster communication between the public and private sector concerning energy-planning needs in the region.
- Achieve objectives and carry out activities in a manner consistent with the National Energy Strategy.

The mission of the Energy Policy Program for the northern Great Plains can best be achieved through an information clearing house/data center. We are proceeding in this direction with the development of the Energy Policy Information Center (EPIC) for the northern Great Plains.

3.0 YEAR 1 GOALS/ACTIVITIES

Year 1 efforts of the Regional Energy Policy Program for the northern Great Plains were designed to initiate the development of an up-to-date listing of energy resources, production, and consumption in the region, as well as a computer-based system to facilitate the efficient identification, collection, and manipulation of energy-related information.

Task A. Development of an Information Management System

The initial efforts of the program will focused on the identification, acquisition, and organization of pertinent energy information and the development of a computer-based system to manage this information.

Task B. Compilation of an Annotated Bibliography

The review of information in Task A formed the basis for initiation of an annotated bibliography.

Task C. Compilation of an Energy Resource Data Base

The review of information acquired in Task A formed the basis for initiation of an energy resource data base.

Task D. Annual Report

4.0 ACCOMPLISHMENTS

To date (the last half of August 1989 to May 1990), activities focused on:

4.1 Work on Tasks A, B, and C

Task A. Development of an Information Management System

The acquisition of computer hardware (subtask a.1) and the identification and assessment of energy-related data bases for the region (subtask a.2; ongoing).

Task B. Completion of an Annotated Bibliography

The design of a review format (subtask b.1) and the acquisition and review of relevant documents (subtask b.2; ongoing). Bibliographic information for these documents has been entered (subtask b.3) in a standardized computer-based Q&A software package format (subtask b.1). The review of these documents and assignment of key words continued during the quarter.

Task C. Energy Resource Data Base

Data base design for the energy resource data bases continued during the quarter.

4.2 Tracking Policy Developments

Efforts in this area were focused on the developing National Energy Strategy (NES). Specific activities included 1) obtaining and reviewing the NES Interim Report, 2) obtaining and reviewing the White Papers prepared in support of the NES ("The Potential for Renewable Energy," "Energy Efficiency: How Far Can We Go," "The Technology Transfer Process," and "Energy and Climate Change"). Federal energy policy from 1970 through the present was reviewed and background materials were prepared.

5.0 TRIPS/PRESENTATIONS

No trips or presentations were made during the quarter.

6.0 FUTURE ACTIVITIES

Activities in the next quarter will include:

1) Continuation of work on Tasks A, B, and C and related activities.

2) Continued tracking of NES developments as the public comment period closes and the preparation of the final policy document is undertaken.

3) Continued contact with energy officials and representatives of the private sector concerning regional policy issues.

4) Continued compilation of historical information on federal and regional energy-related initiatives with the review of state policy measures.

3.0 ADVANCED RESEARCH AND TECHNOLOGY DEVELOPMENT

3.1 Turbine Combustion Phenomena

TURBINE COMBUSTION PHENOMENA

Annual Technical Project Report
for the Period July 1, 1989 through June 30, 1990

Including

the Quarterly Technical Progress Report
for the Period April 1, 1990 through June 30, 1990

by

Michael L. Swanson, Research Supervisor
Michael D. Mann, Research Supervisor
Thomas A. Moe, Research Engineer

University of North Dakota
Energy and Environmental Research Center
Box 8213, University Station
Grand Forks, North Dakota 58202

Contracting Officer's Representative: Leland Paulson

for

U.S. Department of Energy
Morgantown Energy Technology Center
P.O. Box 880
Morgantown, West Virginia 26507-0880

August 1990

Work Performed Under Cooperative Agreement No. DE-FC21-86MC10637

LIST OF FIGURES

LIST OF TABLES

TABLE OF CONTENT

TURBINE COMBUSTION PHENOMENA

1.0 INTRODUCTION

Under DOE sponsorship, coal/water slurry fuels have been investigated as fuels for gas turbine engines for several years, but the major technical problems still inhibiting commercialization are deposits on the pressure and suction sides of the turbine blades, reducing the gas flow area and the turbine efficiency; acceptable coal burnout, given the short residence time inherent with gas turbine engines; corrosion of turbine blades by condensed alkali sulfates; erosion of turbine blades and other components by ash particles entrained in the products of combustion; and control of NO_x, SO_2, and particulate emissions. The release of certain mineral matter species found in both raw and beneficiated coals can lead to ash deposition on surfaces, regardless of the ash content of the fuel. This deposition can lead to corrosion and metal loss of critical turbine components and, ultimately, to derating, unavailability, or catastrophic failure of the power generation system. Alkali metals and sulfur, existing as impurities in coal, have been identified as key components in the initiation of deposition and the onset of corrosion.

Until the last four years, low-rank coals (LRCs) were not considered as potential fuels for gas turbine engines because of their high intrinsic moisture levels. It is extremely difficult to prepare a pumpable slurry of as-mined lignite with a dry solids loading over 35 wt.% due to the high moisture levels in LRCs. However, with the advent of the University of North Dakota Energy and Environmental Research Center's (UNDEERC's) hydrothermal treatment process, micronized lignite slurries have been produced with a solids loading up to 50% and a heating value over 6000 Btu/lb of slurry. Subbituminous coals also respond very well to hydrothermal treatment and produce higher quality slurries. Availability of a slurry with a fuel value high enough to sustain combustion makes it possible to take advantage of the desirable characteristics of low-rank coals, namely the higher reactivity of its nonvolatile carbonaceous components. Thus a low-rank coal slurry should require less residence time in the gas turbine combustor for complete combustion, or inversely, the coal would not have to be micronized as fine to achieve the same level of burnout, thereby reducing fuel preparation costs. Another potential advantage of low-rank coal slurries is their non-agglomerating tendency relative to bituminous slurries, reducing the importance of atomization to very fine droplet sizes.

2.0 GOALS AND OBJECTIVES

The overall objective of this research is to continue to expand the data base on the effects of low-rank coals' unique properties on combustion behavior in pressurized combustion systems such as gas turbine engines. Research will be directed toward understanding the properties of LRC fuels which affect ignition and burn times, combustion efficiency, vaporization and deposition of inorganics on critical gas turbine components. Special emphasis

will be placed on an investigation of LRC high-shear rheology and its effect on atomization and combustion behavior, an evaluation of LRCs' non-agglomerating properties using laser-based diffraction techniques (Insitec PCSV), an investigation of particulate hot-gas cleanup techniques, and inorganic transformations/alkali vaporization using a pressurized drop-tube furnace.

2.1 Year Four Through Six Project Objectives

A. Revise Technology and Market Assessment

This literature review will enable UNDEERC personnel to assess the current status of coal-fired gas turbine research to determine what recent advances have been made by other researchers. This effort will build upon the technology and market assessment made at the start of this program.

B. Characterization of LRCs' Atomization Properties

The objective of this task is to investigate the effects of coal type, particle-size distribution, solids loading, additive package, and shear rate on LRC slurry rheology. High-shear rheology will be measured using a capillary extrusion viscometer modified to perform rheological tests at shear rates up to 200,000 1/sec. This task will also examine the pressurized atomization characteristics of these LRC fuels with a Malvern 2600 particle-size analyzer and still photography in a pressurized spray chamber at UNDEERC. The combustion behavior of these same fuels will be evaluated under similar air-to-fuel and pressure ratios in the gas turbine simulator. This task would also look at different atomizer types in an effort to minimize spray droplet size distributions for a given rheology and atomizing air-to-fuel ratio.

C. Evaluation of LRC Fuel Agglomeration

The objective of this task is to evaluate the agglomerating or non-agglomerating tendencies of LRC fuels by providing optical access for an Insitec PCSV particle-size analyzer at various residence times along the axis of a pressurized drop-tube furnace under construction at UNDEERC. Thus, product of combustion (POC) particle size distributions as a function of residence time, the starting particle-size distribution, and droplet size can be measured to determine if the smaller particle-size distributions found in the LRC fly ash are the result of a gradual burnout of slurry droplet agglomerates or the result of agglomerate disintegration into its original particle-size distribution due to the high thermal friability of LRC fuels.

D. Investigation of Particulate Hot-Gas Cleanup Systems

The objective of this task is to evaluate potential hot-gas particulate cleanup techniques as to their relative probability of success and to test the best two or three systems in the turbine simulator. This task would include a technology assessment building upon a previous literature search performed on hot-gas cleanup techniques. These techniques could include, but would not be limited to, ceramic cross flow filters and filter candles, nested fiber filters, cyclones, and HTHP ESPs. Potential also exists for investigating an alkali vapor cleanup device (i.e., sorbent packed beds, etc.).

E. Ash Transformation and Alkali Vaporization Studies

The objective of this task is to investigate the ash transformations experienced by the mineral matter in beneficiated LRC fuels. Very little research to date has investigated the effects of pressure and coal beneficiation on the reaction pathways taken by the mineral matter present in LRC fuels. These transformations should be dependent on the cleaning techniques used and the level of cleaning achievable on the various coal types. Mineral matter transformations of beneficiated LRC under turbine operating conditions will be investigated in a pressurized drop-tube furnace under construction at UNDEERC. This drop-tube furnace will be capable of combusting both slurry droplets and coal particles. The effects of residence time, temperature, pressure, atmosphere, and gas/fuel flow rates can be varied to examine their effects on ash transformations and carbon burnout. The drop tube will also provide carbon burnout as a true function of residence time, given the laminar gas flow. The effects of deposition probe shape and temperature and approaching gas velocity on the measured deposition rates can also be investigated. Optical ports into the drop tube will enable quantities of alkali vapor/aerosols in the gas streams to be measured using in situ methods. Another advantage of the pressurized drop-tube furnace is the small quantities of fuel (up to 1.5 lbs/hr) needed to conduct extensive deposition and burnout testing as compared to the turbine simulator (approximately 150 lbs/hr).

F. Investigation of Slagging Combustor Design

Should concurrent beneficiation of LRC studies at UNDEERC indicate that acceptable ash levels and composition not be achievable, a vertically fired combustion zone would be built to replace the horizontally fired rich combustion zone on the current turbine simulator. This modification would enable the combustor to operate in a slagging combustor mode versus the current non-slagging combustor mode. Work on this task would be dependent on the results of the work in progress and would be subject to DOE approval.

2.2 Fourth Year Goals and Objectives

Task A - Revise Technology and Market Assessment

This task involves updating the previous literature assessment made at the beginning of the program.

Task B - Characterization of LRCs' Atomization Properties

This task involves the investigation of LRCs' fuel atomization and viscosity properties using a capillary viscometer and a pressurized spray chamber with a Malvern particle-size analyzer and still photography to determine spray droplet sizes. In addition, this task will conduct a parametric investigation of different atomizers for atomization effectiveness. This includes the commercially available Delavan and Parker-Hannifan atomizers, along with the UNDEERC-developed B-II nozzle. This task will also evaluate atomizer combustion performance under the same operating conditions in the turbine simulator combustion rig.

Task C - Evaluation of LRC Fuel Agglomeration

This task consists of using laser-based diagnostics (i.e., Insitec PCSV) and particulate sampling to determine if LRC slurry droplets are friable enough to break into their original particle sizes as hypothesized or remain as agglomerates which must burn out.

Task D - Investigation of Particulate Hot-Gas Cleanup Systems

This task involves evaluating potential hot-gas particulate cleanup techniques for use in direct coal-fired gas turbines to test the two best techniques in combustion tests on the turbine simulator. These techniques could include, but would not be limited to, ceramic cross-flow filters and filter candles, nested fiber filters, cyclones, HTHP ESPs, etc.

Task E - Ash Transformation and Alkali Vaporization Studies

Technical work in this task for Year 4 consists of finishing construction on the PDTF and subsequent combustion tests using selected beneficiated coals to determine the effects of residence time, gas composition, temperature, and pressure on carbon burnout and ash deposition.

Task F - Investigation of Slagging Combustor Design

No technical work in this task will be performed in Year 4. If coal ash properties dictate, construction of a first-stage slagging combustor would begin in Year 6.

3.0 BACKGROUND

3.1 One Million Btu/Hr Gas Turbine Combustor

To meet the objectives of the program, a pressurized combustion vessel was built to allow the operating parameters of a direct-fired gas turbine combustor to be simulated. One goal in building this equipment was to design the gas turbine simulator as small as possible to reduce both the quantity of test fuel needed and the test fuel preparation costs, while not undersizing the combustor such that wall effects would have a significant effect on the measured combustion performance. Based on computer modeling, a rich-lean, two-stage, non-slagging combustor has been constructed to simulate a direct-fired gas turbine. This design was selected to maximize the information that could be obtained on the impact of the unique properties of low-rank fuels and various hot-gas cleanup techniques on the gas turbine combustor and its turbomachinery.

A short description of the gas turbine simulator is given here; a more detailed description is given elsewhere (1,2,3). Figure 1 is a schematic of the 1-MM Btu/hr gas turbine combustor, showing its internal design. Figure 2 is a photograph of the 1-MM Btu/hr gas turbine combustor. The head section of the turbine has an interchangeable, horizontal, flat-bladed air swirler for controlling the primary air-fuel spray and developing a recirculation zone in the rich combustion zone.

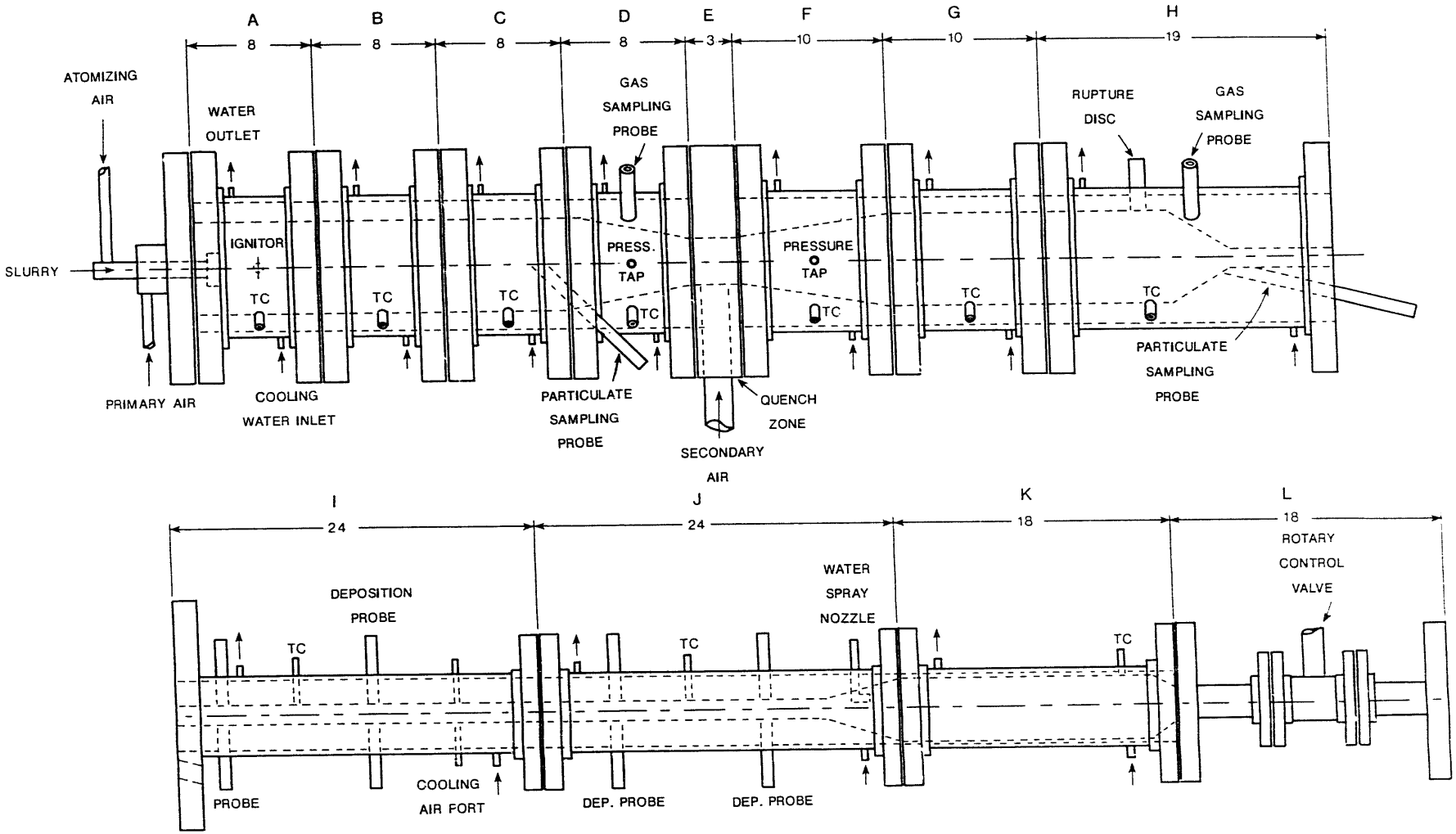

Figure 1. Schematic of 1-MM Btu/Hr gas turbine simulator.

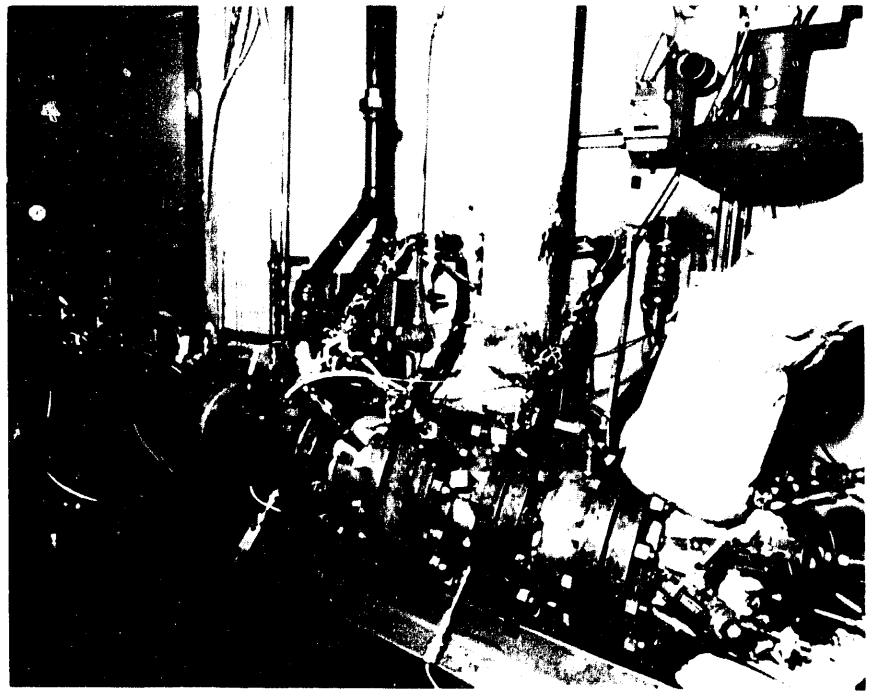

Figure 2. Photograph of 1-MM BTU/hr gas turbine simulator.

A Delavan Swirl-Air nozzle with a 50° spray angle is currently used as the atomizer. The pressurized combustion vessel itself is comprised of several short sections of refractory-lined stainless steel pipe. These sections are water-jacketed to provide cooling of the external pressure vessel wall. This modular design allows the length of the combustion zones to be varied. The removal of some of these modules allows the effect of residence time to be investigated under similar flow conditions.

The quench zone of the turbine simulator was designed to promote rapid mixing of the secondary air with the POC exiting the rich combustion zone, thus minimizing the occurrence of localized "hot spots" and the formation of thermal NO_x. A rotary control valve and a high-temperature guided seat control valve are used to control the flow of combustion air entering the air preheater and the distribution of air between the rich and lean zones, respectively. The combustor is designed to operate at pressures up to 250 psig and a lean zone exit temperature of 2000°F.

A reduced flow area in the deposition section is used to increase the gas velocities up to those typically seen in the expander section of a gas turbine (400 to 800 ft/sec). Four air-cooled probes with various contact angles were machined from thick-walled high-temperature alloy tubing and were installed to simulate the leading edge of turbine blades. Additional cooling air was added after the first two probes to cool the exit gas stream up to 200°F, such

that gas temperature as well as metal temperature can be investigated for their effects on deposition/erosion/corrosion (DEC). A spray water quench zone is located after the deposition section to spray high-pressure water into the combustion gases to cool the gases before passing them through the rotary control valve used to back-pressure the turbine simulator. A natural gas-fired fluidized-bed preheater is used to preheat the high-pressure combustion air to temperatures as high as 1000°F. Combustion efficiencies of the test fuels fired in the turbine simulator are calculated from gas and isokinetic particulate samples taken from both the rich and lean zones of the combustor.

Seventeen successful combustion tests using CWF were completed. These tests included seven tests with a commercially available Otisca Industries produced Taggart seam bituminous fuel and five tests each with physically and chemically cleaned Beulah-Zap lignite and a chemically cleaned Kemmerer subbituminous fuel. Analyses of the emission and fly ash samples highlighted the superior burnout experienced by the LRC fuels as compared to the bituminous fuel, even under a longer residence-time profile for the bituminous fuel. While the LRC fuels are experiencing better burnout than the bituminous fuels, it is possible that differences in slurry rheology (and therefore in atomization) might account for some of the difference in the observed burnout rather than differences in fuel reactivity. Future work will attempt to clarify these differences. The LRC fly ash shows a decrease in particle size as compared to the starting fuel while the bituminous fuel showed an increase in particle size as compared to the starting fuel. These particle size analyses provide some evidence of LRCs' nonagglomerating properties as compared to bituminous fuels.

Statistical analysis of the carbon burnout data generated in a series of parametric combustion tests generated simple models to predict the carbon burnout achievable under a given range of operating conditions. These models indicate that fuel type has a significant effect on the measured carbon burnout. The LRC fuels have high carbon burnouts (97.5%) and appear to be relatively unaffected by other operating parameters, however, the bituminous fuel was significantly affected by combustion air temperature, atomizing air-to-fuel ratio and fuel firing rate. In these models, bituminous fuel carbon burnouts comparable to those of the LRC fuels can be achieved but only under the most optimum conditions. Operating conditions for this model were between the ranges studied for the combustion air temperature (400-800°F), atomizing air-to-fuel ratio (0.75-1.25) and fuel firing rate (0.7-1.0 MM Btu/hr). The models for estimating the carbon burnout (CB) as calculated using uncoded data are as follows:

$$\text{Lean Zone CB} = 97.5035 - 55.4839 * XO + 21.6551 * XO\_3 + 0.03134 * XO\_7 \quad (2)$$

Model R-square = 0.6648

$$\text{Cyclone Ash CB} = 98.6788 - 59.3907 * XO + 15.7727 * XO\_3 + 0.0227 * XO\_7 + 1.699E\text{-}5 * XO\_29 \quad (3)$$

Model R-square = 0.7407

where X0 = fuel type, Otisca = 1, Kemmerer = 0, Beulah-Zap = 0;
X3 = atomizing air-to-fuel ratio;
X7 = combustion air temperature, (°F);
X29 = fuel firing rate, (Btu/hr);
X0_3 = fuel type/atomizing air-to-fuel ratio interaction;
X0_7 = fuel type/combustion air temp interaction
X0_29 = fuel type/fuel firing rate interaction

Note: Interactions were calculated as the product of the two parameters.
i.e.) X0_3 = X0 * X3

As might be expected with the relatively high ash and lower ash fusion temperatures and in the Beulah-Zap coal, significant ash deposition and slagging occurred in the turbine simulator.

The XRD analysis suggests that the residual magnetite left from the physical cleaning process remains as magnetite in the reducing atmosphere of the rich zone but is converted to hematite when it reaches the highly oxidizing atmosphere encountered in the lean combustion zone. As indicated by material balances, the low-rank slurries had significantly larger deposits than the Otisca slurry, primarily due to its high ash content and lower ash fusion temperatures. The composition of the constituents in the ash does not indicate the preferential deposition of any component in a single area of the turbine. These material balances indicated that the Beulah-Zap lignite fuel had a much higher deposition potential as demonstrated by high levels (approximately 70 wt%) of ash recovered in the combustor. The Kemmerer also showed higher deposition levels than the Otisca fuel with approximately 12-13 wt% of the ash being retained in the combustor. With the Otisca fuel combustion tests approximately 8 wt% of the ash was retained in the combustor while over 40 wt% of the Otisca fly ash was recovered in the cyclone pot. This is probably the result of the cyclone ash containing high levels of carbon (60% or greater), thus a large percentage of the fine mineral grains is still tied up in the char cenospheres and has not been released from the char particle where it could contact internal surfaces to form deposits. In addition, the agglomerating nature of the bituminous fuel tends to increase the efficiency of the cyclone on the exhaust of the turbine simulator, thereby collecting a higher percentage of particulate entering the cyclone.

3.2 Scanning Electron Microscope Techniques

Computer-controlled scanning electron microscopy (CCSEM) is used to characterize minerals in unaltered coal samples and inorganic phases in combustion products such as char or fly ash. A computer program is used to locate, size, and analyze particles. Because the analysis is automated, a large number of particles can be analyzed quickly and consistently. The heart of the CCSEM analysis system is a recently installed annular backscattered electron detector (BED). The BED system is used because the coefficient of backscatter (the fraction of the incoming beam that is backscattered) is proportional to the square root of the atomic number of the scattering atoms. This permits a high degree of resolution between sample components based on their atomic numbers. This means that coal minerals can be easily discerned from the coal matrix, and fly ash particles can be differentiated from epoxy

in polished sections. Brightness and contrast controls are used to optimize threshold levels between the coal matrix and the mineral grains or fly ash particles. When a video signal falls between these threshold values, a particle is discerned, and the particle center is located. A set of eight rotated diameters about the center of the particle are measured, and the particle area, perimeter, and shape are calculated. The beam is then repositioned to the center of the particle, and an X-ray spectrum is obtained. The information is then stored to a Lotus™ transportable file for data reduction and manipulation. The CCSEM data provides quantitative information concerning not only the mineral types which are present, but their size and shape characteristics as well. Since the same analysis can be performed on the initial coal and resultant fly ash or char, direct comparisons can be made and inorganic transformations inferred.

In order to quantitatively determine the distribution of phases in fly ashes, deposits, and slags, the scanning electron microscopy point count technique (SEMPC) was developed. The method involves microprobe analysis of a large number of random points in a polished cross section of a sample. The quantitative analysis of each point is transferred for data base analysis. The software is used to calculate molar and weight ratios for each point. Using these ratios, the points which have compositions of known phases (common to ashes and coal minerals) are identified and counted. The software then finds the relative percents of all the identified points as well as the percent number of unknown phases. The unknown phases are those for which there is no known phase corresponding to the chemical composition. In addition, the average chemical composition of all the points in the sample is calculated. Previous work at UNDEERC has shown that the SEMPC average composition corresponds very well to the bulk chemical analysis (4). The quantitative ability of the SEMPC allows for detailed comparisons to be made between different samples.

4.0 Accomplishments

4.1 Design of a High-Pressure High-Temperature Cyclone

A high-temperature, high-pressure cyclone was selected as the first stage in a particulate hot-gas cleanup device. The design goal was to remove 85% of 5-micron particulates. The cyclone should also be designed to fit in-line with the current turbine simulator located at the UNDEERC. Design conditions were selected to match those experienced in the turbine simulator at its 1 MM Btu/hr firing rate. These conditions result in a gas flow rate of approximately 400 scfm entering the cyclone at 2000°F and 160 psig. Cyclone dimensions were selected using the dimensions reported by Perry (4) and Stairmand (5). Figure 3 shows all of the dimensions of the cyclone. These dimensions are all factors of the cyclone diameter. Table 1 shows the 50% cut point size, pressure drop and collection efficiency for a typical turbine simulator fly ash for several different cyclone diameters. Using the methodology reported by Lapple (6), a cyclone diameter of 5 inches was calculated to provide the best compromise on a collection efficiency and pressure drop.

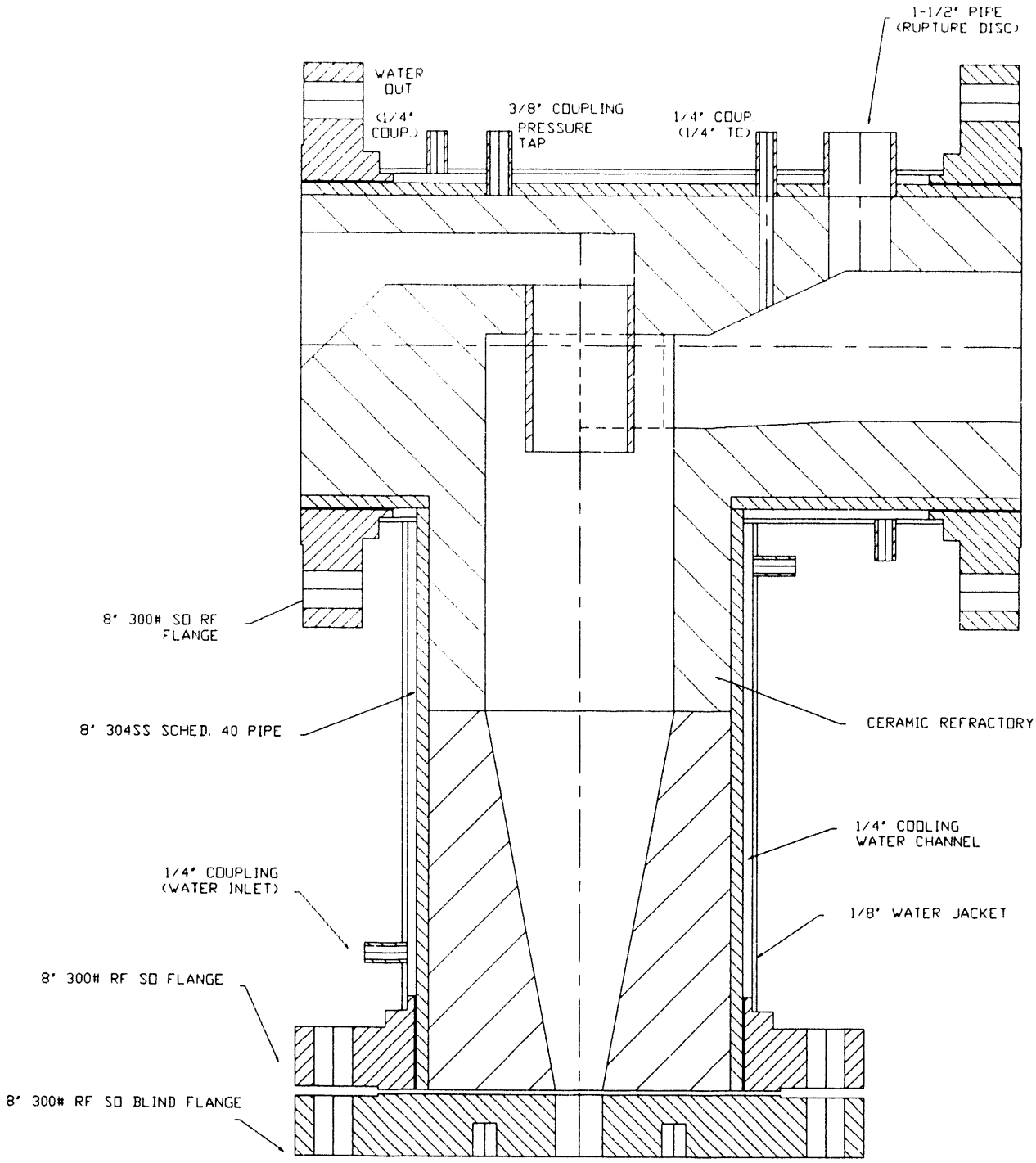

Figure 3. Design of HPHT cyclone for testing in 1MM BTU/hr gas turbine simulator

TABLE 1

HIGH-PRESSURE, HIGH-TEMPERATURE CYCLONE DESIGN RESULTS AT 400 SCFM, 175 PSIA AND 2000°F

Cyclone Diameter (in)	50% Cut size (μm)	Collection Efficiency @ 5μm	Differential Pressure (in H_2O)
5.5	2.51	0.80	46.7
5.0	2.17	0.84	68.3
4.5	1.86	0.88	104.1
4.0	1.56	0.91	166.8
3.5	1.27	0.94	284.5

Figure 3 is a drawing showing the design of the high temperature, high pressure (HTHP) cyclone which will be inserted in the turbine simulator combustion system located at the UNDEERC. This cyclone is fabricated from 8 inch schedule 40 pipe which is welded to form an off-center tee. This pipe is water-jacketed to keep the metal wall temperatures low. As shown in Figure 3, the cyclone dimensions are cast in refractory inside the tee. This cyclone will replace the last section of the lean combustion zone shown in Figure 3. Figure 4 shows the HTHP cyclone inserted in the gas turbine simulator combustion system. Openings have been included in the vessel walls for measuring the inlet and outlet combustion gas temperatures and pressures. In addition openings have also been included for taking upstream particulate samples while an existing port will allow downstream particulate samples to be collected for measuring the cyclone efficiency. A second opening was added for a water-jacketed and sealed boroscope viewing system which is currently ordered. This boroscope will allow the flame quality and stability to be monitored during combustion tests.

4.2 Design of a Pressurized Atomization Spray Chamber

An existing pressure vessel has been modified to include observation ports to perform atomization studies under typical turbine operating pressures and air flows. The main objective of this work is to determine if differences in atomization quality account for the improvements in carbon burnout experienced with the LRC fuels. The design of the spray chamber involves an existing 11.25" ID pressure vessel which has been modified to provide optical access perpendicular to the direction of the atomized spray. The optical access consists of two diametrically opposite 3" sight ports for the use of high-speed photography. In addition, a 2" sight port opposite a 1" NPT port through which a sight pipe can be inserted has also been added. The use of a sight pipe reduces the length of the spray which the Malvern 2600's laser beam must pass through and eliminates the potential for vignetting which could occur if the beam were to pass through the complete spray cone. A honey-comb catalyst support is used as a flow straightener to provide a laminar flow of air around the atomizing nozzle. The height of the atomizer in relationship

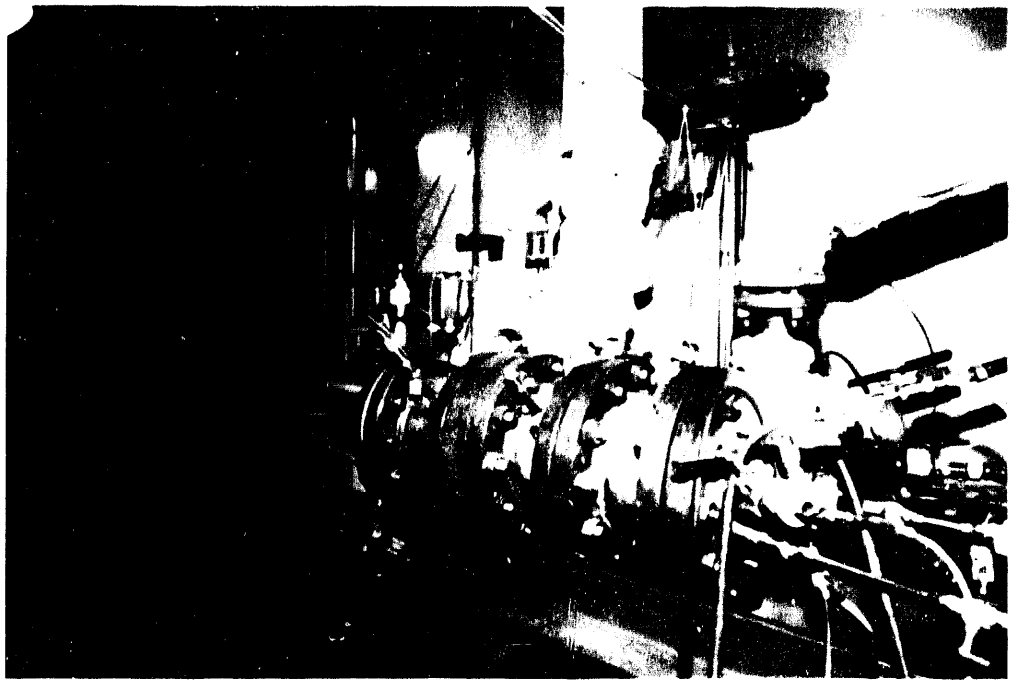

Figure 4. Photograph of the HTHP cyclone in the 1MM Btu/Hr gas turbine simulator combusiton system

to the optical ports will be adjustable from outside the pressure vessel thus allowing the atomizer position to be changed during a single atomization test.

Figure 5 shows the internal details of the pressurized spray chamber. Figure 6 is a photograph of the pressurized spray chamber. The atomized slurry is collected in a funnel at the bottom of the spray chamber where it is drained off to a pressurized separation vessel. Pneumatic control valves are used to control the air flow rate and to back-pressure the spray chamber. High speed photography is accomplished using a high-speed strobe to back light the slurry droplets during atomization. The use of high-speed photography allows droplet sizes larger than 564 microns (the top size for a Malvern particle size analyzer with a 300 mm lens) to be detected and also provide information about the spray angle obtained under a given set of operating conditions.

4.3 Design and Construction of a Pressurized Drop-Tube Furnace

The emergence of advanced coal combustion technologies such as coal slurry-fired gas turbines requires fundamental knowledge of the fuel combustion processes at elevated pressures. Of critical importance is the basic combustion kinetics and the fate of coal mineral matter in such systems.

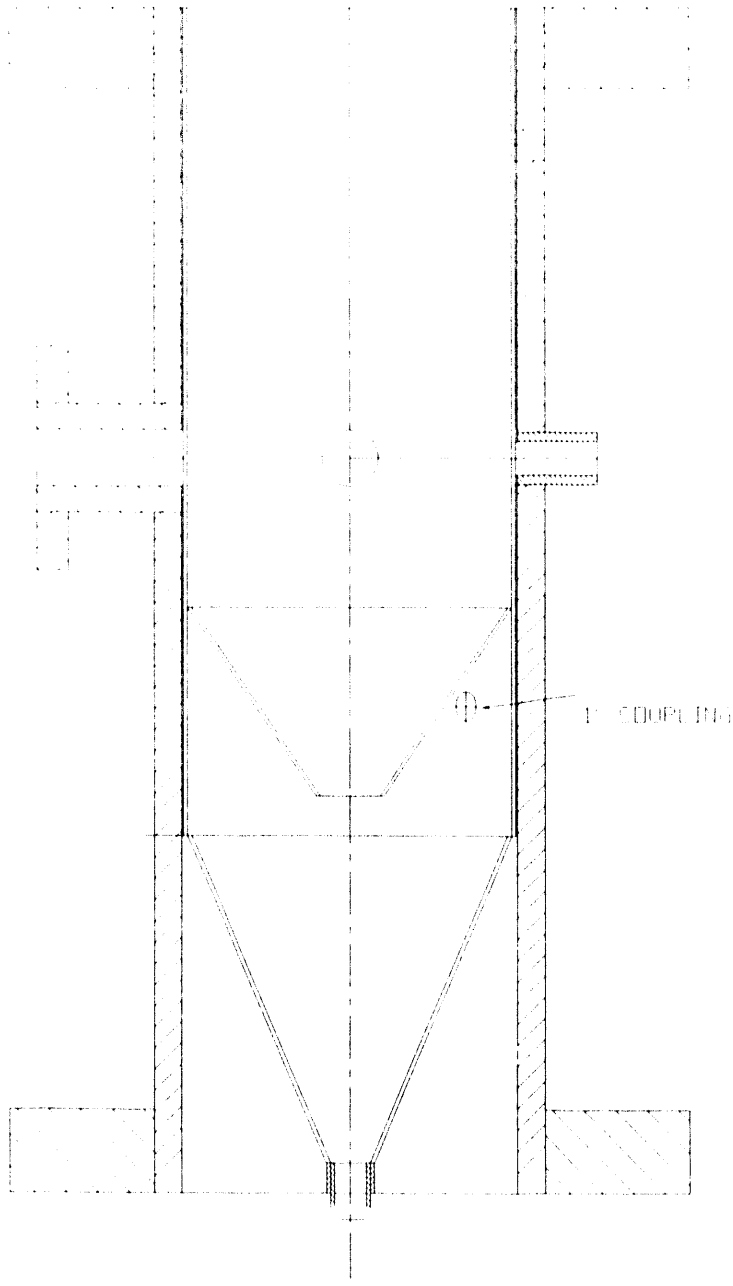

Figure 5. Schematic of pressurized spray chamber

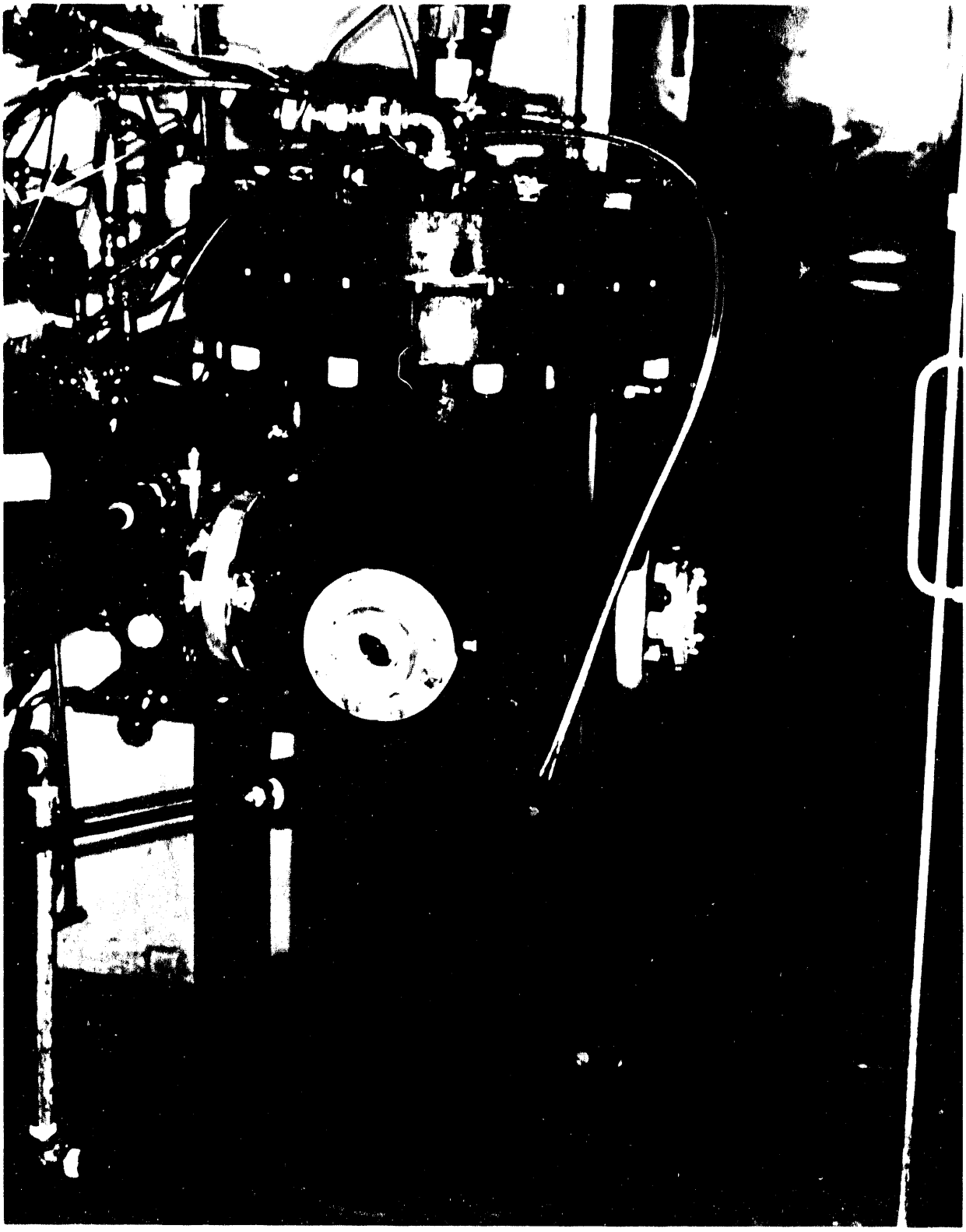

Figure 6. Photograph of pressurized spray chamber.

To address these issues, a pressurized drop-tube furnace was constructed. The pressurized drop-tube furnace (PDTF) is capable of operating under the following conditions:

Temperature:	ambient to 2732°F (1500°C)
Pressure:	ambient to 300 psi (20 atm)
Oxygen:	0 - 20 mole%
Gas Flow:	0 to 14.2 scfm (400 slpm)
Residence Time:	0 to 0.50 sec

- Optical access at any residence time
- Provision for char and ash collection
- Provision for ash deposition studies

The design of the PDTF incorporates several novel features which will allow the design goals to be met. A drawing of the PDTF facility is given in Figure 7. The entire PDTF is constructed of standard 24" and 6" flanged pipe sections. The large pressure vessel contains the furnace sections of the PDTF as shown in Figure 8. Figure 9 is a photograph of the PDTF after assembly for shakedown testing. The walls of the vessel are water-cooled to dissipate the heat from the furnaces. There is a preheater and two furnace sections located above the optical sight ports and one furnace below the optical sight ports to reduce the temperature gradient across the optical access section. Optical access is provided by four 3" diameter ports in the pressure vessel. Electrical power is supplied to the furnaces by electrical feed through terminals in the bottom blind flange of the pressure vessel.

Above the large pressure vessel shown is the injector section containing the injector assembly. The injector is a 1" diameter water-cooled probe sheathed in high-temperature insulation. Figure 10 is a photograph showing the translating mechanism used for raising and lowering the injector into the ceramic tube inside the furnace assembly. The injector may be retracted completely out of the furnace when not in use or may be lowered into the furnace to give the desired residence time between zero and 0.5 seconds. Small viewports in the pipe crosses at the bottom and top of the injector section allow visual inspection of the probe and the sample-feeding behavior.

Below the large pressure vessel is a similar collection assembly and translation mechanism. The collector may be raised to the level of the optical access ports and retracted completely from the furnace for the removal of sample deposits or when not in use. Two pipe crosses with small sight ports allow inspection of the collection probe operation, and the removal of a blind flange provides access for the removal of sample deposits. Both assemblies are interchangeable to allow for feeding powdered or slurry fuels and for collecting deposition or fly ash samples.

The sample feeder assembly is a blank flanged 6" pipe cross which is pressurized to slightly above the furnace pressure. Figure 10 also shows the sample feeder pressure vessel located next to the sample injector translating mechanism. Figure 11 is a schematic of the coal feeder used in the PDTF. The design allows the actual sample feeder to be constructed of lightweight material, since it does not have to withstand more than slight pressure

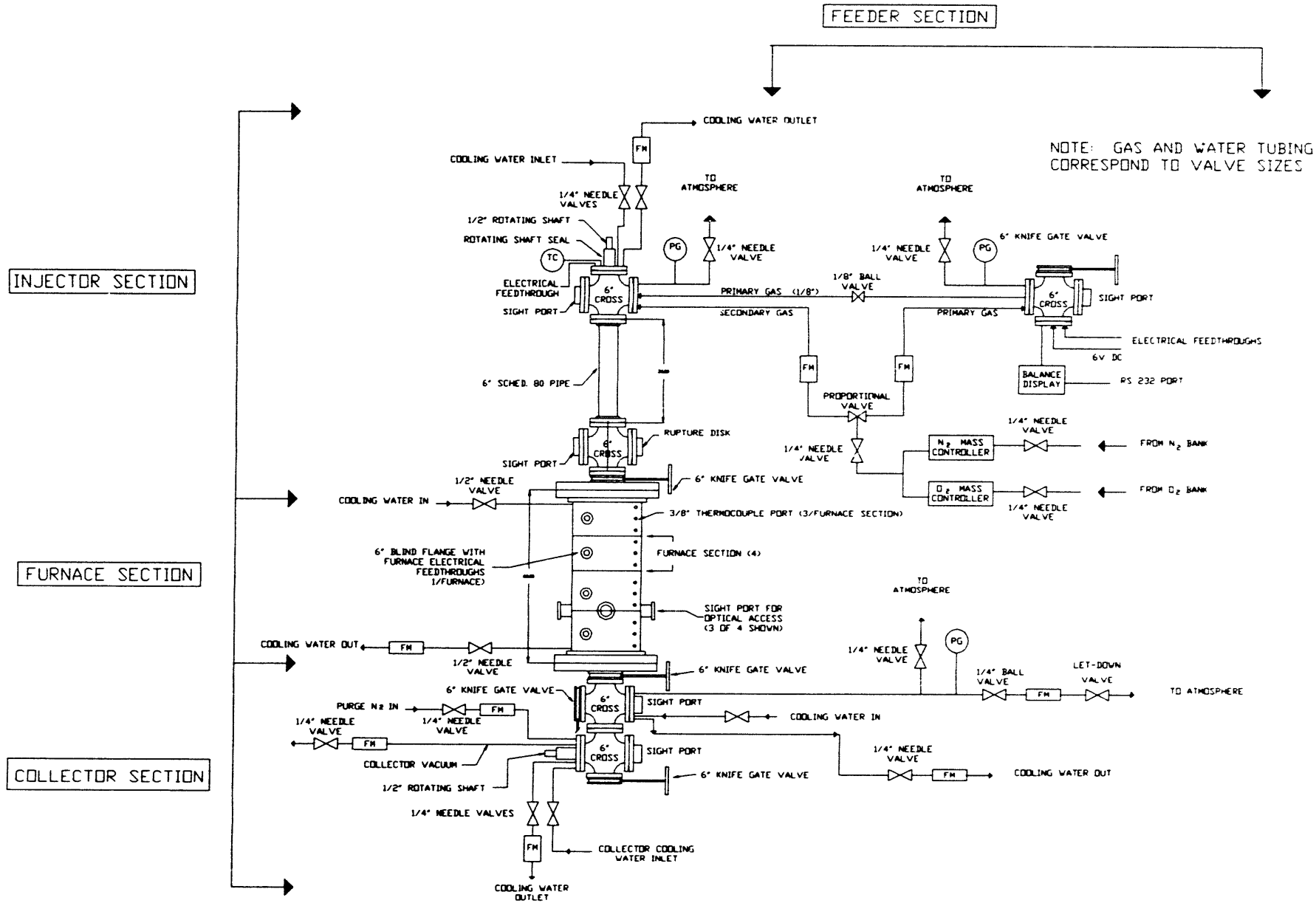

Figure 7. Pressurized drop-tube furnace process schematic.

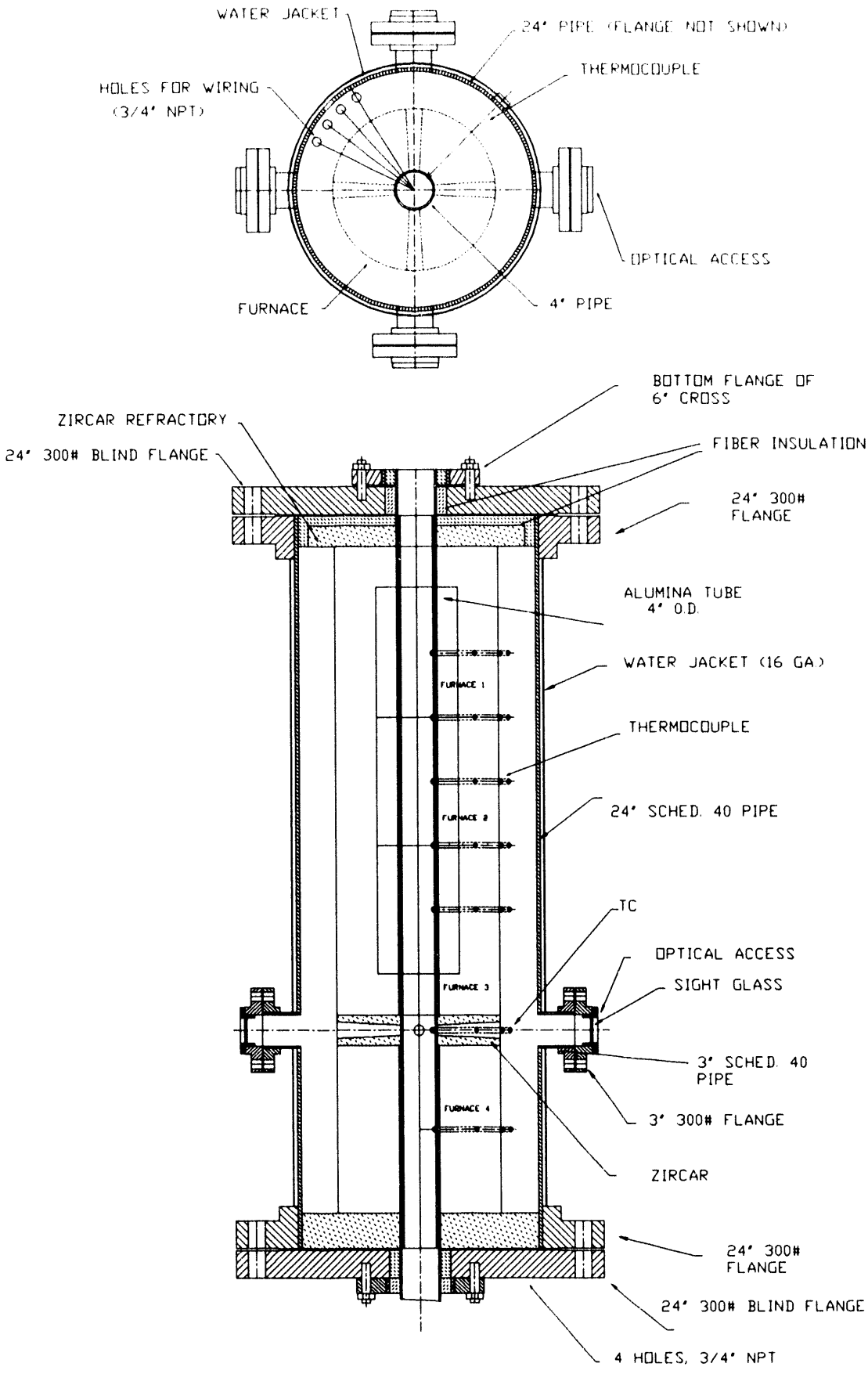

Figure 8. Furnace assembly in PDTF vessel.

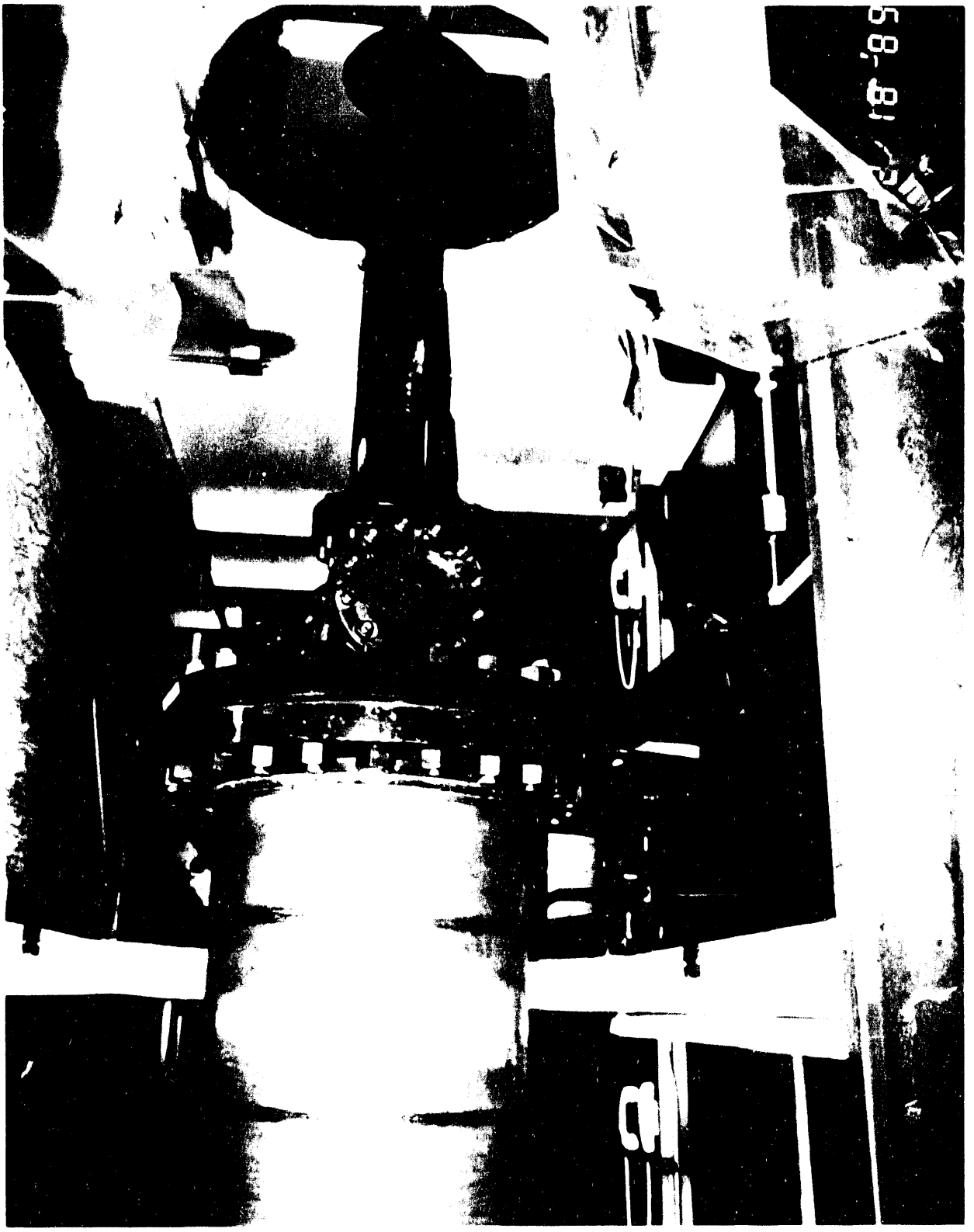

Figure 9. Photograph of PDTF vessel.

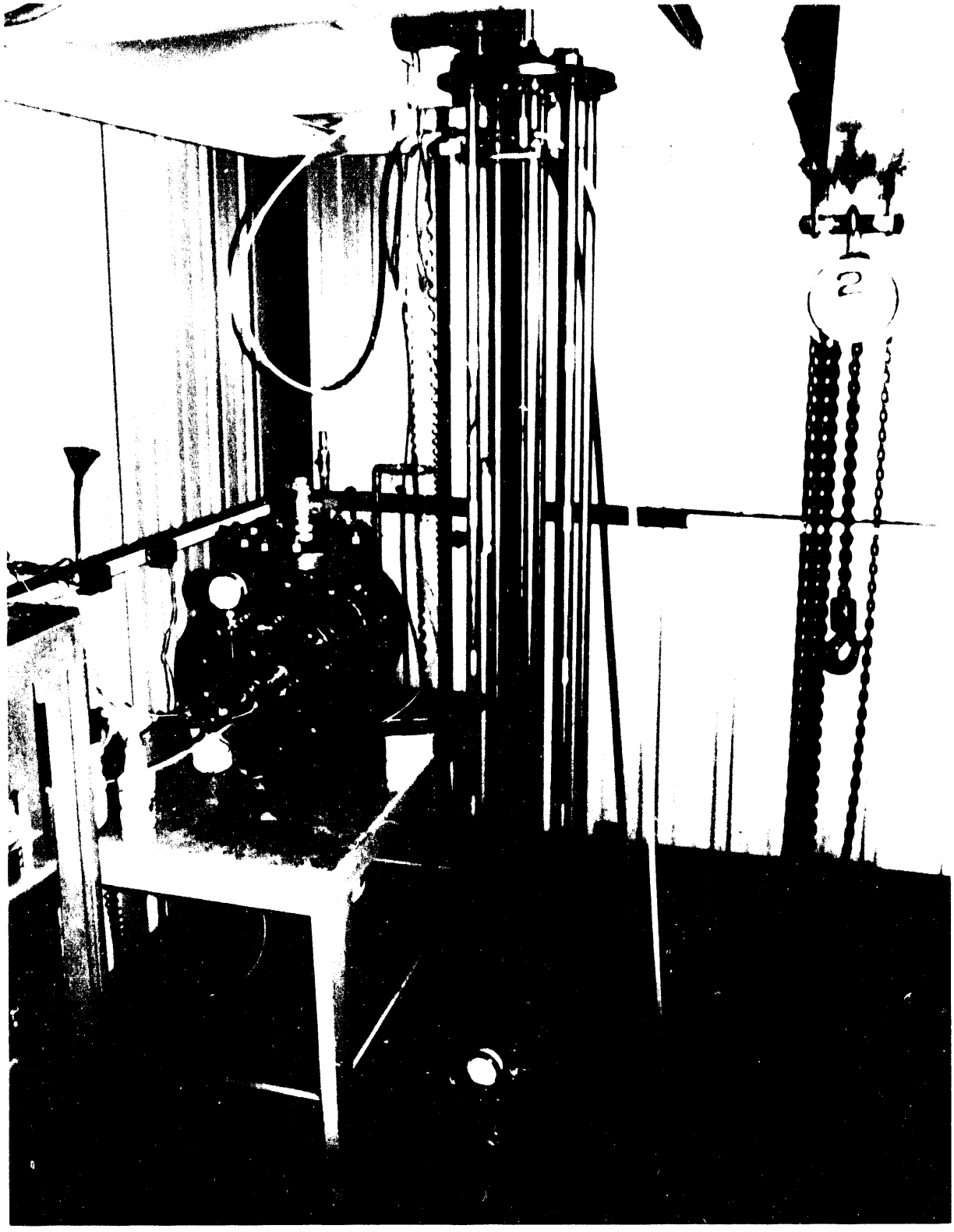

Figure 10. Photograph of PDTF translating mechanisms.

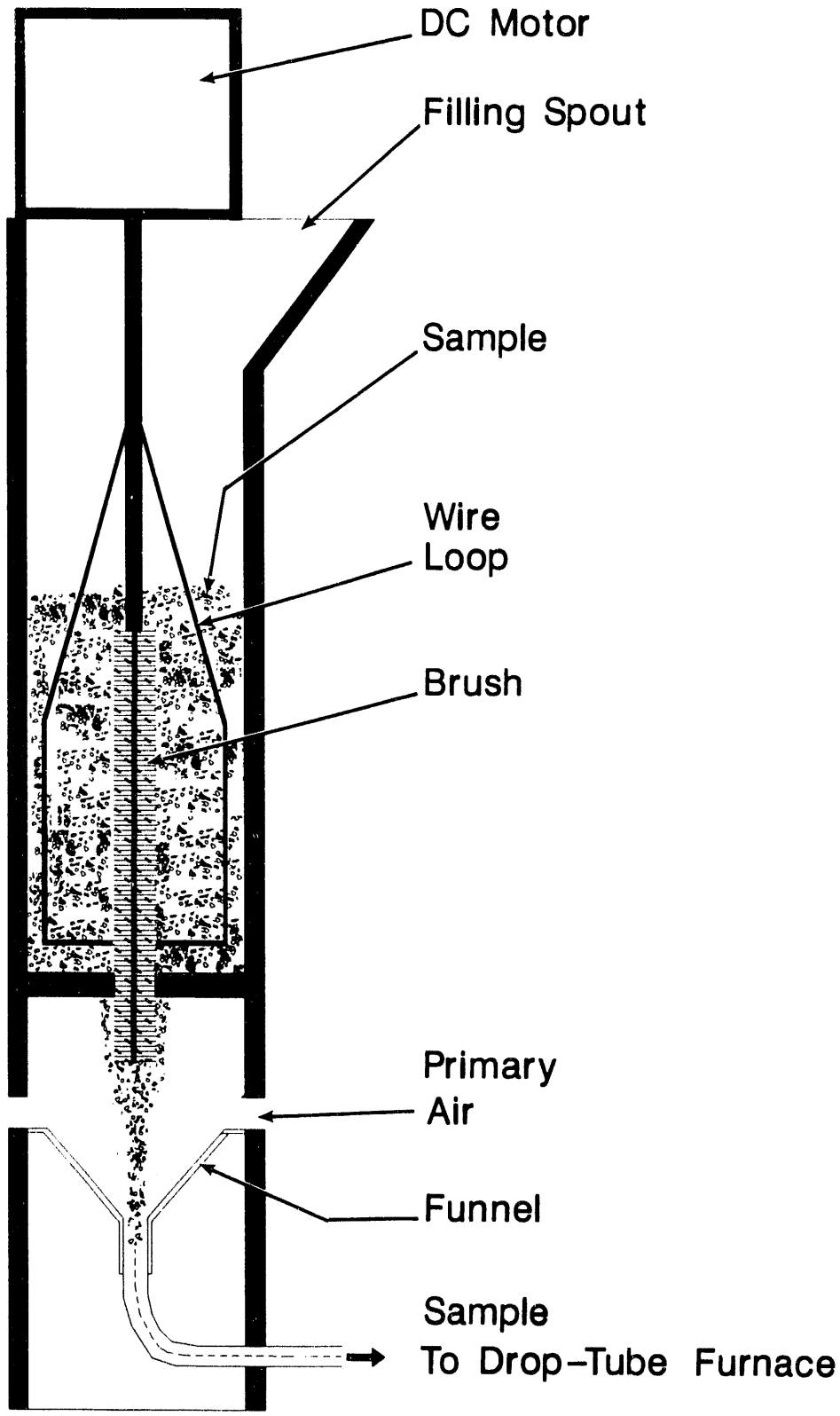

Figure 11. Schematic of coal feeder for pressurized drop tube furnace.

differentials. A small sight port allows inspection of the feeder operation, and the removal of a blind flange gives access to the vessel for filling or adjustment of the feeder. The lightweight feeder can then hang from a load cell in the pressure vessel to provide a continuous record of the sample feed rates. The gas composition and flow rate of gas into the PDTF is controlled by oxygen and nitrogen mass flow controllers. Gas composition can be controlled between 0-20 mole% at flow rates up to 400 liters/minute. The furnace pressure is controlled by a letdown control valve at the exit of the furnace.

Shakedown testing was performed to test the complete PDTF system. During this shakedown testing, several problems were encountered. One problem was that the load cell for monitoring the coal feed rate was too small; thus, the coal feeder used most of the load cell range before any coal was loaded into the feeder. In addition, problems were encountered when feeding coal, due to the PDTF gas flowmeters being sized too small, thus limiting the gas velocity used to pneumatically convey the coal particles into the PDTF.

Further examination indicated that the coal was plugging close to the tip of the injection probe. It was also observed that the deposition substrate temperature was too low due to the substrate being mounted right on the end of the water-cooled deposition probe. A thermal barrier, such as ceramic insulation, will have to be inserted between the probe and the substrate in order to achieve higher metal temperatures. During this testing, the heating elements for the bottom furnace burned out, leading to extremely low gas temperatures being measured in the optical access area. The PDTF will have to be partially disassembled and the furnace repaired before any meaningful testing can be accomplished.

4.4. SEM Analytical Results

CCSEM analyses were performed on the original CWF tested in the 1-MM Btu/hr gas turbine simulator in order to establish a baseline for comparison with deposits generated at 1100°C from these fuels in the PDTF facility. The Otisca CWF is a Taggart seam, VA bituminous coal bought commercially from Otisca, Ind. (Syracuse, NY). The Kemmerer and Beulah-Zap fuels were prepared at UNDEERC. The Kemmerer fuel was acid-cleaned only, while the Beulah-Zap fuel was both physically and chemically cleaned, and both were then hydrothermally treated and micronized. Tables 2 and 3 show the proximate and ultimate analyses, ash fusion temperatures, particle-size and X-ray fluorescence analyses previously performed on these fuels.

Tables 4, 5, and 6 show the CCSEM analysis performed on these same fuels. The first seven columns are all in weight percent on a mineral basis which fall in a certain size distribution, while the last column is the total weight percent on a coal basis, regardless of size. The analysis for the Otisca CWF shows that there were no minerals above 10 microns and only 16 wt.% of mineral particles were over 4.6 microns. In addition, two compounds (aluminosilicate and pyrite) comprise 60 wt.% of the minerals. The identified mineral phases account for approximately half of the ash level reported in the proximate analysis. For the Kemmerer CWF, quartz, aluminosilicate, and pyrite are the major mineral types. About 38 wt.% of all the minerals are greater than 10

TABLE 2
PROXIMATE AND ULTIMATE ANALYSES OF LRC FUELS TESTED IN TURBINE PROGRAM

Sample: PDU Test No.	Otisca N/A	Kemmerer 38	Beulah-Zap 40
Prox. Analysis (wt%, MF)			
Vol. Matter	36.10	41.10	42.66
Fixed Carbon	63.07	56.62	54.78
Ash	0.83	2.28	2.56
Ult. Analysis (wt%, MF)			
Hydrogen	5.39	5.03	4.29
Carbon	82.90	75.72	70.89
Nitrogen	1.59	1.30	1.20
Sulfur	0.78	0.26	0.78
Oxygen (by diff.)	8.49	15.40	20.26
Ash	0.83	2.28	2.56
Heating Value (MF, Btu/lb)	15,060	12,925	12,014
Ash Fusion Temperatures (°F-Reducing Atm)			
Init. Deform. Temp.	2119	2000	1942
Softening Temp.	2187	2095	1986
Hemisph. Temp.	2362	2140	2068
Fluid Temp.	2370	220[illegible]	2329
Part. Size-Mean (microns)	4.6	10.1	15.9
Top Size (99%<) (microns)	15.2	34.9	59.6

TABLE 3

X-RAY FLUORESCENCE ANALYSIS OF LRC FUELS TESTED IN TURBINE PROGRAM

High-Temperature Ash Results (% of ash, SO_3-free)	Otisca Fuel	Kemmerer Fuel	Beulah Fuel
SiO_2	37.0	49.0	25.2
Al_2O_3	28.8	2.0	20.5
Fe_2O_3	20.1	4.5	9.2
TiO_2	4.4	1.2	1.8
P_2O_5	0.4	0.4	1.5
CaO	5.7	9.1	16.3
MgO	1.6	3.5	4.8
Na_2O	0.0	0.0	0.0
K_2O	1.8	0.2	0.7

TABLE 4

SUMMARY OF CCSEM RESULTS FOR OTISCA FUEL

	Wt%, Mineral Basis							
Particle Size (μm)	<2.2	2.2-4.6	4.6-10	10-22	22-46	>46	Total	Coal Basis
Quartz	3.5	3.1	1.0	0.0	0.0	0.0	7.6	0.03
Iron Oxide	0.7	1.1	2.6	0.0	0.0	0.0	4.4	0.02
Aluminosilicate	14.6	15.7	7.0	0.0	0.0	0.0	37.3	0.16
Ca Al-Silicate	0.1	0.0	0.0	0.0	0.0	0.0	0.1	0.00
Fe Al-Silicate	3.8	1.6	0.0	0.0	0.0	0.0	5.3	0.02
K Al-Silicate	3.2	4.3	4.4	0.0	0.0	0.0	11.9	0.05
Pyrite	16.4	5.1	1.0	0.0	0.0	0.0	22.5	0.10
Gypsum	0.8	1.7	0.0	0.0	0.0	0.0	2.4	0.01
Barite	0.1	0.0	0.0	0.0	0.0	0.0	0.1	0.00
Ca Silicate	0.0	0.2	0.0	0.0	0.0	0.0	0.2	0.00
Gyp/Al Silicate	0.1	0.0	0.0	0.0	0.0	0.0	0.1	0.00
Alumina	0.1	0.4	0.0	0.0	0.0	0.0	0.5	0.00
Calcite	0.0	0.4	0.0	0.0	0.0	0.0	0.4	0.00
Rutile	0.5	0.3	0.0	0.0	0.0	0.0	0.8	0.00
Pyrrhotite/Sulfa	1.0	0.0	0.0	0.0	0.0	0.0	1.0	0.00
Si-Rich	0.5	0.4	0.0	0.0	0.0	0.0	0.9	0.00
Unknown	3.2	1.4	0.0	0.0	0.0	0.0	4.6	0.02
Total	48.5	35.5	16.0	0.0	0.0	0.0	100.0	0.43

microns. It is interesting to note that quartz comprises approximately 57.5 wt.% of the minerals, and aluminosilicate constitutes another 24 wt.% of the minerals. Approximately 83 wt.% of the ash in the coal is in the mineral form, which is consistent with this fuel being acid-cleaned only.

The major minerals identified in the Beulah CWF are quartz and pyrite; however, the iron oxide level is higher than would be expected for the Beulah fuel and is probably the result of some of the magnetite used in the heavy media separation remaining with the fuel. Approximately 43 wt.% of the minerals in the Beulah fuel are greater than 10 microns. The high level of unknowns is also unusual and merits further examination. Only 9 wt.% of the ash in the Beulah fuel was identified as minerals in the CCSEM analysis. From CCSEM analysis, most of the 2.56% ash in the Beulah was either organically bound or less than 1 μm in average diameter, the detection limit of CCSEM. The Beulah organically bound fraction has much larger quantities of Fe_2O_3 and CaO than the other coals, and only a fraction of these components are accounted for by discrete minerals. The Fe_2O_3 and CaO may act as fluxing agents, effectively lowering the ash fusion temperature in an aluminosilicate system. This would help induce slag and deposit formation at the 2000°F temperatures present in the gas turbine simulator. Ash fusion temperatures were much lower for the Beulah-Zap as compared to the other test coals.

TABLE 5
SUMMARY OF CCSEM RESULTS FOR MICRONIZED KEMMERER

	wt %, Mineral Basis							
Particle Size (μm)	<2.2	2.2-4.6	4.6-10	10-22	22-46	>46	Total	Coal Basis
Quartz	7.5	8.8	8.6	13.3	19.4	0.0	57.7	1.09
Iron Oxide	0.8	0.6	1.0	0.0	0.0	0.0	2.4	0.05
Aluminosilicate	7.3	5.0	8.5	3.6	0.0	0.0	24.4	0.46
Ca Al-Silicate	0.2	0.3	0.0	0.0	0.0	0.0	0.5	0.01
Fe Al-Silicate	0.1	0.1	0.0	0.0	0.0	0.0	0.2	0.01
K Al-Silicate	1.0	0.7	0.0	0.0	0.0	0.0	1.7	0.03
Pyrite	3.3	1.8	0.0	0.0	0.0	0.0	5.1	0.10
Barite	0.1	0.2	0.0	0.0	0.0	0.0	0.3	0.01
Ca Silicate	0.1	0.0	0.0	0.0	0.0	0.0	0.1	0.00
Ca Aluminate	0.1	0.1	0.3	0.0	0.0	0.0	0.6	0.01
Rutile	0.2	0.6	0.0	0.0	0.0	0.0	0.8	0.02
Dolomite	0.0	0.0	0.7	0.0	0.0	0.0	0.8	0.02
Pyrrhotite/Sulfa	0.1	0.0	0.0	0.0	0.0	0.0	0.1	0.00
Ca-Rich	0.1	0.0	0.0	0.0	0.0	0.0	0.1	0.00
Si-Rich	0.1	0.1	0.0	0.0	0.0	0.0	0.2	0.00
Unknown	1.2	1.7	0.0	2.1	0.0	0.0	5.0	0.10
Total	22.3	20.1	19.2	19.0	19.4	0.0	100.0	1.89

TABLE 6
SUMMARY OF CCSEM RESULTS FOR BEULAH FUEL

	wt %, Mineral Basis							
Particle Size (μm)	<2.2	2.2-4.6	4.6-10	10-22	22-46	>46	Total	Coal Basis
Quartz	16.8	6.2	0.9	1.5	2.8	4.6	32.8	0.08
Iron Oxide	1.3	2.7	0.0	0.0	0.0	0.0	4.1	0.01
Aluminosilicate	1.8	1.6	0.0	2.2	0.0	0.0	5.6	0.01
Ca Al-Silicate	0.2	0.1	0.0	0.0	0.0	0.0	0.3	0.00
Fe Al-Silicate	0.1	0.1	0.0	0.0	0.0	0.0	0.2	0.00
K Al-Silicate	0.2	1.0	0.0	0.8	0.0	0.0	2.0	0.01
Pyrite	10.3	3.1	2.8	0.0	0.0	0.0	16.1	0.04
Gypsum	0.2	0.5	0.4	0.3	0.0	0.0	1.3	0.00
Ca Silicate	0.1	0.6	0.0	0.0	0.0	0.0	0.7	0.00
Gyp/Al Silicate	0.0	0.0	0.0	1.6	2.1	0.0	3.8	0.01
Ca Aluminate	0.1	0.0	0.0	0.0	0.0	0.0	0.1	0.00
Rutile	0.2	0.4	0.0	0.0	0.0	0.0	0.6	0.00
Pyrrhotite/Sulfa	0.1	0.0	0.0	0.0	0.0	0.0	0.1	0.00
Ca-Rich	0.0	0.1	0.0	0.0	0.0	0.0	0.1	0.00
Si-Rich	0.3	0.1	0.0	0.3	0.0	0.0	0.7	0.00
Unknown	2.4	1.4	0.9	6.5	20.3	0.0	31.5	0.08
Total	34.1	17.9	5.0	13.2	25.3	4.6	100.0	0.24

The importance of the CCSEM results as an interpretative tool is more evident when combined with the ash content and composition of the fuels. It can be argued that a larger particle-size distribution of minerals in coal can significantly increase subsequent fly ash particle impaction rates on turbine blades, which in turn increases the potential for deposit development. Larger quantities of minerals were noted in the >10 μm range for the Beulah (43%) and the Kemmerer fuel (38%), as compared to the Otisca fuel (0%) on a mineral basis, which is consistent with the deposition seen in the turbine simulator.

5.0 CONCLUSIONS AND FUTURE PLANS

Spray tests in the pressurized spray chamber using previously tested CWF will be performed. Shakedown testing of the PDTF using the fuels previously tested in the gas turbine simulator will be accomplished. Future plans also include tests to look at what effects various levels of coal cleaning and different types of additives for increasing the ash melting temperatures have on the measured deposition rates and composition. A slurry feed system for the PDTF will be constructed, so fuel agglomeration tests can be completed.

6.0 REFERENCES

1. Swanson, M.L., Mann, M.D., and Potas, T.A., Comparison of Coal/Water Fuels Performance in a Gas Turbine Combustor, Fourteenth Inter. Conf. on Coal & Slurry Technology, April 24-27, 1989, pp 353-364.

2. Swanson, M.L., Moe, T.A., and Mann, M.D., "Advanced Coal Combustion", Proceedings of the Sixth Annual Coal-Fueled Heat Engines and Gas Stream Cleanup Systems Contractors' Review Meeting, DOE/METC-89/6101, March, 1989, pp.419-429.

3. Swanson, M.L., Mann, M.D. and Moe, T.A., Turbine Combustion Phenomena Annual Report, April 1988 to July 1989, in press.

4. Benson, S.A., Zygarlicke, C.J., Toman, D.L., and Jones, M.L. "Inorganic Transformations and Ash Deposition During Pulverized Coal Combustion of Two Western Coals", ASME Ash Deposit and Corrosion Research Committee Seminar on Fireside Fouling Problems, Brigham Young University, Provo, Utah, April 4-6, 1990.

5. Perry, R.H., and Chilton, C.H., Chemical Engineers' Handbook, Fifth Edition, 1973, pp 20-81 - 20-85.

6. Stairmand, C.J., Trans. Inst. Chem. Eng., 29:356, 1951.

7. Lapple, C.E., Ind. Hyg. Q., 11:40, 1950.